UNIVERSITÁ DEGLI STUDI DI CATANIA

FACOLTÁ DI INGEGNERIA

Dipartimento di Ingegneria Industriale e Meccanica

Corso di Dottorato in Meccanica Strutturale, XXIII ciclo

DYNAMIC RESPONSE OF THE COUPLED HUMAN BODY AND SEAT IN VERTICAL AND FORE-AND-AFT DIRECTION

di

Saverio Tufano

Dicembre 2010

Coordinatore e tutor:

Prof. Antonino Risitano

Dipartimento di Ingegneria Meccanica e Strutturale, Facoltà di Ingegneria,

Università degli Studi di Catania

Tutor:

Prof. Mike Griffin

Human Factors Research Unit, Institute of Sound and Vibration Research,

University of Southampton

Abstract

In many environments vibration is transmitted to a person through a seat. Seats can be designed to reduce the discomfort and the injuries caused by vibration. The efficiency of a seat in reducing vibration depends on the characteristics of the vibration, the characteristics of the seat, and the characteristics of the person sitting on the seat (Griffin, 1990).

This research was designed to investigate several aspects of the transmission of vertical and fore-and-aft vibration through polyurethane foams used in seat construction. The research programme was focused on two experiments. The first experiment was designed: (i) to investigate non-linearities in the seat and the human body in the vertical direction and their contributions to seat transmissibility; (ii) to compare the vertical apparent mass of the human body on rigid and soft seats; (iii) to measure and model the vertical dynamic stiffness of polyurethane foam seat cushions and investigate how the dynamic stiffness depends on vibration magnitude and subject characteristics (i.e. sitting weight, and hip breadth). The second experiment was designed: (i) to investigate the dependence of fore-and-aft seat cushion transmissibility on vibration magnitude, foam stiffness and contact with a backrest; (ii) to compare the fore-and-aft apparent masses of the human body on rigid and soft seats; (iii) to measure and model the dynamic stiffness of polyurethane foam seat cushions in the fore-and-aft direction, compare the fore-and-aft and vertical dynamic stiffness of foam, and investigate how fore-and-aft dynamic stiffness depends on subject sitting weight and hip breadth; (iv) to study the linear and non-linear effects of simultaneous vertical and fore-and-aft vibration and investigate whether single-axis transmissibility and single-axis models can be used to predict seat cushion transmissibility in multi-axis vibration environments.

Fifteen subjects attended the two experiments. In the first experiment, the vertical force and vertical acceleration at the seat base and vertical acceleration at the seat-subject interface were measured during random vertical vibration excitation (0.25 to 25 Hz) at each of five vibration magnitudes (0.25 to 1.6 ms^{-2} r.m.s.), with four seating conditions (rigid flat seat and three foam cushions). The measurements are reported in terms of the subject apparent mass on the rigid and foam seat surfaces, and the transmissibility and dynamic stiffness of each of the foam cushions. A frequency domain model was used to identify the dynamic parameters of the foams and to investigate their dependence on subject sitting weight and hip breadth.

In the second experiment, the vertical and fore-and-aft forces and accelerations at the seat base and the vertical and fore-and-aft accelerations at the seat-subject interface were measured during random vibration excitation (0.25 to 25 Hz) in fore-and-aft and vertical directions. Using three acceleration magnitudes in each direction (0, 0.25 and 1.0 ms^{-2} r.m.s.) eight different combinations of vertical and fore-and-aft excitation were investigated with three seating conditions (rigid flat seat and two foam cushions), with and without contact with a rigid vertical backrest.

Both the human body and the foams showed nonlinear softening behaviour, which resulted in nonlinear cushion transmissibility in both the vertical and the fore-and-aft direction. The nonlinearities in vertical cushion transmissibility, expressed in terms of changes in resonance frequencies and moduli, were more dependent on human body nonlinearity than on cushion nonlinearity. The vertical apparent masses of subjects sitting on the rigid seat and on foam cushions were similar, but with an apparent increase in damping when sitting on the foams. Fore-and-aft apparent mass was strongly dependent on the use of the backrest. Fore-and-aft apparent masses on rigid and soft seats had similar shapes. The vertical and fore-and-aft dynamic stiffness of foam was found to be nonlinear with vibration magnitude and showed complex correlations with the characteristics of the human body. Foams were stiffer in the horizontal direction than in the vertical direction. Linear cross-coupling between vertical and fore-and-aft transmissibility was found: a small part of the vertical (or fore-and-aft) vibration at the seat base contributes to fore-and-aft (or vertical) vibration at the subject-seat interface. Nonlinear cross-coupling was found in seat transmissibility and foam dynamic stiffness: the softening of the seat-subject system in one axis is affected by the vibration in the perpendicular direction.

The author believes that this research increased the current state of knowledge of the dynamics of the seated human body and polyurethane foams and so it represents a step forward in the understanding of the mechanisms involved in the vibration isolation provided by seats.

CONTENTS

Introduction

A comfortable and safe seat has to fulfil many requirements. By the 'static' point of view, a seat has to provide a proper support to the body parts, placing the occupant in a comfortable position to undertake appropriate activities requiring the minimal muscular effort. It should also provide ventilation, regulate temperature and distribute contact pressure evenly on the largest possible area, in order to reduce fatigue and avoid ulceration. By the 'dynamic' point of view, a good seat is a seat that insulates the occupant from vibration or shocks according to a relevant criterion, which can be the reduction of discomfort, the minimization of the disturbance of activities or the preservation of health (Griffin, 1990).

Seating dynamics is the science studying the insulating properties of seats respect to vibration. In fact, in many environments, vibration is transmitted to a person through a seat. Seats can be designed to reduce the amount of vibration transmitted to the human body, decreasing the discomfort and the injuries caused by vibration. The efficiency of a seat in reducing vibration depends on the characteristics of the vibration, the characteristics of the seat, and the characteristics of the person sitting on the seat (Griffin, 1990). Using subjects in seat testing, either in laboratory or in field, can be time consuming and expensive. Test procedures for the evaluation of seat performances have been therefore developed (Fairley, 1986; Wei, 2000). Prediction of seat transmissibility involves a deep knowledge of both seat and human body dynamics. It is well know that many factors can influence seat transmissibility. As discussed in (Wei, 2000) and in (Fairley, 1986) factors such as posture, footrest and the use of a backrest can modify seat transmissibility. Their contribution is beyond the aim of this thesis.

The general objective of this thesis is to improve the current knowledge about dynamics of seated people and of polyurethane foams for seat construction, through measurements of human body apparent mass and seat dynamic stiffness in vertical and fore-and-aft direction, and analysing their contribution to seat transmissibility.

For a more exhaustive introduction on the topic, the reader should refer to chapters 1 and 7

Research programme

The programme of the present research can be divided, for simplicity, into two experiments.

The first experiment was designed to investigate: (i) the differences in human body apparent mass when measured on a rigid or on a soft seat; (ii) the non-linearities in the polyurethane foam arising from static loading, contact dimensions and vibration magnitude; (iii) the role of human body and seat in determining the non-linearities in seat transmissibility in vertical direction.

The second experiment was designed to improve the knowledge about the cushion transmissibility in fore-and-aft direction, through the investigation of human body apparent mass on rigid and soft seat and seat stiffness.

The second experiment also investigated the existence of linear and non-linear cross-coupling in seat transmissibility. This is a basic requirement to understand the usability of single-axis dynamic models and to improve the knowledge of the mechanism of non-linearity.

1. Literature review and Introduction to Experiment no. 1

Seat transmissibility

The response of seat to vibration can be evaluated in different ways. The most common way to measure the characteristics of an occupied seat is to measure its transmissibility. Seat transmissibility is defined as the ratio of the motion at the seat surface over base of the seat.

$$\text{seat transmissibility} = \frac{\text{vibration on the seat}}{\text{vibration on the floor}}$$

The motion is usually expressed in terms of acceleration. In the frequency domain, it can be defined as the transfer function between the input and the output motion. If the cross-spectral density method is used (Bendat, 2000), the transfer function between two signals is:

$$H_{io}(f) = \frac{G_{io}(f)}{G_{ii}(f)}$$

where $G_{io}(f)$ is the cross-spectral density function (CSD) between the input and the output and $G_{ii}(f)$ is the power spectral density function (PSD) of the input. $H_{io}(f)$ is a complex quantity. Ordinary coherence function gives a value of the linearity of the relationship between input and output and gives also an indication of the level of uncorrelated noise in the measurements.

$$\gamma_{io}^{\,2}(f) = \frac{\left|G_{io}(f)\right|^2}{G_{ii}(f)\,G_{oo}(f)}$$

Seat transmissibility gives an insight into the dynamics of the seat and gives an indication of the possible improvements of the seat (Mansfield, 1998).

A way of summarising the performances of a seat has been proposed by Griffin (1978). The SEAT ('Seat Effective Amplitude Transmissibility') is defined as the frequency-weighted (e.g. according to weightings defined in ISO 2631-1:2001 or BS 6841:1997) time averaged acceleration measured on the seat surface divided by the frequency-weighted time averaged acceleration at the seat base. SEAT value may be considered as the ratio of the ride experienced on the seat to the ride which would be experienced if the seat were rigid, expressed as a percentage

$$SEAT\% = \left[\frac{\int G_{ss}(f)\,W_i^2(f)\,df}{\int G_{ff}(f)\,W_i^2(f)\,df}\right]^{1/2} x\ 100$$

where $G_{ss}(f)$ and $G_{ff}(f)$ are the seat and floor acceleration power spectra and $W_i(f)$ is the frequency weighting for the human response to vibration which is of interest (Griffin, 1990).

Seat transmissibility is usually calculated from signals measured by accelerometers. One accelerometer measures the vibration input, and is placed at the base of the seat. Another accelerometer has to be placed at the seat-human interface. Devices such as the SAE-pad or the SIT-BAR have been developed in order to firmly and comfortably place accelerometers between the seat pan and the subject buttocks.

Human body mechanical impedance and apparent mass

In biodynamics measures of human body driving-point mechanical impedance (or apparent mass) are commonly used, as they give an insight in the dynamic behaviour of the human body, indicating frequencies at which the human body is most responsive to acceleration (Mansfield, 2005), and providing useful information for modelling.

The single-point mechanical impedance is defined as the ratio between the force and the velocity measured at a certain point. Apparent mass is the ratio of the force and the acceleration at a certain point.

$$\text{Mechanical Impedance } = \mathrm{Z(f)} = \frac{F(f)}{v(f)}$$

$$\text{Apparent Mass } = M(f) = \frac{F(f)}{a(f)}$$

Usually human body apparent mass is preferred to mechanical impedance for several reasons. Apparent mass can be directly obtained from the signals of force and acceleration transducers. It is easily linked to Newton's law of motion $F = ma$. Furthermore the apparent mass is easier to interpret: 0 Hz value corresponds to the sitting weight of the person and the resonance frequency of a single degree of freedom system apparent mass is the same of the transmissibility resonance. This is not true in the case of mechanical impedance. The apparent mass can be obtained as the transfer function between the acceleration input and the force output:

$$M(f) = \frac{F(f)}{a(f)}$$

Apparent mass is simply measured by supporting the body on a force platform (a rigid plate mounted on force transducers) secured to a vibrator (Griffin, 1990). The force platform has to be rigid (have constant apparent mass) in the range of interest of the

measurements, so forces coming from the plate above the force transducers can be subtracted: this process is known as ‘mass cancellation’ (Griffin, 1990)

Seat dynamic stiffness

The seat dynamic properties are usually expressed in terms of seat dynamic stiffness. Dynamic stiffness is measured with an indenter attached to a force transducer. The seat is placed on a vibrator, so that it can be subjected to an acceleration input. Dynamic stiffness is the measured as the ratio between force and acceleration, multiplied per the squared frequency in radians per second

$$S(f) = \frac{F(f)}{a(f)}(2\pi f)^2$$

The indenter shape and area, the static load and the vibration magnitude determine the dynamic stiffness of the seat (Wei, 1997). Seat dynamic stiffness properties, to the author knowledge, have not been directly related to static properties.

* * *

The extent to which a seat modifies the vibration on the floor in any form of transport depends on the characteristics of the vibration, the characteristics of the seat, and the characteristics of the person sitting on the seat. Since the vibration on a seat can influence human comfort, the performance of activities, and human health, it is appropriate to select vehicle seats for their efficiency in isolating the vibration that has the greatest adverse influence (Griffin, 1978). The laboratory measurement of the vibration transmissibility of a seat usually involves the exposure of human subjects to vibration using specialised simulation facilities with the need for safety precautions. Differences between people lead to the requirement to test a group of representative subjects and consequent costs in both time and money. For this reasons research has investigated methods of predicting seat transmissibility without involving human subjects.

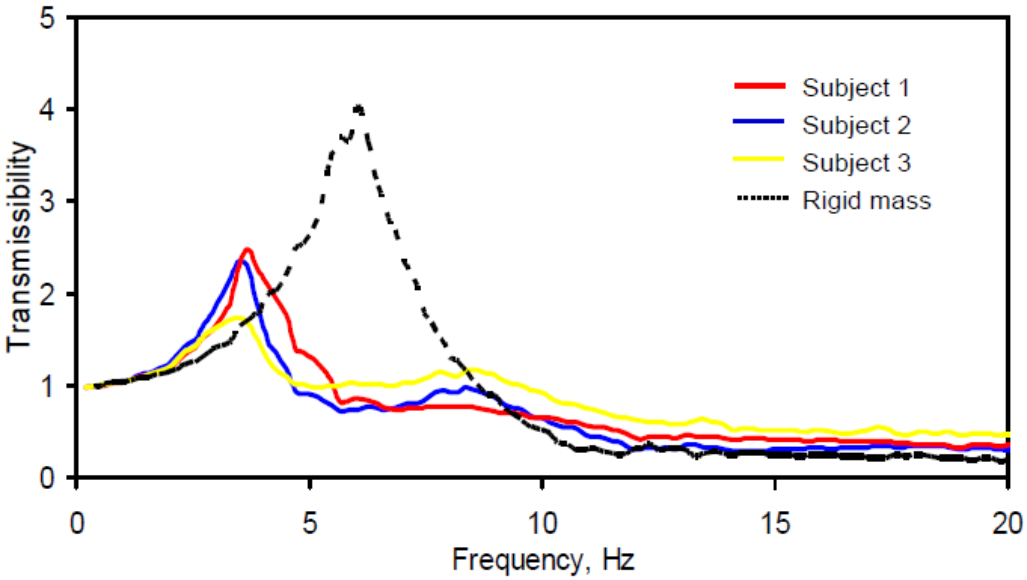

Figure 1.1: from (Toward, Short course on the Human Response to Vibration handouts)

Figure 1.1 shows that transmissibility of a seat measured with rigid mass quite different from that measure with human subjects and shows large inter-subject variability.

The vertical transmissibility of a seat in laboratory and field test can be determined without human subjects by using passive anthropodynamic dummies (e.g. Mansfield, 1996; Toward, 2000). Results usually showed good agreement with those obtained with human subjects and, usually, a better repeatability. Unfortunately, as addressed by Lewis and Griffin (2002), a mechanical dummy suitable for measuring seat transmissibility in laboratory conditions and in vehicles (on and off-road), would need to be capable of representing the driving point frequency response of human subjects over a wide range of vibration magnitudes. Mechanical suspension components, such as dampers, tend to have limitations that modify their dynamic performance when the excitation magnitude is lower, or higher, than an optimum operating range and result in non-linearities in mechanical dummies. That's the reason why active anthropodynamic dummies have been developed (e.g. Lewis and Griffin, 2002).

Figure 1. Anthropodynamic dummy.

Figure 1.2: passive dummy (Toward, 2000)

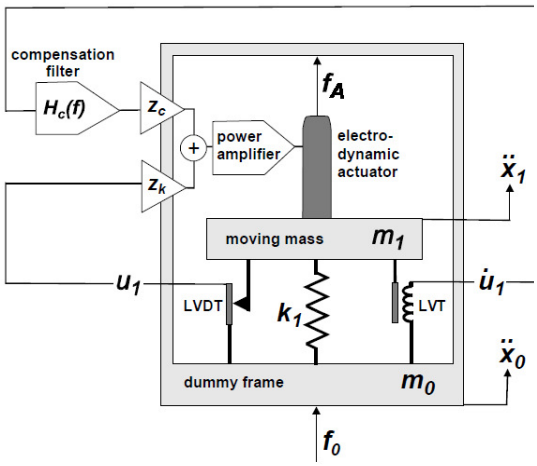

Figure 4. Schematic diagram of the active anthropodynamic dummy.

Figure 1.3: active dummy (Lewis and Griffin, 2000)

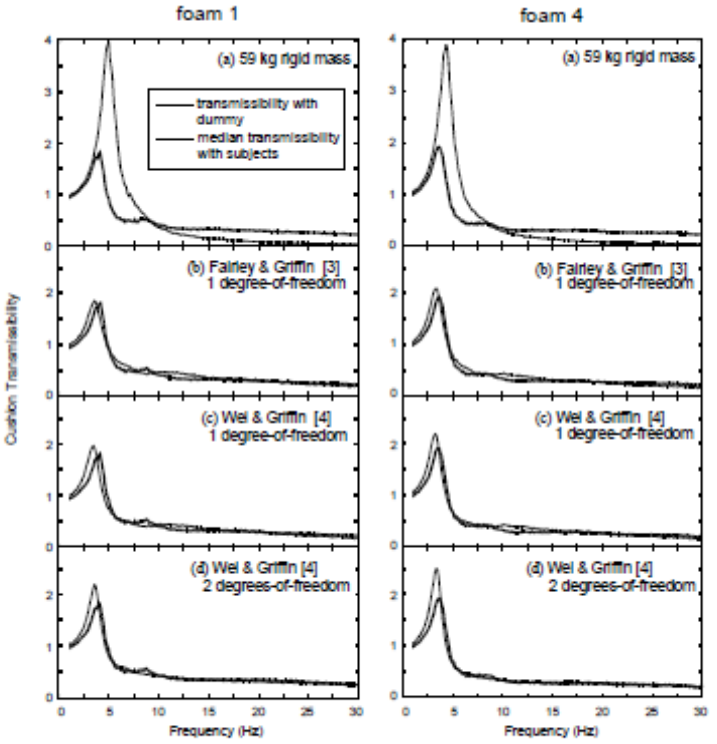

Figure 9. Mean cushion transmissibility measured with nine subjects compared with cushion transmissibilities measured with a rigid mass, and with the three dummy configurations shown in Figure 8. Broadband random excitation at 1·0 m/s² r.m.s. (signal 1 in Figure 7). Resolution = 0·125 Hz.

Figure 1.4: transmissibility prediction with an active anthropodynamic dummy in different configurations (Lewis and Griffin, 2002)

The vertical transmissibility of a seat can be predicted in a laboratory, by means of spectral techniques, from the measured seat dynamic stiffness and the measured apparent mass of the human body (e.g. Fairley and Griffin, 1986). Measurements of seat dynamic stiffness, given a model such the one in Figure 1.4, can be combined with apparent mass measurements to obtain transmissibility prediction. Main limitation of this method is that linear behaviour of seats and human body has to be assumed, meaning that the dependence of seat and body response respect to vibration input magnitude and spectral content cannot be implemented. In fact, human body apparent masses and seat dynamic stiffness are the optimum linear approximation for the conditions in which are measured and therefore could not be applicable in other cases. Furthermore, as showed in Figure 1.6, agreement between measured data and prediction is not perfect. This is probably due to (i) the difficulty of modelling the backrest contact or to (ii) the different condition in which apparent mass and dynamic stiffness measurements are taken.

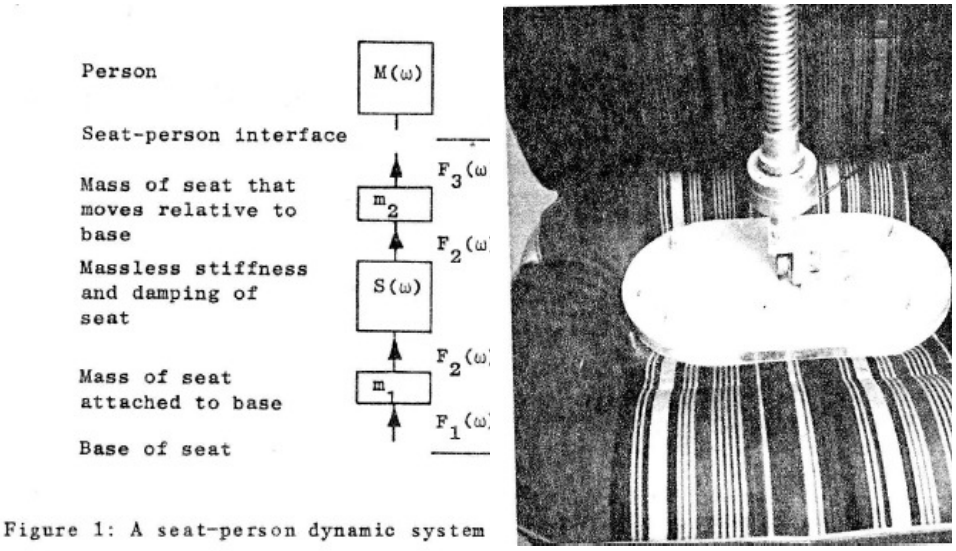

Figure 1.5: seat person dynamic stiffness and indenter rig for dynamic stiffness measurement (taken from (Fairley and Griffin, 1986))

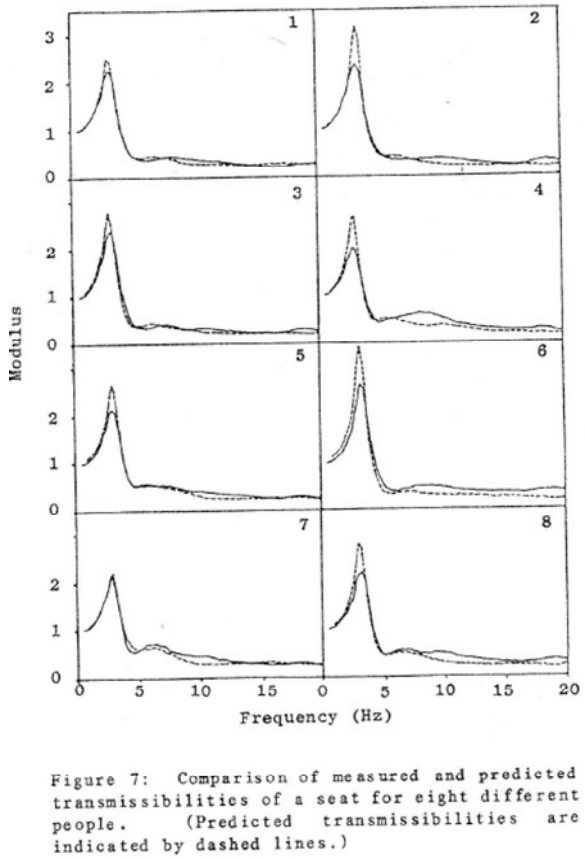

Figure 1.6: seat transmissibility prediction (Fairley and Griffin, 1986)

Another way of predicting seat transmissibility is by using mathematical models of the dynamic response of the seat and the human body (e.g. Wei and Griffin, 1998).

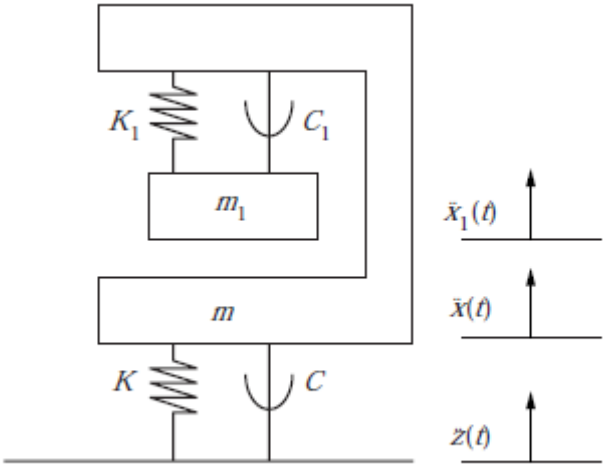

Figure 9. First seat–person system model.

Figure 1.7: human-seat model (Wei and Griffin, 1998)

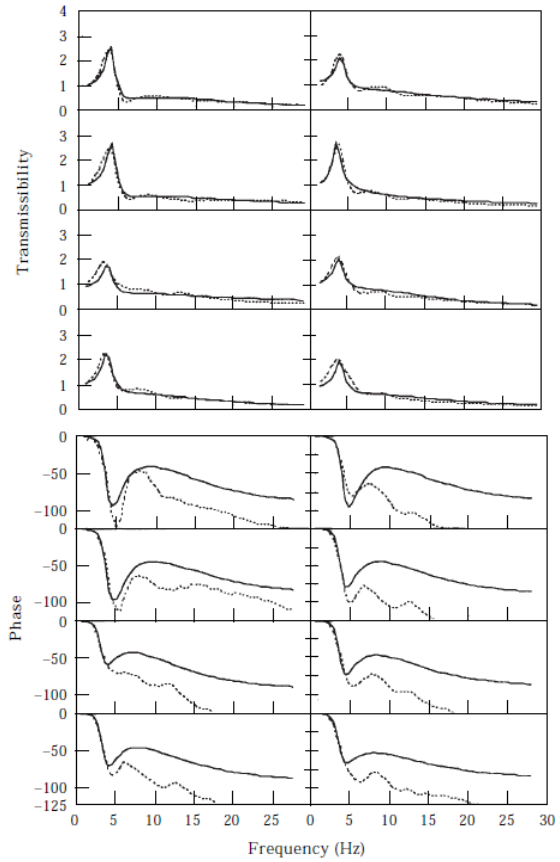

Figure 12. Comparison of measured and predicted seat transmissibility and phase when using single-degree-of-freedom model for eight different male subjects. - - -, Measured transmissibility; —, predicted transmissibility; – – –, measured phase; ——, predicted phase.

Figure 1.8: transmissibility prediction (Wei and Griffin, 1998)

Predictions of vertical seat transmissibility show differences from the transmissibility measured with human subjects, suggesting there are limitations to the models (e.g.

difficulties in modelling posture changes, effect of a backrest, effects of multi-axial vibrations) or the associated assumptions (e.g. linear behaviour)

It is commonly assumed that the apparent mass of the body and the dynamic stiffness of a seat do not change when they are coupled together. Changes might arise from differences in the contact conditions or differences in the vibration magnitude and spectral content. The apparent mass of the human body is usually measured on rigid flat surfaces: different pressure distributions and contact areas may alter the responses of soft tissues to vibration (Wu and Rakheja, 1989; Mansfield and Griffin, 2002).

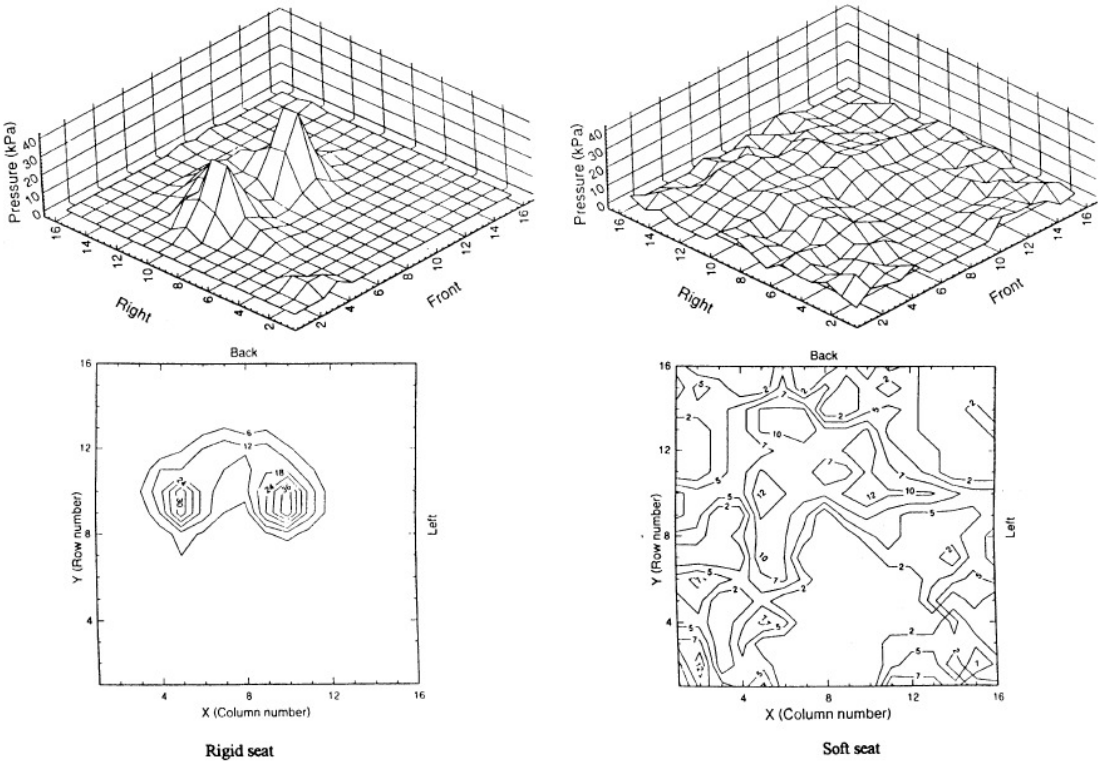

Fig. 2. Static interface pressure distributiion measured on the rigid and soft seat surface.

Figure 1.9: differences in seat-buttocks contact pressure distribution on a rigid and soft seat in static conditions (Wu et al., 1999)

The dynamic stiffness of a seat is measured using rigid indenters of specific size and shape, with little study of the effect of contact area or contact shape on seat dynamic stiffness (Wei, 1997).

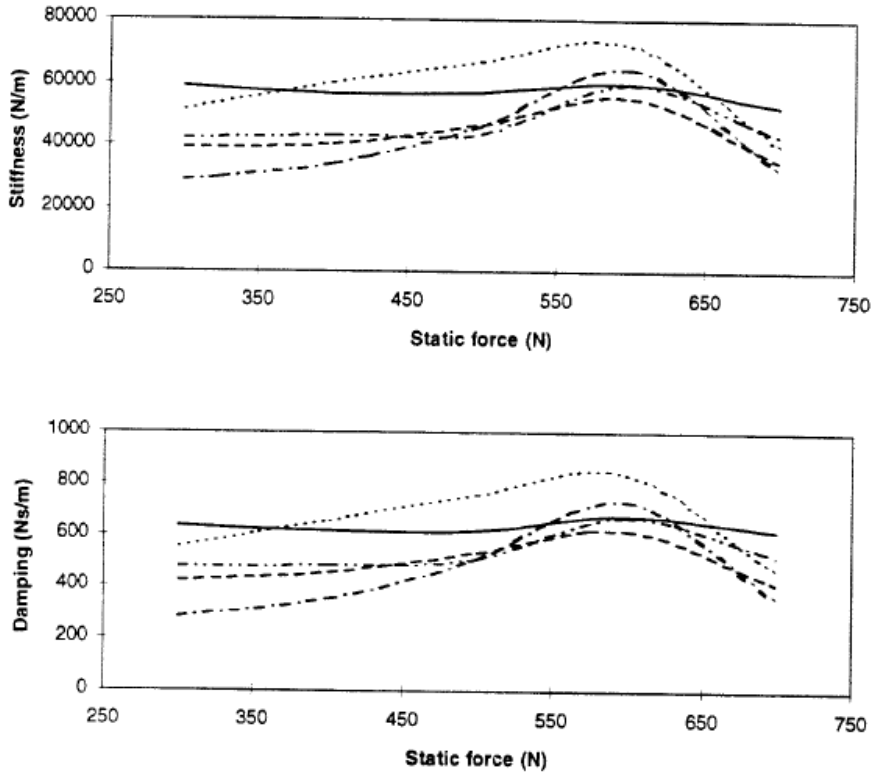

Figure 7. The effect of static force on measured foam stiffness and damping with the mean of five different foams at an input magnitude of 1.5 m/s² (disk 15 ———, disk 20 - - - - - -, disk 25 · · · · · · ·, buttocks - · - · - · - · -, SIT-BAR - · · - · · - · · -).

Figure 1.10: influence of static load and contact area on seat dynamic stiffness (Wei and Griffin, 1997)

The dynamic stiffness of foam also varies with changes in the weight it supports (Fairley and Griffin, 1986; Wei and Griffin, 1998), and it is not clear how vibration magnitude, subject weight, and contact area combine to determine the dynamic stiffness of seating foam (Hilyard, 1984; Hilyard, 1994; Wei, 1997).

Although linear behaviour is commonly assumed, both the human body (e.g. Fairley and Griffin, 1989) and polyurethane foams used in seat construction (e.g. Patten and Pang, 1998) are nonlinear systems that soften with increasing magnitude of vibration.

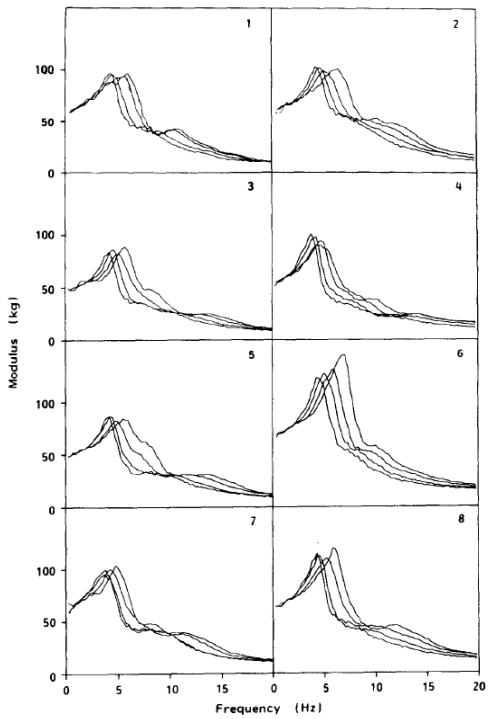

Fig. 6. Effect of vibration magnitude (0.25, 0.5, 1.0 and 2.0 ms^{-2} r.m.s.) on the apparent masses of eight people—the resonance frequency, and the apparent mass at frequencies above resonance, consistently decrease with increasing magnitude for every person.

Figure 1.11: nonlinear softening effect of vibration magnitude on human body vertical apparent mass (Fairley and Griffin, 1989)

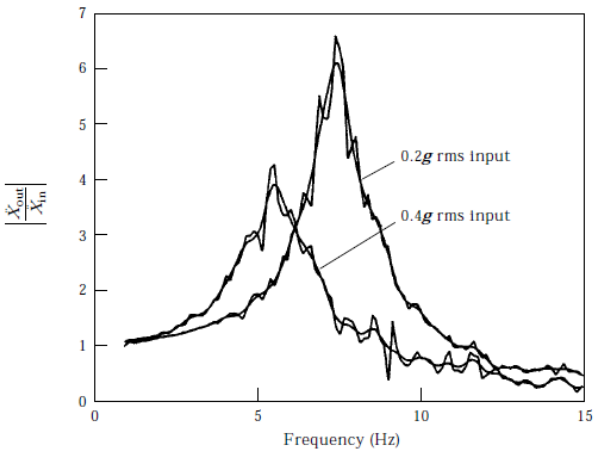

Figure 7. Experimental transfer function of a sport car seat for 356 N (80 lb) seat load (raw data and smoothed data shown).

Figure 1.12: nonlinear softening effect of vibration magnitude on seat transmissibility measured with a mass (Patten and Pang, 1998)

Consequently, the vertical transmissibility of seats is nonlinear, with the resonance frequencies reducing as the vibration magnitude increases (Figure 1.13). While the effect

of vibration magnitude (e.g. Mansfield and Griffin, 2000) and spectral content (Mansfield et al., 2006) on human apparent mass has been studied, it is not yet possible to predict the apparent mass of the human body for any type of vibration input. The apparent mass of the body and the dynamic stiffness of seats may be measured using broadband random vibration with equal energy over a specified frequency range, so as to ensure generality and allow repeatability, but this is not representative of the vibration in transport (Griffin, 1990). The nonlinearity in both systems results in the measured apparent mass of the body and the measured dynamic stiffness of the seat not being representative of the conditions in which the seat is used. When using a specific apparent mass for the human body and a specific dynamic stiffness for a seat, the linear prediction of seat transmissibility will only apply to a limited range of vibration conditions.

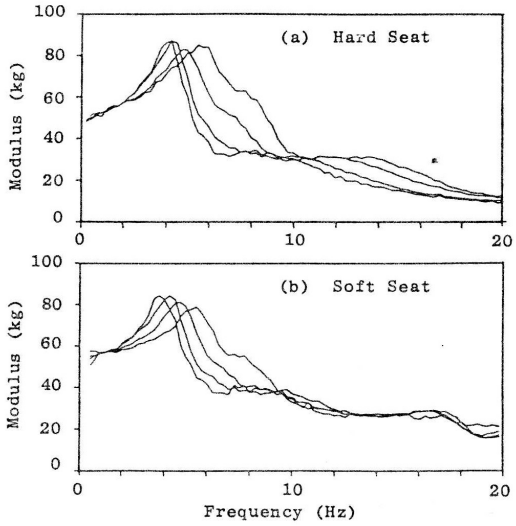

Figure 10: Effect of vibration magnitude on the apparent mass of a person, measured on (a) a hard seat and (b) a soft seat.

Figure 1.13: effect of human body and seat nonlinearity on seat transmissibility (Fairley and Griffin, 1986)

Models of the human body and seats vertical dynamics could be developed with model parameters that are dependent on the magnitude and spectra of the input vibration (e.g. Muksian, 1976; Patten and Pang, 1998; Patten *et al.*, 1998). However, it has recently been shown that the non-linearity of the human body is also influenced by vibration in other directions (e.g. Hinz *et al.*, 2006), and so useful non-linear models of the body that are generally applicable are not yet available.

Ebe (1993) found a strong correlation between transmissibility measured on conventional full-dept foam seats and rectangular blocks of foam made from the same material,

meaning that measurements made on a foam sample, although slightly different from those on a real seat, can help seat manufacturers in choosing the best material for vibration insulation in a seat.

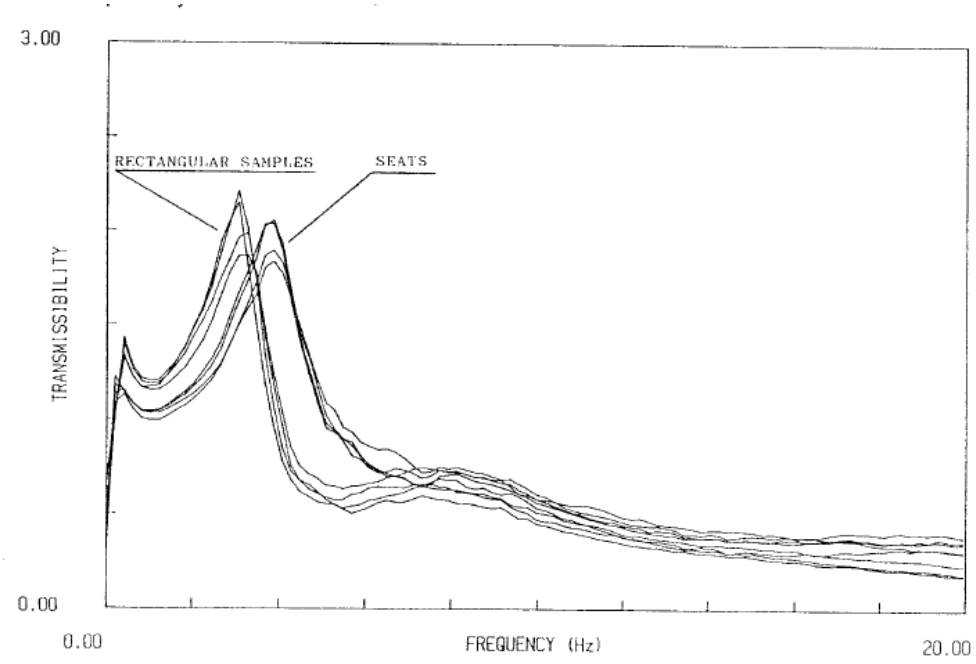

Figure 5 The median transmissibilities of the rectangular samples and the seats

Figure 1.14: seat transmissibility measured with rectangular foam blocks and seats

The first part of this thesis was designed to investigate some common assumptions by simultaneously measuring the human body apparent mass and the dynamic stiffness of a foam cushion. It was hypothesised that:

(i) the apparent mass of the body and the dynamic stiffness of the foam would change with changes in vibration magnitude and that there would be a consequent differences between the apparent mass of the body sitting on a rigid seat and the apparent mass of the body supported on a foam cushion;

(ii) increases in subject weight and increases in foam contact area would increase the elastic stiffness of the foam;

(iii) the dynamic nonlinearity in the human body would have a greater influence on seat transmissibility than any nonlinearity on the dynamic response of the foam (Griffin, 1996; Wei, 1997).

2. Method – experiment 1

2.1 Apparatus

The vertical force was measured using a Kistler force platform (model 9281B) with an aluminium top plate secured to a rigid seat attached to a 1-m stroke vertical hydraulic vibrator in the laboratories of the Human Factors Research Unit at the Institute of Sound and Vibration Research (Figure 2.1). The charge signal from vertical force cells at the four corners of the force platform were summed and amplified by a Kistler 5001 amplifier.

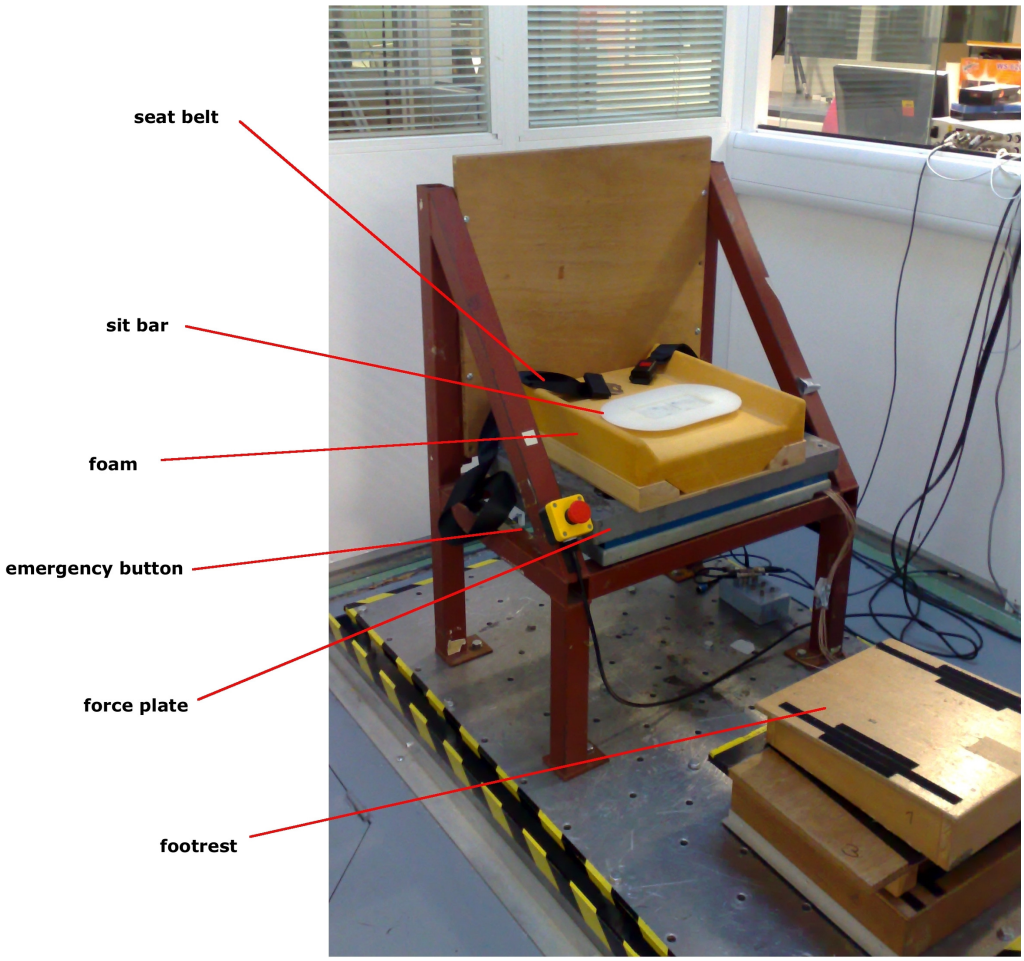

Figure 2.1: experimental setup

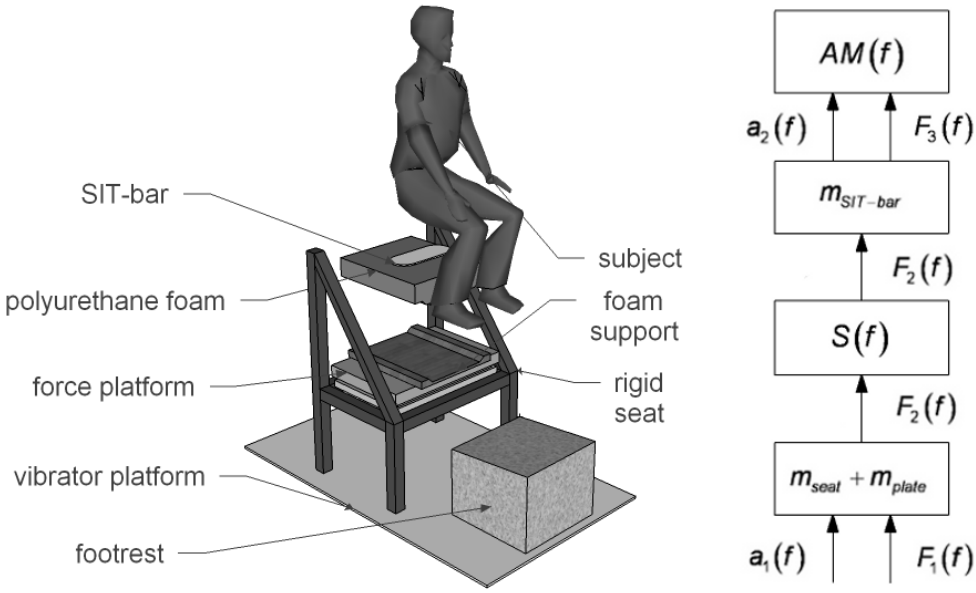

Figure 2.2: Experimental setup (left), and seat-person dynamic model from [3], right.

The vertical acceleration was measured using an Endevco 2265/10 accelerometer at the centre of the force plate and a 2265/20 accelerometer in a SIT-bar placed between the seat cushion and the subject buttocks (Whitham and Griffin, 1977).

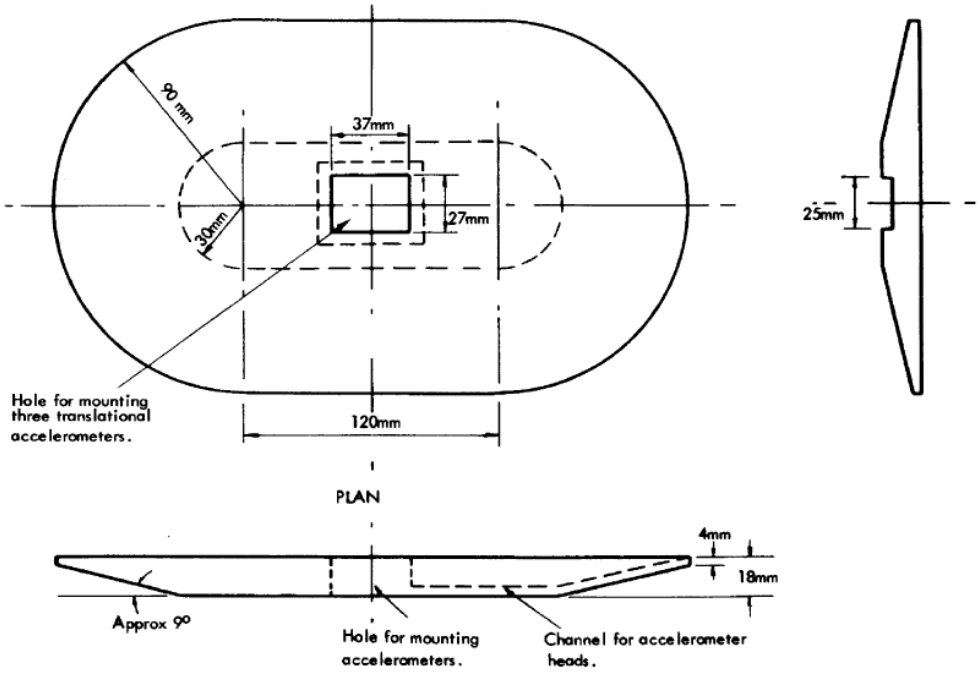

Figure 2.3: Design of the SIT-BAR (Seat Interface for Transducers indicating Body Acceleration Received) seat indenter (Whitham and Griffin, 1978).

The force and acceleration signals were amplified and low-pass filtered (3-pole Butterworth, 50-Hz cut-off frequency) by Fylde signal conditioning before being acquired to computer at 256 samples/second via a National Instrument NI-USB-6251 DAQ, controlled by *HVLab* Matlab Toolbox software.

Table 2.1 Foam properties.

	Dynamic stiffness	Composition	Density (kg/m^3)	Maximum thickness (mm)	Weight (kg)
foam 1	soft	MDI	75	110	1.35
foam 2	medium	TDI	50	110	0.89
foam 3	hard	MDI	75	80	0.93

Three blocks of polyurethane foams suitable for automotive seats were selected from a larger sample so as to represent a broad range of dynamic characteristics (Table 2.1). The upper flat surface of each foam block was 400 mm wide by 450 mm deep. The lower surfaces of the foams were flat, apart from a 40-mm reduction in thickness over 60-mm wide strips on both sides. The foams (with no covers) were supported on a wooden base (weighing 2.1 kg) resting on the aluminium plate secured to the force platform.

2.2 Experimental design

Fifteen male subjects participated in the study. Their ages, standing weights, statures, and hip breadths were measured as described by Pheasant (1988) (see Table 2.2). The sitting weight shown in Table 2.2 for each subject is the median measured apparent mass at 0.625 Hz, as determined when sitting on the seat foams and measured as described below. The ratio of the sitting weight to the standing weight had a median of 72%.

Table 2.2 Subject characteristics (Pheasant, 1988)

	Age (years)	Stature (cm)	Weight (kg)	Sitting weight (kg)	Hip breadth (cm)
Median	27	178	76	55	36
Minimum	21	169	56	41	31
Maximum	41	186	93	65	41
Interquartile range	8	10	21	12	5

The apparent masses of the subjects were determined in four conditions: while they sat on the force plate without a cushion (i.e. rigid seat condition) and while they sat on each of the three blocks of foam placed on the force plate. The subjects were instructed to sit in an erect posture with no backrest contact, with their lower legs vertical and their hands on their laps. A footrest supported on the moving platform of the vibrator was adjusted in height so as to maintain the uncompressed cushion surface 300 mm above the feet. So as to reduce the influence of foam relaxation on seat properties, the subjects sat on the foam blocks for at least 3 minutes before starting the dynamic tests.

For each of the four seating conditions, the force plate was excited for 60 seconds using 0.25 to 25 Hz Gaussian random vibration at each of five magnitudes: 0.25, 0.4, 0.63, 1.0, and 1.6 ms^{-2} r.m.s.

The order of presenting the four seating conditions was randomised, as well as the order of presenting the vibration magnitudes with each seat.

2.3 Human-seat model

Using the signals from the two accelerometers and the force transducer, it was possible to calculate: the foam transmissibility, $T(f)$, between the seat base acceleration, $a_1(f)$, and the seat pan acceleration, $a_2(t)$; the apparent mass of the subject, $AM(f)$; and the dynamic stiffness of the foam, $S(f)$. As derived from Figure 2.2b (redrawn from Fairley and Griffin, 1986), $AM(f)$ is the complex ratio (i.e. the transfer function) of $F_3(f)$ to $a_2(f)$. While the acceleration at the human-seat interface, $a_2(t)$, was directly measured by the accelerometer in the SIT-bar, $F_3(t)$ was derived (see below).

The foam was supported on the force platform, so $F_1(t)$ was the gross force measured by force transducers. The foam was assumed to be a pure complex stiffness element, with its mass m_{seat} added to the mass of the plate m_{plate} for mass cancellation. It follows that (Fairley and Griffin, 1986):

$$F_2(t) = F_1(t) - \left(m_{plate} + m_{seat}\right) a_1(t) = F_3(t) + m_{SIT-bar} a_2(t)$$

$$\Delta a(t) = a_2(t) - a_1(t)$$

$$S(f) = \frac{F_2(f)}{\Delta a(f)} (2\pi f)^2 = M(f)(2\pi f)^2$$

$$AM(f) = \frac{F_3(f)}{a_2(f)}$$

$$T(f) = \frac{a_2(f)}{a_1(f)} = \frac{M(f)}{M(f) + AM(f) + m_{SIT-bar}} \quad (1)$$

Mass cancellation for the mass of the force platform above the force sensors and the mass of the seat and wooden frame was performed in the time domain, while *S*(*f*) and *AM*(*f*) are frequency domain response functions and were determined from the ratio of the input-output cross spectrum to the power spectral density of the input (Bendat, 2000):

$$H_{io}(f) = \frac{G_{io}(f)}{G_{ii}(f)}.$$

For each quantity, the coherence function was calculated as (Bendat, 2000):

$$\gamma_{io}^{\ 2}(f) = \frac{\left|G_{io}(f)\right|^2}{G_{ii}(f)G_{oo}(f)}$$

The transfer functions were determined with a resolution of 0.125 Hz and 32 degrees-of-freedom.

The normalized apparent masses of the subjects were determined from their apparent mass function divided per their quasi-static sitting weights calculated from their apparent mass at 0.625 Hz.

2.4 Evaluation of nonlinearity

For each subject sitting on each seat foam, the resonance frequencies of both the apparent mass and the seat transmissibility were determined from the maxima of the absolute values of apparent mass and transmissibility, respectively, with each of the five vibration magnitudes (0.25, 0.4, 0.63, 1.0, and 1.6 ms^{-2} r.m.s.). The maximum difference in the resonance frequency across the five magnitudes was used as the measure of nonlinearity. Equation (1) was used to estimate the separate influences of the nonlinearity in the human body and the nonlinearity of the seat foam on the seat transmissibility. To evaluate the influence of the human body nonlinearity, the subject apparent mass at each of the five magnitudes was substituted in Equation (1), with the dynamic stiffness held constant at the appropriate reference magnitude (0.25, 0.4, 0.63, 1.0, or 1.6 ms^{-2} r.m.s.). As result, five estimated transmissibility functions were obtained for each vibration magnitude. To evaluate the influence of seat nonlinearity on transmissibility, the subject apparent mass was held constant at the value measured with each vibration magnitude and the five dynamic stiffness functions were substituted in Equation (1). The maximum difference in the resonance frequency over the five vibration magnitudes in each case

(either the dynamic stiffness held constant or the apparent mass held constant) was used as the measure of nonlinearity.

2.5 Seat Dynamic Stiffness model

Previous studies (Hilyard, 1984; Lewis, 2000) and preliminary data indicated that the real and imaginary stiffness of foam tends to increase with increasing frequency of vibration. It was therefore considered appropriate to model the dynamic stiffness of the foam using a linear model composed of pure stiffness, *k*, and viscous damping, c, with the addition of a linear frequency dependency in the stiffness, *k'*, and an hysteretic component, *c'* (Conza, 2007):

$$S(f) = k + \omega k' + i(\omega c + c') \tag{2}$$

where $\omega = 2\pi f$ is the frequency in radians per second. The foam stiffness, *k*, results in a force in-phase with the foam displacement. The frequency-dependency in the stiffness, *k'*, may be explained by reduced airflow through the foam at increased deformation rates: the air is trapped in the foam and contributes to the stiffening. The damping, *c*, represents the energy loss resulting from the movement of air through the polymer cellular matrix, while the viscous equivalent hysteretic damping, *c'*, is related to the characteristics of the base polymer (Hilyard, 1984).

Curve fitting was performed by minimising the least square error function between the measurements and Equation (2) at frequencies over the range 4 to 20 Hz.

3. Experiment 1 - Results

3.1 Apparent Mass – Rigid and soft seat

The effects of vibration magnitude on the median apparent mass, median normalised apparent mass, and median phase over the 15 subjects are shown for each of the four conditions (sitting on the rigid seat and sitting on the three foams) in Figure 3.2. The apparent mass had a main resonance peak at about 5 Hz, with some subjects showing a second resonance with lower apparent mass in the range 8 to 17 Hz. An increase in the modulus of the apparent mass was occasionally apparent at about 2 Hz, and was associated with a positive phase.

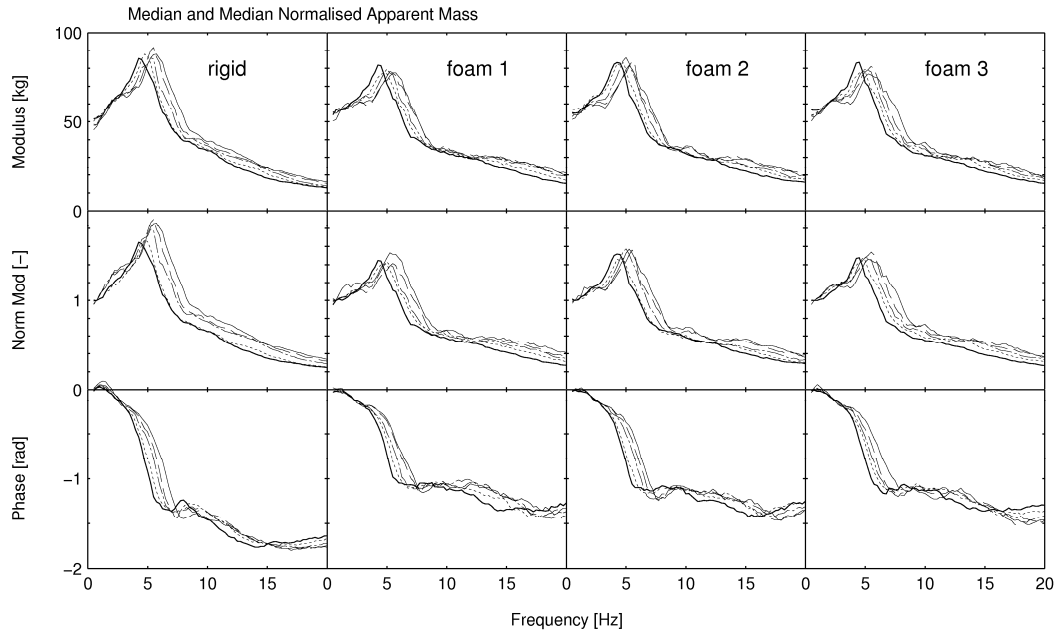

Figure 3.2: Effect of acceleration magnitude on apparent mass, normalised apparent mass and phase of the apparent mass (medians of 15 subjects): — 0.25, – – 0.4, –·– 0.63, ····1, — 1.6 ms^{-2} r.m.s.

With all four seating conditions there was a significant overall effect of vibration magnitude on the apparent mass resonance frequency (Friedman two ways analysis of variance (Siegel, 1988), $p < 0.05$). The frequency of the main resonance decreased with each incremental increase in the vibration magnitude (Wilcoxon matched pairs signed rank test (Siegel, 1988), $p < 0.05$), except for foam 3 from 0.25 to 0.4 ms^{-2} r.m.s., consistent with a softening system. There was no significant effect of vibration magnitude on the modulus of the apparent mass at resonance (Friedman, $p > 0.05$). Increases in vibration magnitude decreased the apparent mass at 20 Hz (Wilcoxon, $p < 0.05$), except

for foam 1 (from 0.25 to 0.4 ms^{-2} r.m.s.), foam 2 (from 0.25 to 0.4 ms^{-2} r.m.s.), and foam 3 (from 0.25 to 0.4 ms^{-2} r.m.s., and from 0.4 to 0.63 ms^{-2} r.m.s.).

The effects of seating condition on the median apparent mass, median normalised apparent mass, and median phase over the 15 subjects are shown for each magnitude of vibration in Figure 3.3. Although the footrest height was the same for each seating condition, the quasi-static mass (i.e. the apparent mass at 0.625 Hz) was slightly less (by about 4 kg) when sitting on the rigid seat than when sitting on any of the foams. There were no significant differences in the resonance frequencies of the apparent mass between the four seats at any vibration magnitude (Friedman, $p > 0.05$). However, at all five vibration magnitudes, the apparent mass at resonance was about 9 kg greater on the rigid seat (Wilcoxon, $p < 0.05$). It may be seen that the phase lag was greater for the rigid seat at frequencies from 5 to 20 Hz. Comparing Figures 3.2 and 3.3, it can be seen that subject apparent mass was more influenced by changes in vibration magnitude than changes in seating condition (i.e. sitting on a rigid seat or sitting on a block of foam).

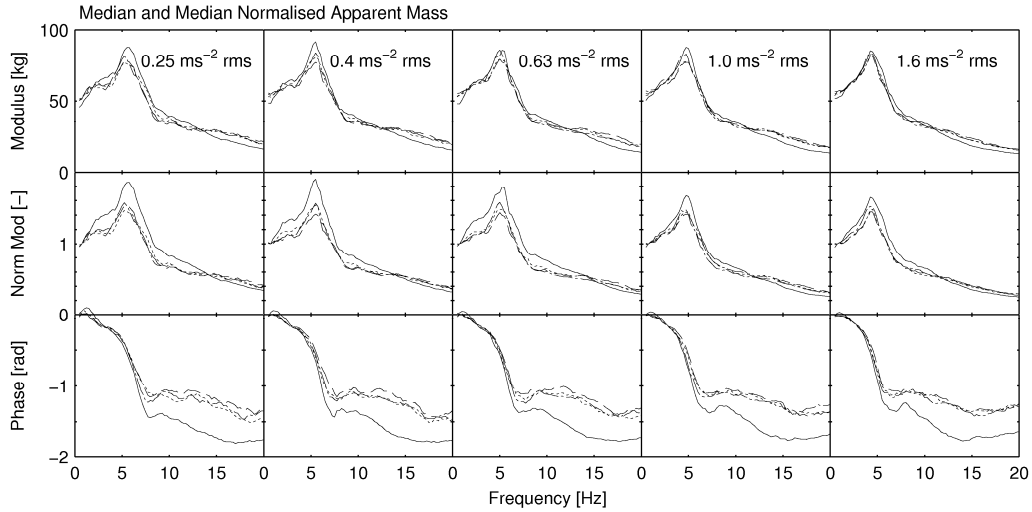

Figure 3.3: Effect of seating condition on subject apparent mass at each vibration magnitude (medians of 15 subjects): — rigid seat; – – foam 1; –·– foam 2; ····· foam 3.

At 20 Hz, the normalised apparent mass at all vibration magnitudes was significantly less on the rigid seat than on the foam (Wilcoxon, $p < 0.01$)

3.2 Dynamic Stiffness – Effect of Magnitude

The measured dynamic stiffness, $S(f)$, seemed to be well represented by the model using the four parameters in Equation (2) (Figure 3.4). The coefficient of determination R^2 of the linear regression had a mean of 0.924 (range 0.736 to 0.988).

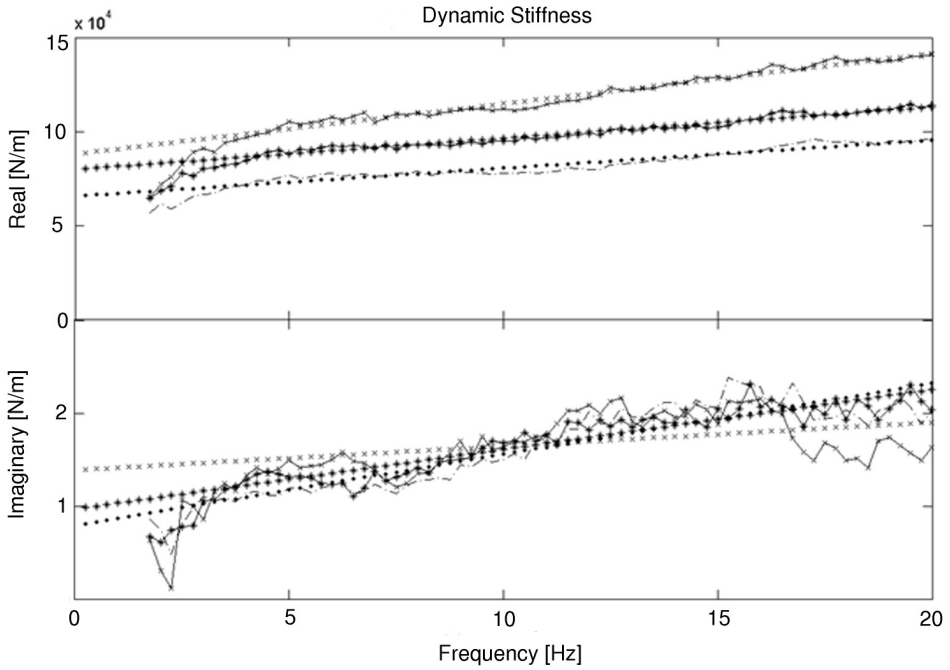

Figure 3.4 Example of dynamic stiffness curve fitting (subject 1, 0.63 ms^{-2} r.m.s., foam 1 measured data, foam 2 measured data, foam 3 measured data, foam 1 fitted, foam 2 fitted, foam 3 fitted).

There were significant effects of vibration magnitude on the stiffness parameters *k* and *k'* (Friedman, $p < 0.05$). As the vibration magnitude increased, the dynamic stiffness of each of the three foams showed significant overall trends for a decrease ($p < 0.05$, Wilcoxon) in stiffness, *k*, and the stiffness frequency-dependence stiffness, *ωk*' (Figure 3.5). However, some increases in the magnitude of vibration did not produce statistically significant changes in dynamic stiffness, *k* (foam 1: 0.25 to 0.4, and 0.4 to 0.63 ms^{-2} r.m.s.; foam 2: 0.25 to 0.4, and 0.4 to 0.63 ms^{-2} r.m.s.; foam 3: 0.25 to 0.4, 0.25 to 0.4 and 0.4 to 0.63, and 0.63 to 1.0 ms^{-2} r.m.s.; $p > 0.05$, Wilcoxon) or *k'* (foam 1: 0.4 to 0.63 ms^{-2} r.m.s.; foam 2: 0.25 to 0.4 and 0.4 to 0.63 ms^{-2} r.m.s.; foam 3: 0.4 to 0.63 ms^{-2} r.m.s.; $p > 0.05$, Wilcoxon). The magnitude of the vibration had no effect on the viscous damping, *c*, ($p > 0.05$, Friedman). The hysteretic damping, *c'*, was significantly dependent on vibration magnitude for foam 3 ($p < 0.05$, Friedman), with a significantly lower value with the lowest magnitude of vibration (0.25 ms^{-2} r.m.s.) compared to the other magnitudes ($p < 0.05$, Wilcoxon).

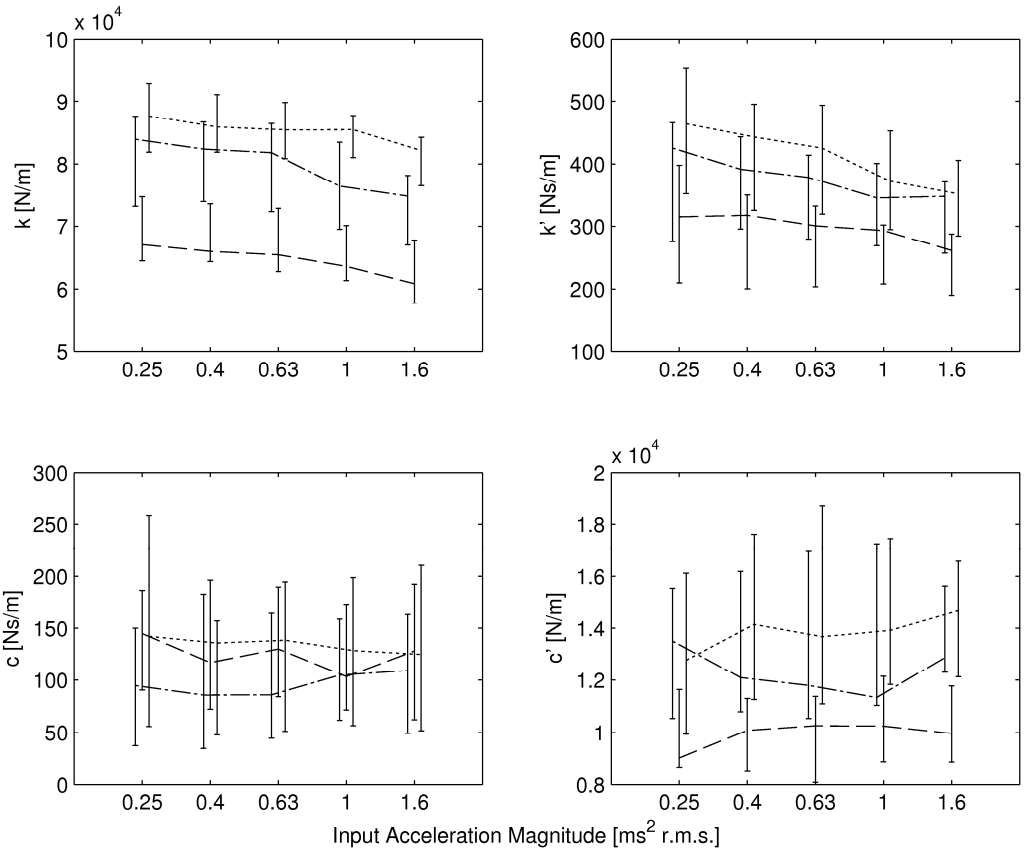

Figure 3.5 Effect of vibration magnitude on foam dynamic stiffness for each of the three foams (medians and inter-quartile ranges for 15 subjects) (– – foam 1; –·– foam 2; ····· foam 3).

3.3 Dynamic Stiffness – Effect of subject characteristics

Associations between the foam dynamic stiffness and subject characteristics were investigated using the Spearman rank-order correlation coefficient (Siegel, 1988) at each vibration magnitude. The stiffness, *k*, of foam 2 and foam 3 generally increased with increasing sitting weight and increasing hip breadth (Table 3a). The frequency-dependent stiffness, *ωk'*, was insensitive to subject weight and hip-breadth ($p > 0.05$). The damping, *c*, generally increased with increasing hip breadth and increasing subject weight with all three foams (Table 3b). The hysteretic damping, *c'*, was independent of both subject weight ($p > 0.05$) and hip breadth ($p > 0.05$).

Table 3 Correlations involving foam stiffness, *k*, and foam damping, *c*.

a) Spearman correlations between stiffness, *k*, and subject weight and hip breadth

	Vibration magnitude (ms^{-2} r.m.s.)	foam 1	foam 2	foam 3
Weight	0.25	ns	ns	**
	0.4	ns	*	**
	0.63	ns	*	**
	1.0	ns	*	**
	1.6	ns	*	**
Hip breadth	0.25	*	**	**
	0.4	ns	**	**
	0.63	ns	**	**
	1.0	ns	**	**
	1.6	*	**	**

b) Spearman correlation between damping, *c*, and subject weight and hip breadth

	Vibration magnitude (ms^{-2} r.m.s.)	foam 1	foam 2	foam 3
Weight	0.25	**	**	**
	0.4	**	**	**
	0.63	**	**	*
	1.0	**	**	**
	1.6	**	**	**
Hip breadth	0.25	**	ns	**
	0.4	**	ns	ns
	0.63	**	*	**
	1.0	**	**	**
	1.6	**	**	*

c) Spearman partial correlation between stiffness, *k*, and subject weight and hip breadth

	Vibration magnitude (ms^{-2} r.m.s.)	foam 1	foam 2	foam 3
Weight controlling hip breadth	0.25	ns	ns	ns
	0.4	ns	*	ns
	0.63	ns	*	ns
	1.0	ns	*	ns
	1.6	ns	ns	ns
Hip breadth controlling weight	0.25	*	**	ns
	0.4	ns	**	ns
	0.63	*	**	*
	1.0	ns	**	ns
	1.6	*	**	ns

d) Spearman partial correlation between damping, *c*, and subject weight and hip breadth

	Vibration magnitude (ms^{-2} r.m.s.)	foam 1	foam 2	foam 3
Weight controlling hip breadth	0.25	*	ns	*
	0.4	ns	ns	ns
	0.63	**	ns	ns
	1.0	*	*	ns
	1.6	ns	*	ns
Hip breadth controlling weight	0.25	ns	ns	ns
	0.4	ns	ns	ns
	0.63	ns	ns	ns
	1.0	ns	ns	ns
	1.6	ns	ns	ns

ns = not significant, $p > 0.05$; * = significant, $p < 0.05$; ** = significant, $p < 0.01$.
Note: All the correlation coefficients are positive.

The weights and hip breadths of subjects were highly correlated ($r = 0.859$, $p < 0.001$), so Spearman partial correlation analysis (i.e. Pearson partial correlation on ranked data) was used to identify which of these parameters was influencing the stiffness and damping of the foam. For foam 1 and foam 2, the stiffness, k, was generally correlated with hip breadth when controlling for the effect of weight ($p < 0.05$, Table 3c). Only for foam 2, the stiffness, k, was correlated with subject weight after controlling hip breadth ($p < 0.05$, Table 3c). When controlling for weight none of the foams showed a significant correlation between damping, c, and hip breadth ($p > 0.05$, Table 3d). When controlling for hip breadth, the damping, c, showed correlation with weight in some conditions (Table 3d).

3.4 Seat transmissibility

With increasing magnitude of vibration, there were significant reductions in the resonance frequency of the transmissibility of all three foams ($p < 0.05$, Wilcoxon; Figure 3.6). Similarly, the modulus of the transmissibility at resonance decreased with increasing magnitude of vibration ($p < 0.05$, Wilcoxon).

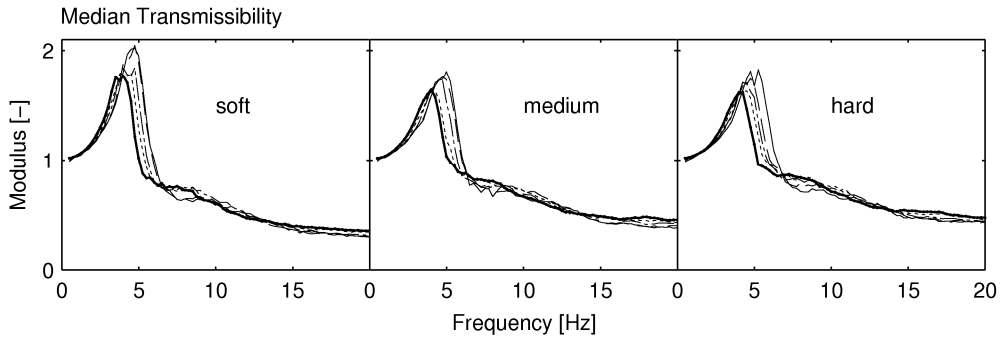

Figure 3.6 Effect of acceleration magnitude on foam transmissibility (medians of 15 subjects): — 0.25, – – 0.4, –·– 0.63, ·····1, — 1.6 ms^{-2} r.m.s.

For the three foams, Figures 3.7, 3.8, and 3.9 show the inter-subject variability in the measured apparent mass, measured dynamic stiffness, measured foam transmissibility and predicted foam transmissibility, for the intermediate vibration magnitude (0.63 ms^{-2} r.m.s.).

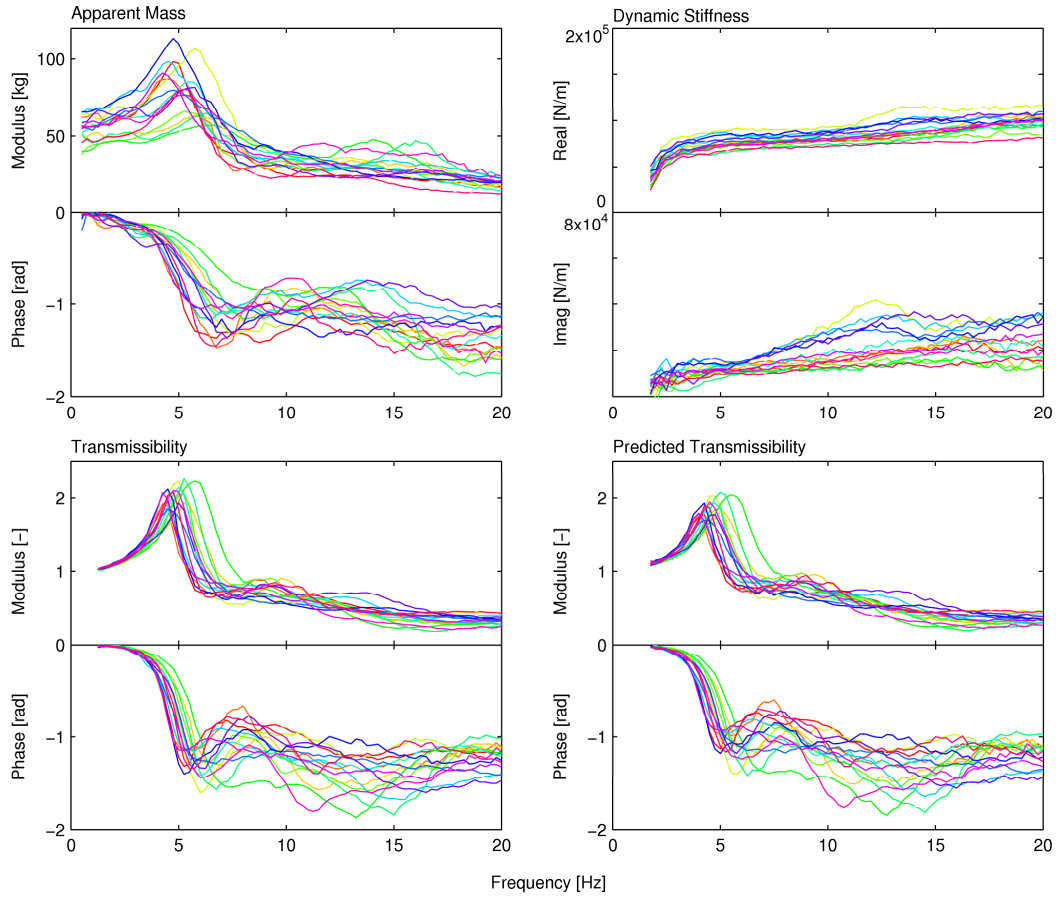

Figure 3.7: Inter-subject variability in subject apparent mass and foam transmissibility (foam 1, 0.63 ms^{-2} r.m.s.).

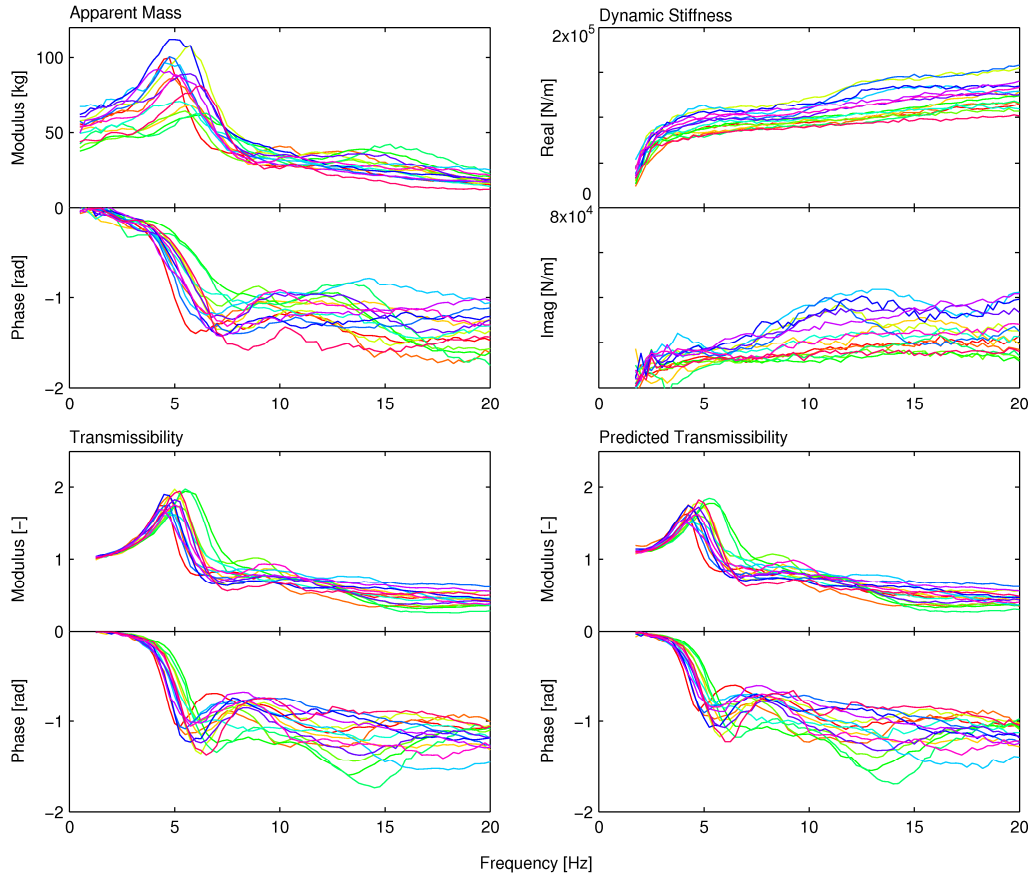

Figure 3.8 Inter-subject variability in subject apparent mass and foam dynamic stiffness (foam 2, 0.63 ms^{-2} r.m.s.)

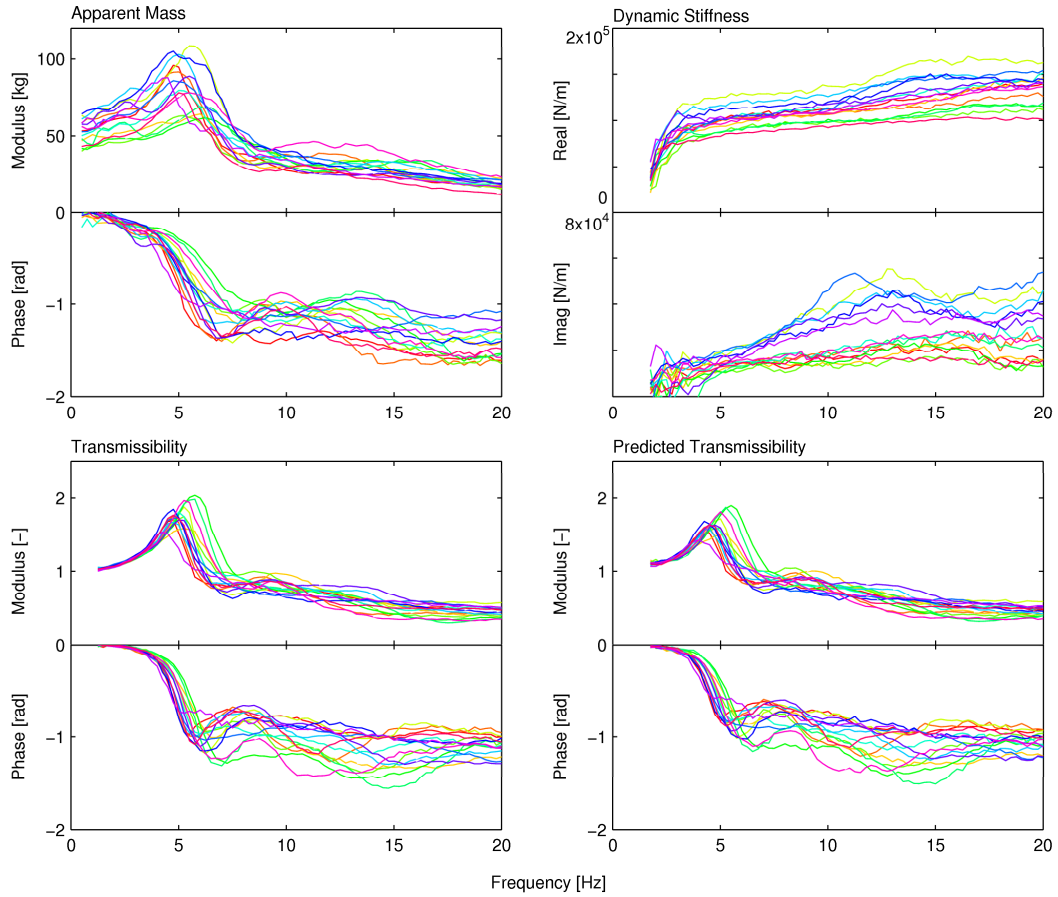

Figure 3.9 Inter-subject variability in subject apparent mass and foam dynamic stiffness (foam 3, 0.63 ms^{-2} r.m.s.).

As described in Section 2.4, the transmissibility resonance frequencies and the transmissibility moduli at resonance were calculated at each of the five vibration magnitudes when either: (i) substituting the five apparent masses with a fixed foam dynamic stiffness, or (ii) substituting the five foam dynamic stiffnesses with a fixed apparent mass. In each case (i.e. 15 subjects, 3 foams, and 5 reference vibration magnitudes), the maximum changes in the resonance frequency and in modulus at resonance when substituting the apparent mass at each magnitude were greater than those obtained by substituting the seat dynamic stiffness at each magnitude (Tables 4 and 5). So the nonlinearity in the seat transmissibility (i.e. reduction in seat resonance frequency and reduction in transmissibility modulus at the resonance frequency) due to the nonlinearity in the apparent mass was greater than that due to the nonlinearity in the foam (Wilcoxon, $p < 0.001$). An example is illustrated in Figure 3.10.

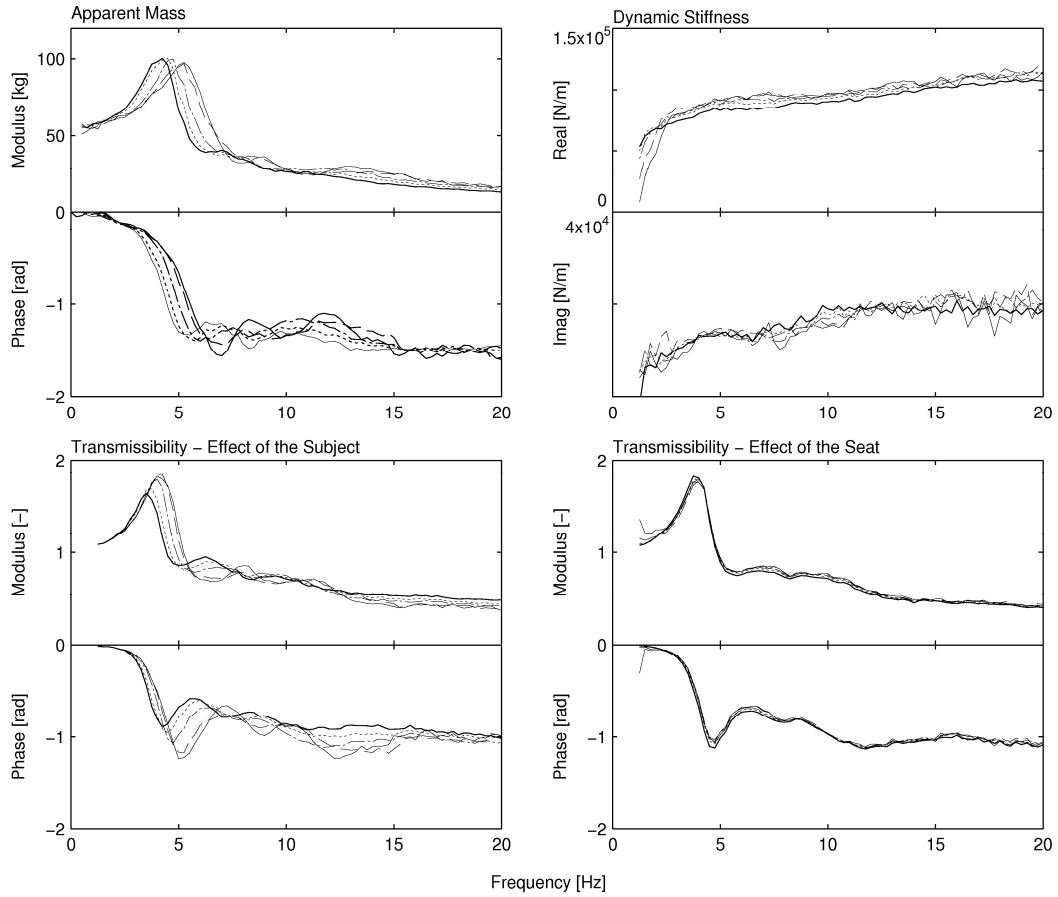

Figure 3.10 Example of the relative effects on seat transmissibility of non-linearity in subject apparent mass and non-linearity in foam dynamic stiffness (Subject 1, Foam 2, 0.63 ms^{-2} r.m.s. reference magnitude, ── 0.25, – –0.4, –·– 0.63, ····· 1.0, — 1.6 ms^{-2} r.m.s.).

The associations between foam transmissibility and both body weight and hip breadth were investigated using the non-parametric Spearman correlation coefficient. The resonance frequency evident in the foam transmissibility was negatively correlated with sitting weight at all magnitudes of vibration for foam 1 ($p < 0.05$), at the three highest magnitudes of vibration for foam 2 ($p < 0.05$ at 0.63, 1.0, and 1.6 ms^{-2} r.m.s.), but at only one magnitude of vibration for foam 3 ($p < 0.05$ at 0.4 ms^{-2} r.m.s.). The resonance frequency was also negatively correlated with hip breadth at three magnitudes of vibration for foam 1 ($p < 0.05$ at 0.4, 1.0, and 1.6 ms^{-2} r.m.s.), at one magnitude for foam 2 ($p < 0.05$ at 0.63 ms^{-2} r.m.s.) and at two magnitudes for foam 3 ($p < 0.05$ at 0.4 and 1.6 ms^{-2} r.m.s.). The negative correlations mean that an increase in weight or hip breadth decreased the transmissibility resonance frequency. There were no significant

correlations between the modulus of the foam transmissibility at resonance and either subject weight or hip breadth ($p > 0.05$).

Table 4 Median, maximum and minimum changes in transmissibility resonance frequency, f_r, of the fifteen subjects when substituting the foam dynamic stiffness, *S(f)*, at each vibration magnitude or when substituting the human body apparent mass, *AM(f)*, at each vibration magnitude (spectral resolution: 0.125 Hz)

	foam 1					
	effect of *S(f)* nonlinearity			effect of *AM(f)* nonlinearity		
Reference vibration magnitude (ms^{-2} r.m.s.)	Median f_r change (Hz)	Max f_r change (Hz)	Min f_r change (Hz)	Median f_r change (Hz)	Max f_r change (Hz)	Min f_r change (Hz)
0.25	0.25	0.5	0	0.75	1.125	0.5
0.4	0.125	0.375	0	0.75	1.125	0.5
0.63	0.125	0.375	0	0.75	1	0.5
1.0	0.125	0.375	0	0.625	1	0.375
1.6	0.125	0.25	0	0.625	0.875	0.375
	foam 2					
	effect of *S(f)* nonlinearity			effect of *AM(f)* nonlinearity		
Reference vibration magnitude (ms^{-2} r.m.s.)	Median f_r change (Hz)	Max f_r change (Hz)	Min f_r change (Hz)	Median f_r change (Hz)	Max f_r change (Hz)	Min f_r change (Hz)
0.25	0.125	0.5	0	0.875	1.25	0.625
0.4	0.125	0.375	0	0.875	1.125	0.625
0.63	0.125	0.5	0	0.875	1.125	0.625
1.0	0.125	0.375	0	0.75	1.125	0.5
1.6	0.125	0.375	0	0.875	1	0.625
	foam 3					
	effect of *S(f)* nonlinearity			effect of *AM(f)* nonlinearity		
Reference vibration magnitude (ms^{-2} r.m.s.)	Median f_r change (Hz)	Max f_r change (Hz)	Min f_r change (Hz)	Median f_r change (Hz)	Max f_r change (Hz)	Min f_r change (Hz)
0.25	0.125	0.375	0	0.75	1.125	0.625
0.4	0.125	0.5	0	0.75	1	0.5
0.63	0.25	0.625	0	0.875	1.125	0.625
1.0	0.25	0.5	0	0.75	1	0.5
1.6	0.125	0.375	0	0.75	1	0.625

Table 5 Median, maximum and minimum changes in transmissibility modulus at resonance, $H(f_r)$, of the fifteen subjects when substituting the foam dynamic stiffness, $S(f)$, at each vibration magnitude or when substituting the human body apparent mass, $AM(f)$, at each vibration magnitude (spectral resolution: 0.125 Hz)

	foam 1					
	effect of $S(f)$ nonlinearity			effect of $AM(f)$ nonlinearity		
Reference vibration magnitude (ms^{-2} r.m.s.)	Median $H(f_r)$ change (-)	Max $H(f_r)$ change (-)	Min $H(f_r)$ change (-)	Median $H(f_r)$ change (-)	Max $H(f_r)$ change (-)	Min $H(f_r)$ change (-)
0.25	0.15	0.32	0,04	0.41	0.77	0.12
0.4	0.12	0.23	0.02	0.42	0.94	0.21
0.63	0.12	0.30	0.03	0.44	0.84	0.12
1.0	0.14	0.27	0.04	0.43	0.95	0.18
1.6	0.10	0.32	0.03	0.48	0.85	0.19
	foam 2					
	effect of $S(f)$ nonlinearity			effect of $AM(f)$ nonlinearity		
Reference vibration magnitude (ms^{-2} r.m.s.)	Median $H(f_r)$ change (-)	Max $H(f_r)$ change (-)	Min $H(f_r)$ change (-)	Median $H(f_r)$ change (-)	Max $H(f_r)$ change (-)	Min $H(f_r)$ change (-)
0.25	0.11	0.33	0.03	0.35	0.75	0.12
0.4	0.11	0.30	0.04	0.35	0.60	0.21
0.63	0.12	0.22	0.04	0.36	0.61	0.14
1.0	0.13	0.20	0.04	0.36	0.63	0.07
1.6	0.10	0.18	0.07	0.40	0.71	0.14
	foam 3					
	effect of $S(f)$ nonlinearity			effect of $AM(f)$ nonlinearity		
Reference vibration magnitude (ms^{-2} r.m.s.)	Median $H(f_r)$ change (-)	Max $H(f_r)$ change (-)	Min $H(f_r)$ change (-)	Median $H(f_r)$ change (-)	Max $H(f_r)$ change (-)	Min $H(f_r)$ change (-)
0.25	0.08	0.20	0.04	0.31	0.58	0.13
0.4	0.09	0.17	0.01	0.36	0.55	0.20
0.63	0.06	0.14	0.03	0.31	0.53	0.16
1.0	0.10	0.15	0.02	0.36	0.57	0.16
1.6	0.09	0.22	0.03	0.34	0.48	0.18

3.5 Coherence functions

As shown in Figure 3.11, ordinary coherence functions were greater than 0.75 for each computed transfer function.

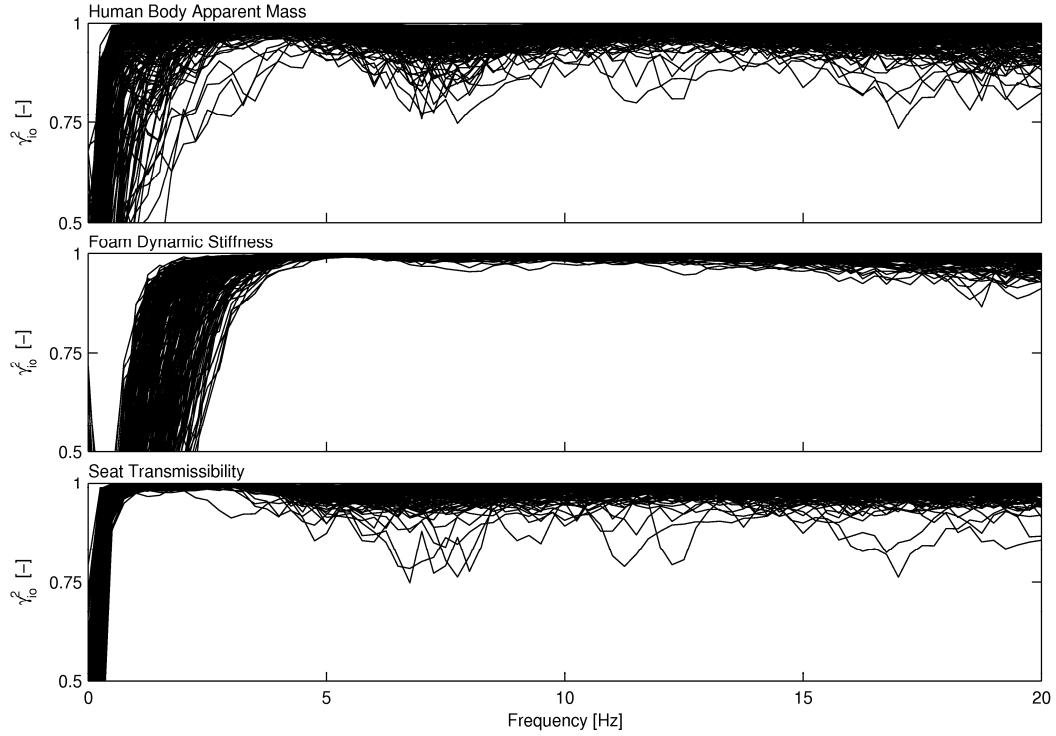

Figure 3.11: Coherence functions for all the calculated transfer functions: human body apparent mass, foam dynamic stiffness, and seat transmissibility.

4. Experiment 1 - Discussion

4.1 Apparent Mass – Rigid and soft seat

The apparent masses of subjects measured on the rigid seat have similar shapes to those reported in previous studies (e.g. Fairley and Griffin, 1989). With increasing magnitude of vibration, previous studies have reported similar reductions in the apparent mass resonance frequency (e.g. Mansfield and Griffin, 2000). The absence of an effect of vibration magnitude on the apparent mass at resonance is consistent with some previous measurements (e.g. Mansfield and Griffin, 2002; Mansfield *et al.*, 2006), but not others (e.g. Mansfield and Griffin, 2000; Hinz *et al.*, 2006).

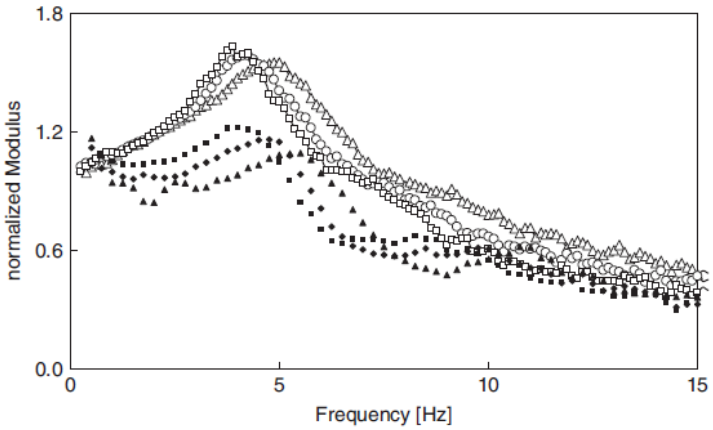

Fig. 9. Normalized mean moduli of the apparent masses calculated by the forces and accelerations measured at rigid seat (AMR): △ during the vibration magnitude I1, ◇ during the vibration magnitude I2, □ during vibration magnitude I3, and calculated by the forces and accelerations at the seat cushion (AMS): ▲ during the vibration magnitude E1, ♦ during the vibration magnitude E2, ■ during the vibration magnitude E3.

Figure 4.1: normalized mean apparent masses moduli on hard and soft seats with varying vibration magnitude (Hinz *et al.*, 2006)

A device for measuring pressure distributions has been used to estimate apparent mass on a soft seat (Hinz *et al.*, 2006). Consistent with the present study, two peaks in the modulus of the apparent mass were found, with the same dependence of the resonance frequency of the first peak with respect to vibration magnitude. There was a similar resonance frequency when measuring apparent mass on a rigid and soft seat, but the modulus of the apparent mass on the rigid seat was remarkably greater than on the soft seat. Although the contact conditions different between the seats (e.g. there was a backrest on the soft seat) and the vibration spectra reaching the subjects will have differed between seats, it is doubtful whether these factors can sufficiently explain why subject apparent mass showed a large difference between the soft and rigid seats, unlike the present study.

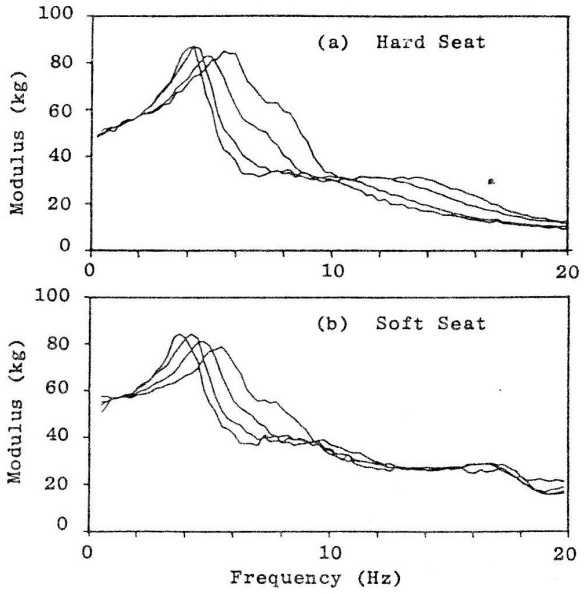

Figure 10: Effect of vibration magnitude on the apparent mass of a person, measured on (a) a hard seat and (b) a soft seat.

Figure 4.2: effect of vibration magnitude on apparent mass on a hard and soft seat (Fairley and Griffin, 1986)

Fairley and Griffin (1986) estimated the apparent mass of the body sitting on a soft seat using a method similar to the present study, but with a conventional car seat without a backrest and a flat broadband spectrum on the surface of the soft seat. Similarly to the present study, a SIT-bar was used to place the accelerometer at the seat-human interface. Although no statistical tests were reported, the apparent masses on the soft and rigid seats were very similar, except at high frequencies (12.25 to 18.25 Hz), consistent with the present findings. The effect of vibration magnitude on apparent mass when sitting on the soft seat was investigated with one subject and showed a reduction in apparent mass resonance frequency with increasing magnitude of vibration, consistent with the present research. Apart from these studies, there are no known previous reports of the apparent mass of the human body sitting on a soft seat.

In the present study, the human body was subjected to a different spectrum of vibration when sitting on the foam than when sitting on the rigid seat: the effect of the foam transmissibility was to amplify low frequency vibration and attenuate high frequency vibration giving an overall reduction in the r.m.s. acceleration magnitude to about 74%. It is evident in Figure 3.3 that the apparent mass of the body sitting on the three foams was very similar, although not identical, to the apparent mass when sitting on the rigid seat.

The resonance frequency did not differ significantly, but the modulus of the apparent mass at resonance was slightly increased and the apparent mass at 20 Hz was slightly reduced on the rigid seat. The phase lag was also reduced on the rigid seat over the 5 to 20 Hz range.

If the human body is represented as a single degree-of-freedom lumped parameter model with one or two masses as fitted by Fairley and Griffin (1989) or Wei and Griffin (1998b), the changes in body apparent mass from the foam to the rigid seat are represented by a decrease in the internal damping of the body. The reduction might be partially due to differences in the contact area and pressure distribution: tissues around the ischial tuberosities are more compressed when sitting on a flat rigid seat because the weight of the body is supported on a smaller contact area than when sitting on foam (Hinz, 2006; Wu, 1999: Figure 1.9). Although the subjects were sitting on a SIT-bar, the compliance of the foam resulted in a greater contact area when sitting on the soft seat and a more uniform pressure distribution. There is some evidence that increased contact area (obtained by sitting on a 'bead cushion') may slightly increase body internal damping whereas increased contact area may tend to decrease the apparent mass resonance frequency (at 1.0 and 2.0 ms^{-2} r.m.s. in Mansfield and Griffin, 2002). The decrease in the apparent mass at 20 Hz associated with no significant change in the apparent mass at resonance suggests the increase in vibration magnitude decreased the internal damping of the body.

The overall decrease in the vibration magnitude on the soft seat (by around 25%) might be expected to increase the resonance frequency due to the non-linearity in the body apparent mass, so offsetting any decrease associated with the different contact conditions between rigid and soft seat. However, the overall reduction in vibration magnitude was due to attenuation of high frequencies, and the foam amplified the low frequencies that may have a greater influence on the nonlinearity in the apparent mass (Mansfield *et al*., 2006).

4.2 Dynamic Stiffness – Effect of Magnitude

The use of a four parameter model to describe the response of the foam, based on the observation of the frequency response functions, resulted in better curve fitting than the $S(f) = k + i2\pi fc$ or $S(f) = k(1 + id)$ models (Wei and Griffin, 1998; Fairley and Griffin, 1986), and assisted the interpretation of the data. In this study, the dynamic stiffness was similar to that reported by Lewis and Griffin (2000), showing a dependence on frequency, unlike the conventional seat ('foam supported on wire springing') with cover response reported by Fairley and Griffin (1986). As suggested by Hilyard (1994) and Patten and Pang (1998), polyurethane foams have a nonlinear softening behaviour. Present research

findings show that nonlinearity affects not only *k*, but also the stiffness rate of increase with frequency, *k'*. In the conditions of the present study, with relatively low magnitude vibration and a spectral content influenced by the human body impedance and not a rigid mass (e.g. Patten and Pang, 1998; Patten *et al.*, 1998), which is likely to enhance the influence of seat nonlinearities as greater seat dynamic deflection is likely than when a seat supports the human body (Griffin, 1990), the softening of the foam with increasing vibration magnitude was not dramatic. The conditions in which there was no statistically significant change in foam dynamic stiffness (foam 1: and 0.25 to 0.4 and 0.4 to 0.63 ms^{-2} r.m.s.; foam 2: 0.25 to 0.4 and 0.4 to 0.63 ms^{-2} r.m.s.; foam 3: 0.25 to 0.4, 0.4 to 0.63, and 0.63 to 1.0 ms^{-2} r.m.s) suggest that the harder the seat, the greater the change in acceleration magnitude required to trigger nonlinearity.

The energy loss parameters were not affected by the magnitude of vibration: *c'* changed with changing vibration magnitude in only one condition with one of the three foams (foam 3 at 0.25 ms^{-2} r.m.s).

4.3 Dynamic Stiffness – Effect of Subject Build

The present findings are not easily compared with either the literature on cellular polymers, that mainly present fully compressive stress-strain static curves or dynamic transmissibility curves obtained with rigid masses, or studies of seat dynamics that have used different models to fit the experimental data (e.g. Fairley and Griffin, 1986; Wei and Griffin, 1998). Deflection measures were not obtained in this study, but it is possible to consider the static force to which the foam was subjected (i.e. subject seating weight) and the dimensions of the 'indenter' (i.e. subject hip breadth). The dynamic stiffness parameter *k* had a clear dependence on hip breadth, showing that increased dimensions of the 'indenter' (and so of the foam supporting area) increased the stiffness of the foam. The significant stiffening of the foam stiffness, *k*, with increasing subject weight (for foams 2 and 3) is consistent with previous research (Hilyard, 1984; Fairley and Griffin, 1986; Wei and Griffin, 1998). However the behaviour of the softest foam (foam 1) demonstrates that stiffening may not always occur. Furthermore, the stiffness of foam 3 showed no dependence on subject weight after controlling for subject hip breadth, demonstrating that the stiffening of the foam may depend on the contact dimensions more than the supported weight. However, in this study, the range of seated weights resulted in only 240 N variation in the force applied to the foam, whereas Fairley and Griffin (1986) and Wei and Griffin (1998) varied the static indentation force applied to foam by 600 N and 500 N, respectively.

The positive correlation between viscous damping, *c*, and the static weight on the foam is consistent with results presented by Wei and Griffin (1998) (Table 1), although they used

a different dynamic model. The correlation between viscous damping, *c*, and hip breadth dropped drastically when controlling for weight, while some correlation remained between *c* and weight when controlling for hip breadth (Table 3d). This may suggest that changes in damping, *c*, are mediated by another variable.

The absence of a correlation between either subject weight or hip breadth and the hysteretic damping coefficient, *c'*, was expected, since *c'* has been reported to depend on the cellular geometry and on the viscoelastic behaviour of the base polymer (Hilyard, 1984).

4.4 Seat Vertical Transmissibility

As reported in the literature (e.g. Griffin, 1990; Fairley and Griffin, 1986), vertical seat transmissibility is nonlinear with acceleration magnitude. The prediction of the transmissibility from the apparent mass and the dynamic stiffness measured at different magnitudes gave definitive evidence that the human body contributed most to the nonlinearity, as suggested by Fairley and Griffin (1986). Although variations in the vibration magnitude resulted in variations in the seat dynamic stiffness (in some cases *k* varied by up to 30%), this had relatively little effect on seat transmissibility.

The correlations between foam transmissibility and subject weight and hip breadth are not easily interpreted. Whether the statistical tests were significant or not, the correlation coefficients were negative, indicating that increased subject weight or increased hip breadth decreased the transmissibility resonance frequency. This implies that the increase in the mass supported by the foam was not fully compensated by an increase in the stiffness of the foam (this is the case for foam 1). Non-significant statistical tests imply that increased weight or increased hip breadth was compensated by increased seat stiffness, so that transmissibility resonance frequency remained constant (this is the case for foam 2 and foam 3).

7. Literature review and Introduction to Experiment no. 2

The second experiment regards: (i) the effects of foam stiffness, acceleration magnitude and backrest on fore-and-aft transmissibility of seats; (ii) the human body fore-and-aft apparent mass on a rigid and soft seat; (iii) the linear and nonlinear effects of multi-axis acceleration on seat vertical and horizontal transmissibility; (iv) the polyurethane foam dynamic stiffness in fore-and-aft and vertical directions.

7.1 Seat horizontal transmissibility

Although most of the research regarding dynamic behaviour of seat has been focused on vertical vibration, this is not the only seat input to the body (Griffin, 1990). Horizontal vibration can be dominant in vehicles such as tractors, tanks, earth-moving machines, trains and aircrafts (Griffin, 1990; Fairley and Griffin, 1984; Mandapuram et al., 2005; Fleury and Mistrot, 2006, Smith, *multi aircraft*; Bovenzi, Pinto, Stacchini, 2002; Kumar et al., 2001, Fairley, UK group 1984).

Some data suggest that there is often a near-unity transfer of x-vibration through conventional seat squab (Griffin, 1990; Griffin, 1978).

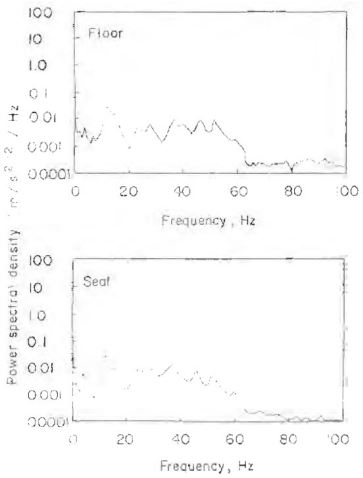

Figure 7.1: floor and seat acceleration PSD in one vehicle (Griffin, 1978)

This is one of the reasons why suspended seat are used when attenuation of horizontal vibration is required (Fleury, 2006; Bluthner, 2008; Bovenzi et al., 2002; Kumar et al., 2001). Anyway, in some cases (i.e. military aircrafts) suspended seats cannot be used (Smith, 2008) and, anyway, a foam cushion, as a part of the suspended seat, might contribute to its transmissibility (Fairley and Griffin, 1984).

Fairley and Griffin (1984) showed the transmissibility of a seat isolator and a seat squab up to 10 Hz without backrest contact. The squab transmissibility has a resonance

between 3 and 4 Hz, an anti-resonance for higher frequencies, and then increased linearly from 6.5 to 10 Hz. Fairley an Griffin (1984) addressed the poor fore-and-aft vibration insulation of conventional seats.

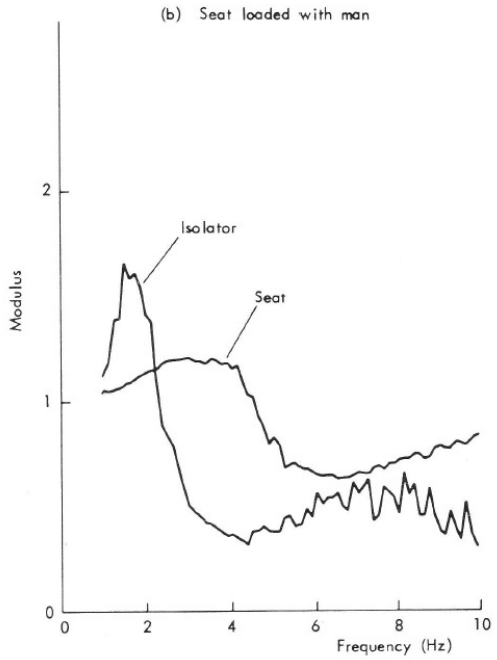

Fig 3 Transmissibilities in the x-axis of a seat isolator and of the remainder of the seat when loaded with (a) mass and (b) subject

Figure 7.2: (Fairley, 1984)

Measurements of transmissibility of a spring and foam seat in a light van riding on a road were taken by Fairley (1984). Fore-and-aft vibration had a resonance at about 2 Hz (Figure 7.3). While transmissibility showed some attenuation between 2 and 14 Hz, it increased at higher frequencies and reached unity at about 15 Hz. Transfer functions had low coherency from 1 to 10 Hz. Causes for this low coherency could have been nonlinear relationship between seat base and seat squab transmissibility or the low signal to noise ratio.

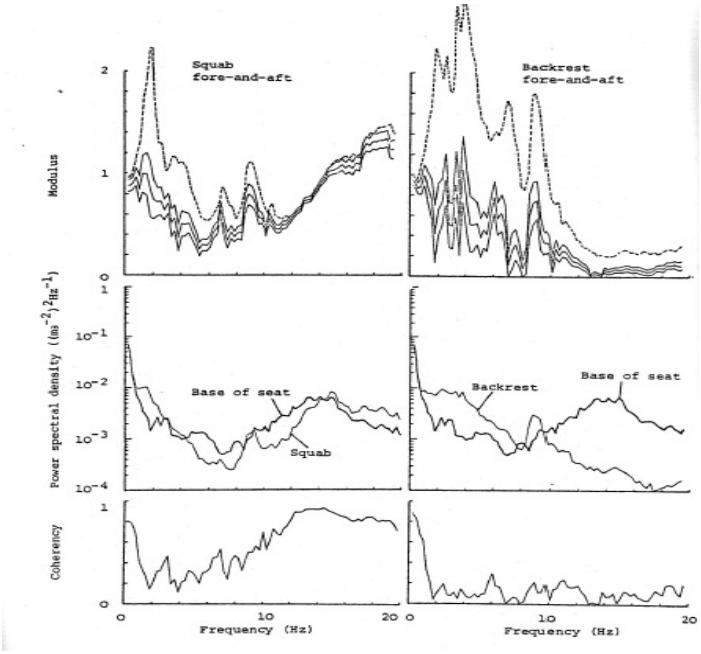

Figure 7.3: Fairley (1984)

A broader frequency range was used by Qiu and Griffin (2003). Backrest and fore-and-aft seat pan transmissibility was measured on a conventional car seat in field and laboratory tests.

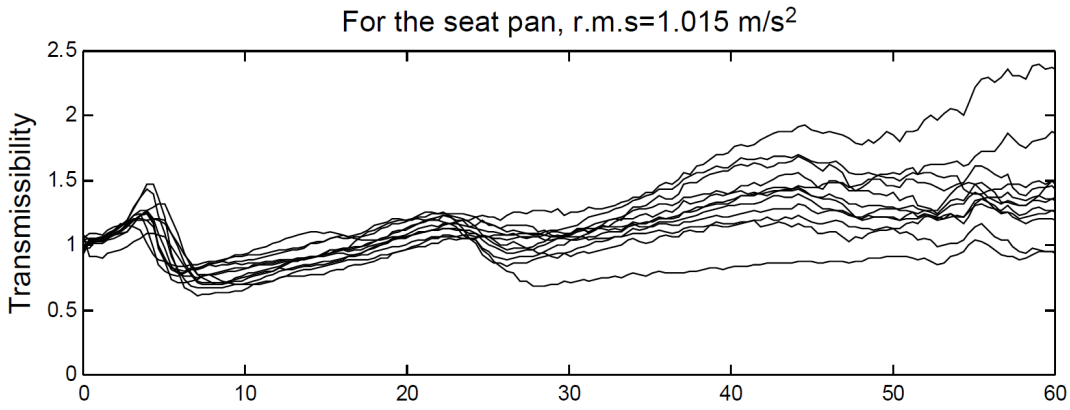

Figure 7.4: fore-and-aft seat pan transmissibility (Qiu and Griffin, 2003)

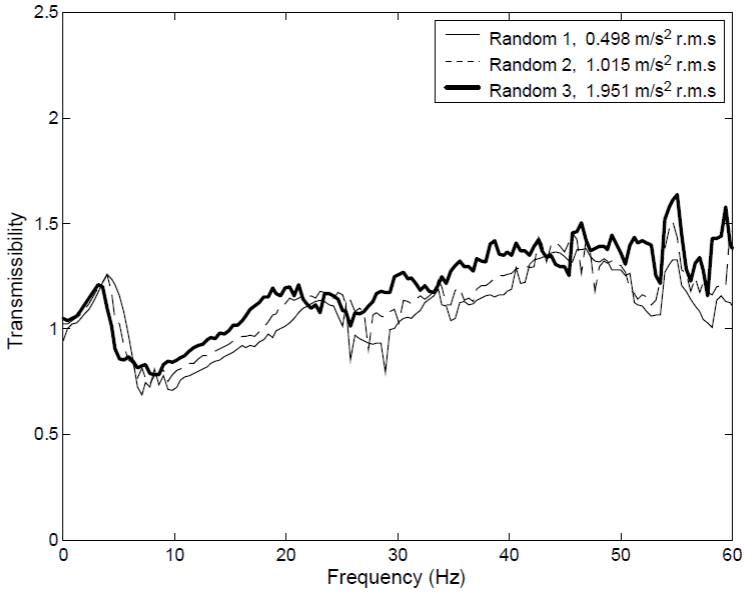

Fig. 16. Median transmissibility of the seat pan from 12 subjects and three random vibration inputs (acceleration r.m.s. values = 0.498, 1.015 and 1.951 $m\,s^{-2}$), laboratory simulation

Figure 7.5: (Qiu and Griffin, 2003)

Seat fore-and-aft transmissibility was evaluated up to 60 Hz. Seat showed a fairly stiff behaviour, with a distinct resonance peak at about 3 to 5 Hz. The first resonance was followed by an anti-resonance and another resonance at about 23 Hz. Significant effects of vibration magnitude were found. Qiu and Griffin (2003) dealt with the bias errors arising from the misalignment of the accelerometer on the seat surface respect to the one on the seat base: "the measurement of fore–aft vibration on seat cushions and backrests can be affected by the angle of inclination of the surfaces: both the seat pan and the backrest are usually inclined rearwards. This inclination means that transducers used to measure vibration at the interfaces between a subject and a seat are not truly orientated in horizontal and vertical directions. The inclination of the transducers will result in them responding to a component of the vertical vibration on the seat pan or backrest $\ddot{z}\sin\theta$, where $\ddot{z}$ is the vertical acceleration and $\ddot{\theta}$ is the angle of inclination. Even small angles (e.g., 10°) can result in significant levels of acceleration appearing in the fore-and-aft direction due to the truly vertical vibration".

Mansfield and Griffin (1996) measured seat transmissibility of a car seat in the three orthogonal directions on different roads with 12 subjects and an anthropodynamic dummy. His data show that there are peaks in fore-and-aft transmissibility at about 1 and 4 Hz.

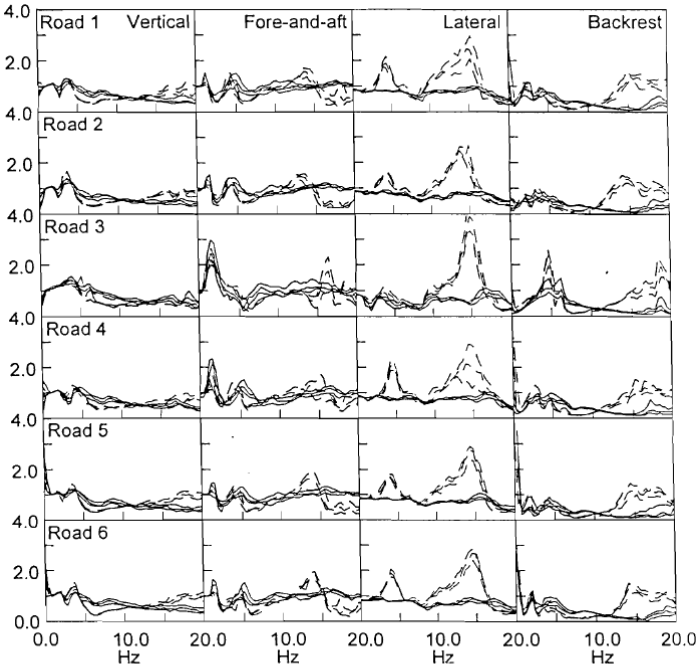

Fig. 2. Transmissibility of a car seat measured on six roads. Median and inter-quartile ranges for 12 subjects (——) and 12 anthropodynamic dummy (- - - - -) tests.

Figure 7.6: Mansfield and Griffin (1996)

Smith and Smith (2005) showed that the choice of the seat cushion can help attenuating fore-and-aft vibration transmission, especially at high frequencies.

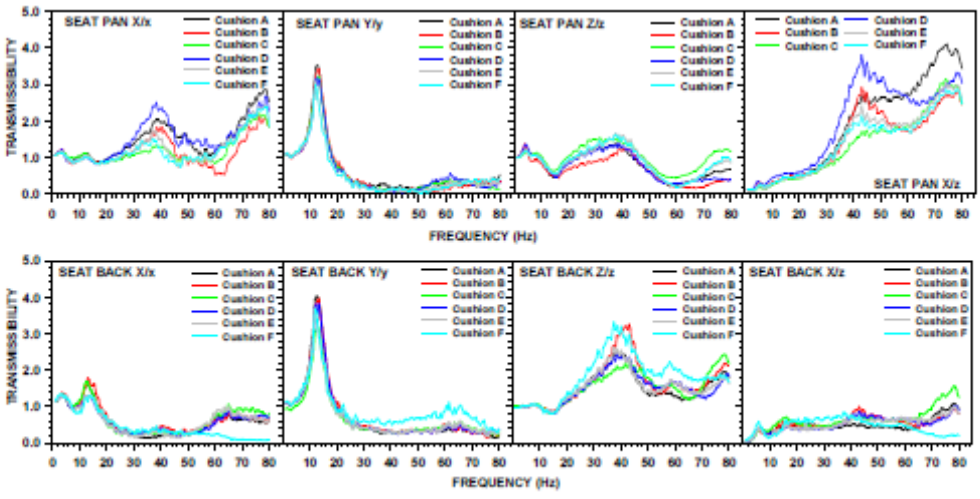

Figure 1.—Mean seat pan and seat back transmissibilities (seven subjects).

Figure 7.7: (S.D. Smith and J.A. Smith, 2005)

Smith et al. (2008) studied the multi-axis transmissibility (and so the fore-and-aft) of two locomotive seats with two vertical suspension configurations and a freight seat in the 1-10 Hz frequency range. Data show a resonance at about 2-3 Hz, then an anti-resonance that caused transmissibility dropping to 0.6 at about 4 Hz and a trend for increase up to 10 Hz.

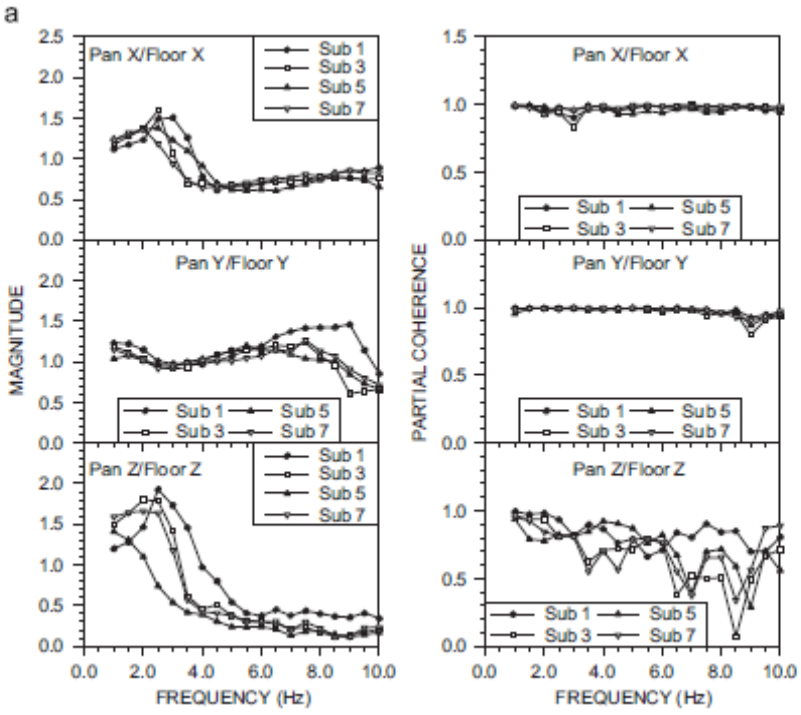

Figure 1.8: Smith et al. (2008)

It is known (Griffin, 1990; Fairley and Griffin, 1984; Fairley and Griffin, 1986) that seat transmissibility is dependent of human body apparent mass, which cannot be considered constant with frequency, and seat dynamic stiffness. Fairley and Griffin (1984) suggested that the fore-and-aft seat transmissibility can be modelled by the following equation:

$$T(\omega) = \frac{k + j\omega c}{k - \omega^2 (AM(\omega) + m) + j\omega c}$$

where *k, c* and *m* are the stiffness, damping and mass of the seat, *AM(ω)* is the apparent mass of the person.

Fore-and-aft apparent mass of a seating human is strongly dependent on the use of a backrest (e.g. Mandapuram et al., 2005; Nawayseh and Griffin, 2005; Fairley and Griffin,

1990) and so it is believed transmissibility will affected by the presence of a backrest. Literature review on the topic is in the next section of the introduction.

After reviewing the above literature (considering also the following paragraphs and the previous experiment), the following hypotheses were generated and the experiment was designed accordingly:
(i) fore-and-aft seat transmissibility is nonlinear with vibration magnitude;
(ii) fore-and-aft seat transmissibility is affected by the backrest;
(iii) fore-and-aft seat transmissibility is affected by foam dynamic stiffness;

7.2 Fore-and-aft human body apparent mass on hard and soft seat

Many researches studied human body apparent mass on rigid seat, with and without backrest (Fairley and Griffin, 1990; Mansfield and Lündstrom, 1999; Nawayseh and Griffin, 2005; Mandapuram et al., 2005; Hinz et al., 2006; Fleury and Mistrot, 2006; Stein et al., 2007).

Fairley and Griffin (1990) measured the fore-and-aft apparent mass of 8 subjects with and without backrest contact. The backrest was rigidly attached to the force plate, so that horizontal forces at the back were added to those at the seat. Two heavily damped modes were found in the 'backrest OFF' condition: one at about 0.7 Hz and the second in the region of 2.5 Hz. The apparent mass second resonance frequency decreased of 1-2 Hz when increasing the magnitude of vibration from 0.5 to 1.0 ms^{-2} r.m.s. The first mode of vibration appeared to arise from a motion of the entire whole body that rocked backwards and forwards. The second mode presumably arose from the response of the musculo-skeletal structure of the body. One resonance, at about 3.5 Hz, was found when the subjects were leaning against the backrest. With the backrest contact, the modulus of the apparent mass increased at all frequencies above 0.8 Hz. The mode of vibration observed with the backrest was probably associated with the second mode, with the backrest providing a stiffening of the upper body and therefore increasing the resonance frequency. Fairley and Griffin (1990) noticed that "subjects, involuntarily or otherwise, were using muscle control in the lower back to restrain the rocking or swaying of the upper body when there was no backrest". This was particularly so with the highest vibration magnitude. This could explain the absence of softening effect on the first peak of resonance. The effects on the second mode of resonance are the same observed on vertical vibration: higher magnitude of vibration reduced the apparent stiffness of the human body.

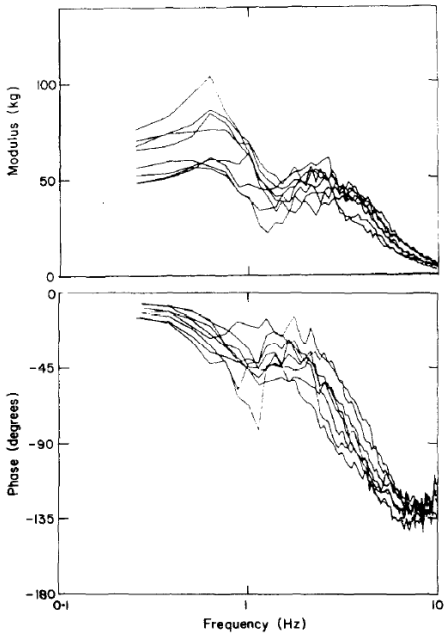

Figure 1. Fore-and-aft apparent masses of eight people; without backrest.

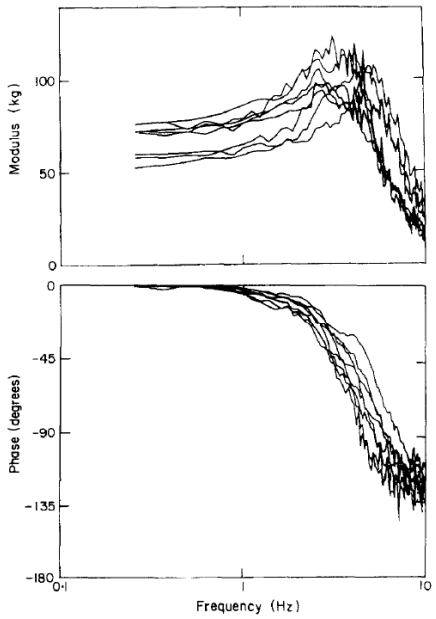

Figure 2. Fore-and-aft apparent masses of eight people; with backrest.

Figure 7.9: (Fairley and Griffin, 1990)

Mansfield and Lundström (1999) measured subjects apparent mass in the frequency range of 1.5 to 20 Hz, at the magnitudes of 0.25, 0.5 and 1.0 m s^{-2} r.m.s. in a comfortable upright posture with arms folded and with a knee angle of 90°. The data indicate two peaks in apparent mass with excitation magnitude of 0.25 ms^{-2} r.m.s. The first peak in the apparent mass occurred at 2-3 Hz and the second at 5-6 Hz. The second peak was more pronounced for female subjects. It has to be noticed that, due to the frequency range of their vibrator, they could not identify the first peak of resonance reported in (Fairley and Griffin, 1990). Both apparent mass peaks decreased in frequency, with the magnitude of the first peak increasing with the vibration magnitude. Conversely, the apparent mass from 4 to 10 Hz, which encompassed the second peak, reduced with increasing vibration magnitude. The first peak increased and the second peak decreased in magnitude with increases in acceleration. The change in the magnitude of the second peak explains why fewer subjects showed a clear resonance at about 5 Hz for the higher magnitudes of motion. As the peak in the apparent mass decreased with increased stimulus magnitude, the response at 5 Hz was dictated by the 2.5 Hz mode.

Nawayseh and Griffin (2003) studied the fore-and-aft apparent mass curves of 12 subjects without backrest contact in the frequency range 0.25 to 20 Hz with four levels of

vibration magnitude and different footrest heights. Three vibration modes were found in the 0-10 Hz range. Considerable vertical forces were found on the seat during fore-and-aft vibration (Figures 7.15 and 7.15).

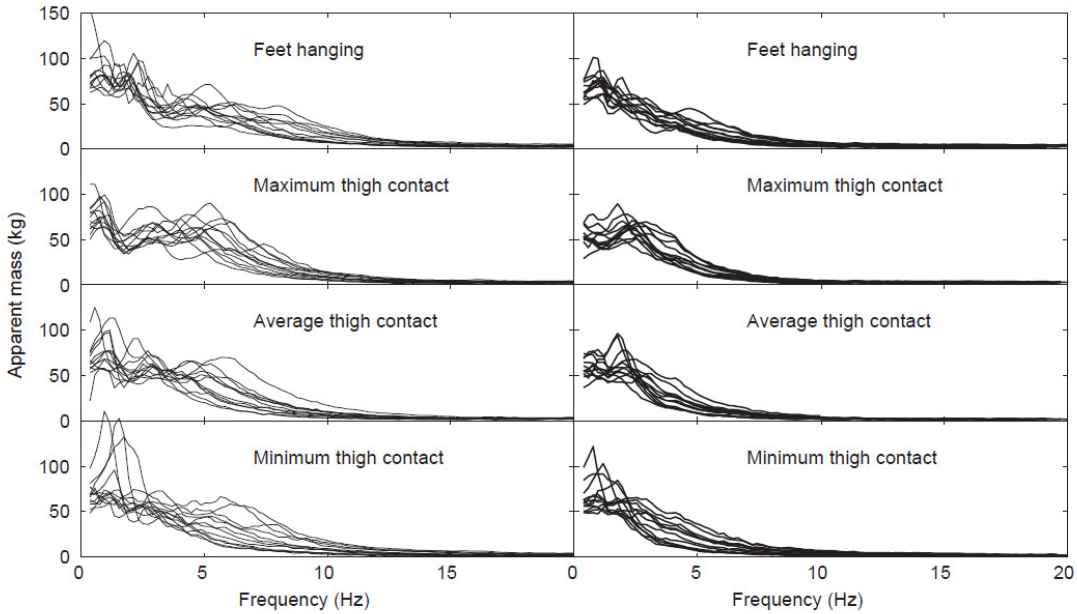

Fig. 2. Inter-subject variability in the fore-and-aft apparent mass at the seat for each posture at two vibration magnitudes. —, 0.125 m s^{-2} rms; —, 1.25 m s^{-2} rms.

Figure 7.10: (Nawayseh and Griffin, 2003)

Mandapuram et al. (2005) measured the fore-and-aft apparent mass of eight subjects in three conditions: (i) upright posture without a backrest; (ii) with a vertical backrest; (iii) with a backrest inclined of 12.5 degrees, in the frequency range 0.5 to 10 Hz. Three different postures, three different seat height and three different vibration magnitudes were used. The authors found strong effects of vibration magnitude, due to nonlinear behaviour of the seated body but also due to excessive upper body movements under higher excitations and to shifting tendencies to realize more stable posture and contribution of the legs. The authors found that the second and third peaks of resonance were more evident under low magnitude vibration. They also found a significant effect of a backrest. The effect of backrest support on fore-and-aft response is far more significant than the one in vertical biodynamics, giving a stiffening of the body.

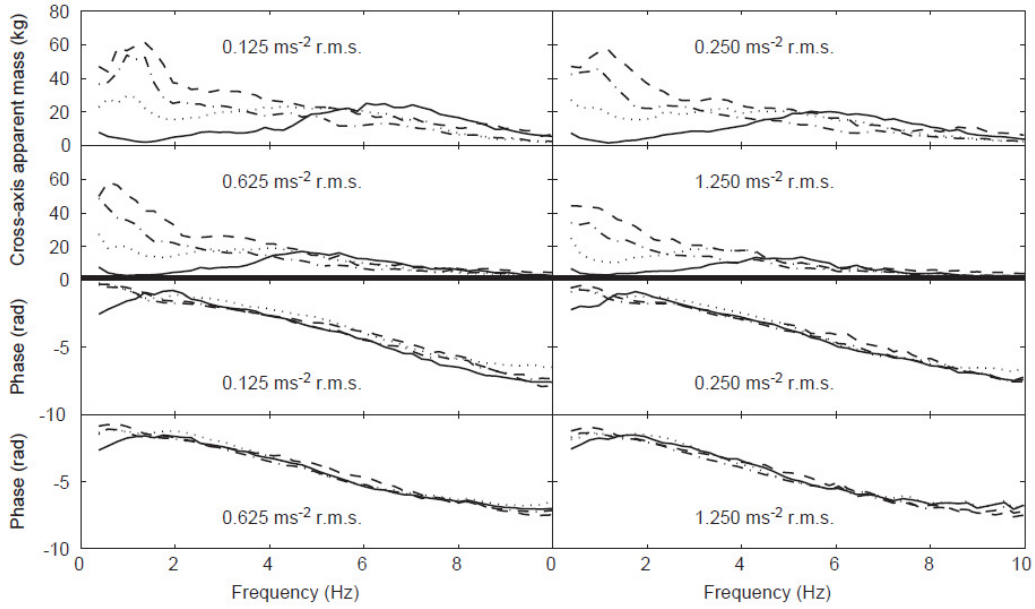

Fig. 6. Median vertical cross-axis apparent mass and phase angle of 12 subjects at the seat: effect of posture. —, feet hanging; ……, maximum thigh contact; –·–·–·–, average thigh contact; – – – –, minimum thigh contact.

Figure 7.11: (Nawayseh and Griffin, 2003)

There have been very few attempts of measuring the human body vertical (Hinz, 2006; Fairley and Griffin, 1986) and fore-and-aft (Stein et al., 2007; Fleury and Mistrot, 2006) apparent mass on a soft seat. Studies regarding vertical apparent mass on soft seat have been reviewed in paragraph no.1.

Stein et al. (2007) measured the apparent mass of the human-seat system by fitting a seat on a force plate and measuring forces and accelerations at the force plate. Results were dependent on the seat apparent mass of the seat and therefore not generally applicable.

Fleury and Mistrot (2006) measured the apparent mass on soft cushion by measuring the forces under the seat and the accelerations at the seat-human interface and then subtracting the seat apparent mass. The authors (2006) fitted the apparent mass data with a model having a translational and a rotational degree of freedom describing the rocking motion of the upper body. The model could take into account postural changes such as leaning against the seat backrest.

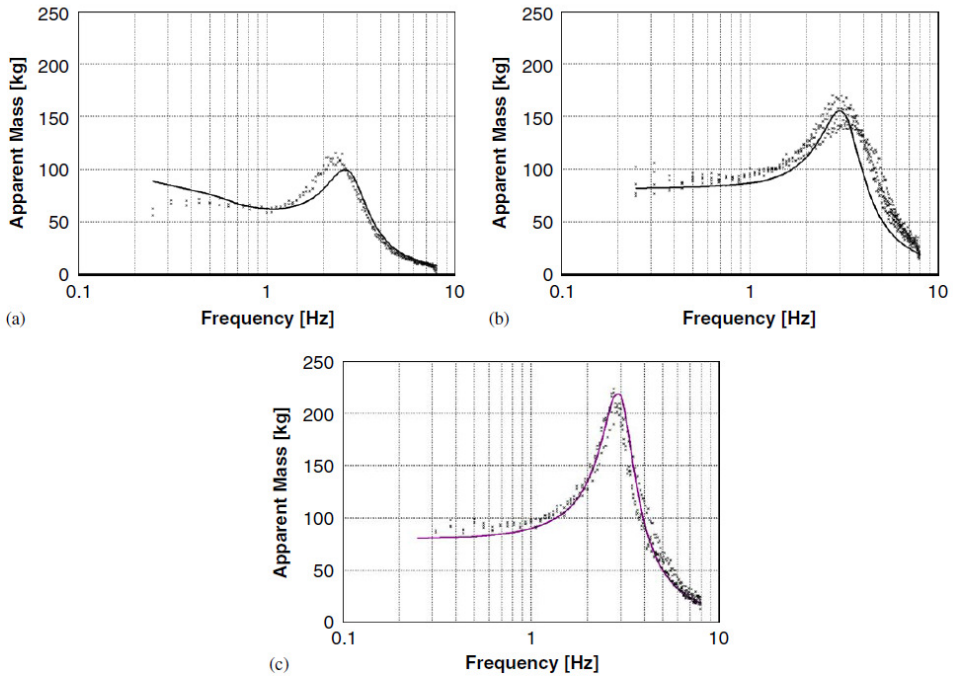

Fig. 11. Comparison between computed (—) and measured (xxxx) apparent mass response for different back supports: (a) no backrest (b) backrest, lumbar support (c) backrest, whole back support.

Figure 7.12: (Fleury and Mistrot, 2006)

Given the above literature review and the introduction to the first experiment, the author generated the following hypotheses: (i) whether the fore-and-aft apparent mass on a soft seat is different from the one measured on a soft seat; (ii) the dependence of apparent mass on vibration magnitude and (iii) on backrest contact.

7.3 Cross-axis effects in seat vertical and fore-and-aft transmissibility

Most of the published studies were focused on the vertical seat transmissibility (or human body apparent mass), while vibrating environments are usually multi-axial and vibration in one axis can produce vibration in another axis or affect transmissibility in another axis (Griffin, 1990).

Since physical systems generally show cross-talk between measurement axes, the validity of using single-axis transmissibility data or models in multi-axis environments has not been verified yet. The effects of a multi-axial vibration environment can be linear and non-linear.

Fairley (1984) addressed importance of fore-and-aft vibration in a car. The author investigated whether, in seat transmissibility, more than one input can contribute to seat vibration output. He did not model the effects of cross-coupling in translational vibration and showed that some fore-and-aft vibration at the seat pan can be attributed to rotational pitching mode of the seat base.

Fairley (1983) investigated, in a laboratory experiment, whether the transmission of vertical vibration through the seat was affected by presence of fore-and-aft vibration.

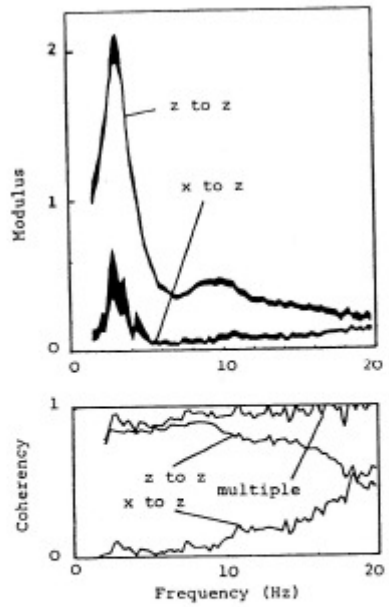

Figure 4.6: Frequency response functions and coherency functions for vertical (z) and fore-and-aft (x) vibration at the base of the base of a seat transmitted to vertical (z) vibration at the seat-person interface.(Black bands indicate 95 percent confidence intervals)

Figure 7.13: (Fairley, 1983)

He found that the cross-coupling, obtained by adding uncorrelated fore-and-aft vibration to vertical vibration, was small at low frequencies and could be attributed to the tilting of the SIT-bar and of the accelerometer attached to it. For frequencies higher than 10 Hz the cross-coupling seemed to increase with increasing frequency. Anyway, the amount of vibration transmitted to the person at high frequencies was small, so the cross-coupling was far from being of any practical significance. The multiple coherence function was

close to unity meant that most of the vertical vibration was accounted for the vertical and fore-and-aft excitation.

Smith et al. (2008) investigated the transmissibility of a suspended seat with two suspension configuration. The authors took into account the full transfer function matrix for the three-input/three-output system. They found that, regardless the seat configuration or the seating posture, the found very low cross-axis effect.

Smith (2008) investigated the transmissibility of a seat on an aircraft. Figure 7.14 shows that the amount of x vibration at the seat base transferred to the vertical vibration at the seat pan increases with vibration frequency.

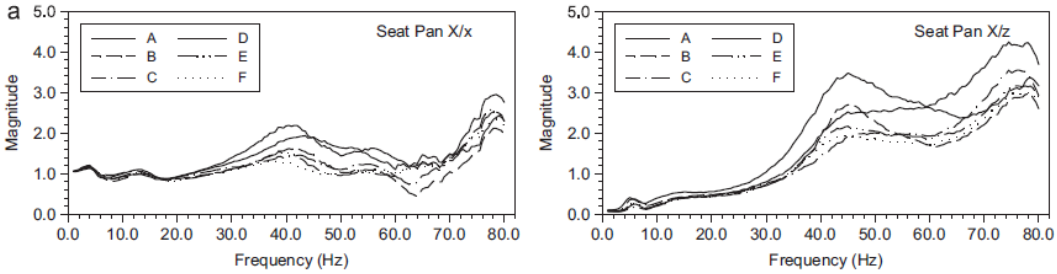

Figure 7.14: (Smith, 2008)

Seat transmissibility depends on both human body and seat (Griffin, 1990; Fairley and Griffin, 1984; Fairley and Griffin, 1986). In the same way, cross-axis effects can depend on both seat and human body characteristics. If so, cross-axis apparent mass could cause cross-axis transmissibility: due to human body characteristics, motion in vertical (or fore-and-aft) direction causes motion in fore-and-aft (or vertical) direction. For example, Nawayseh and Griffin (2003), Mansfield et al. (2006) studied the cross-axis transfer function between fore-and-aft acceleration and vertical force. A similar cross-axis response has been found with fore-and-aft excitation: considerable vertical forces are caused by pure fore-and-aft oscillation of a seat (Nawayseh and Griffin, 2005).

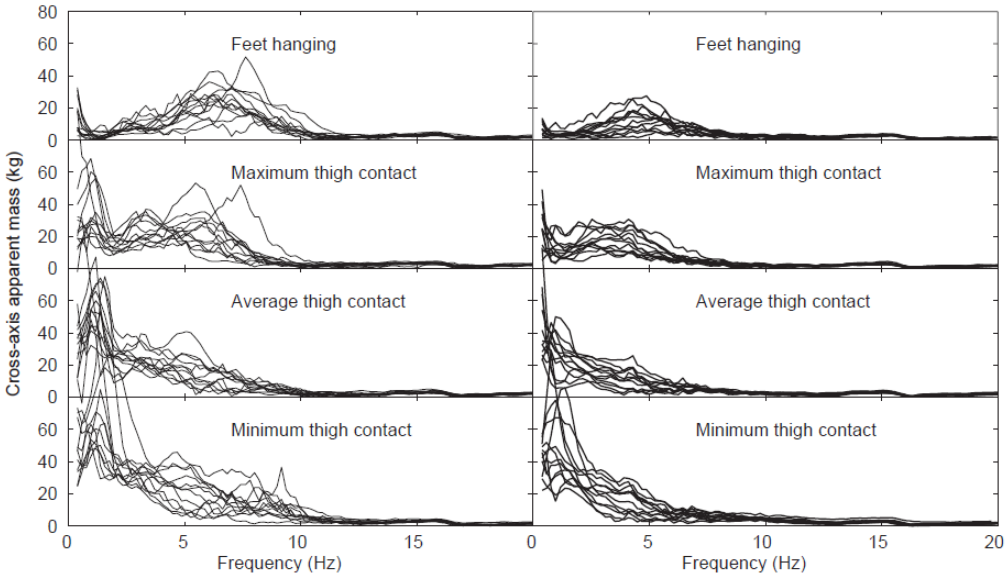

Fig. 4. Inter-subject variability in the vertical cross-axis apparent mass at the seat for each posture at two vibration magnitudes. —, 0.125 m s^{-2} rms; —, 1.25 m s^{-2} rms.

Figure 7.15: from Nawayseh and Griffin (2005)

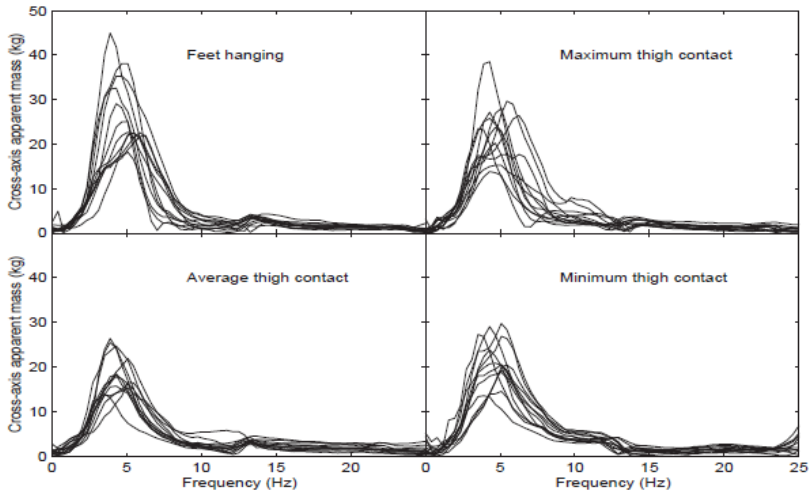

Fig. 4. Inter-subject variability in the cross-axis apparent mass in the fore-and-aft direction for each posture at 1.25 m s^{-2} r.m.s.

Figure 7.16: from Nawayseh and Griffin (2003)

Some studied focused on the non-linear effects of perpendicular vibration on in-line apparent mass. One study by Hinz et al. (2006) showed generally similar results between apparent masses measured using single-axis and tri-axial vibration in one posture, but

that addition of vibration in orthogonal axes showed an effect similar to that of increasing vibration magnitude.

Mansfield and Maeda (2006) found that the apparent mass resonance frequency is a function of the total vibration magnitude in all axes rather than a function of the vibration magnitude in the direction being measured.

Qiu and Griffin (2010) found that with dual-axis excitation (combined fore-and-aft and vertical vibration) the vibration in one axis affects the apparent mass of the body measured in the other axis. The resonance frequency in the vertical apparent mass is reduced as the magnitude of fore-and-aft excitation increases, and the resonance frequency in the fore-and-aft apparent mass is reduced as the magnitude of vertical vibration increases. Due to the non-linear dual-axis response of the human body, it is expected that the seat transmissibility will be non-linearly dependent by motion in other direction.

The second part of this thesis will also investigate the linear and non-linear cross-coupling in seat dynamic stiffness and seat transmissibility. It is hypothesised that there will be (i) linear and (ii) non-linear effects of vertical vibration on fore-and-aft transmissibility and of fore-and-aft vibration on vertical transmissibility. Linear effects will cause part of the input vibration in one axis being linearly transferred to the output vibration spectrum in another axis. Nonlinear effect will cause softening of the system in one direction while the vibration magnitude in that direction is kept constant and vibration in another direction is added.

7.4 Polyurethane foam dynamic stiffness in fore-and-aft direction

Polyurethane foams used in seat construction can be open-cell or closed-cell, depending whether the cell has just the structure made of struts or it has struts and membranes enclosing gas. Polyurethane foams for seat construction are, nowadays, mainly close-cell. Anyway, before completing the production process, the foam is subjected to a ‘crushing’ process in order to break the cells membrane and release the enclosed gas. It is not clear to the author whether an open-cell or a closed-cell model is more suitable for foam used in the present study. In (Gibson and Ashby, 1999) models for the prediction of the elastic compression, E, and the elastic shear Young modulus, G, in cellular materials are presented. E and G are different in open and closed-cell foams.

The complexity of the problem, due to high nonlinear behaviour of the foam (the role of preload and of subject apparent mass can be significant as showed in the first part of this research), effect of contact area, differences between compression and indentation tests (the former is commonly used in literature) etc., do not allow the author giving a quantitative forecast.

The author will test the following hypotheses:
(i) Polyurethane foam fore-and-aft stiffness is different from the vertical stiffness;
(ii) Polyurethane foam fore-and-aft stiffness is dependent on vibration magnitude;
(iii) Polyurethane foam fore-and-aft stiffness is correlated with subject weight and hip breadth;
(iv) there will be cross-axis nonlinearity in foam stiffness, i.e. foam vertical stiffness will be influenced by vibration in horizontal direction.

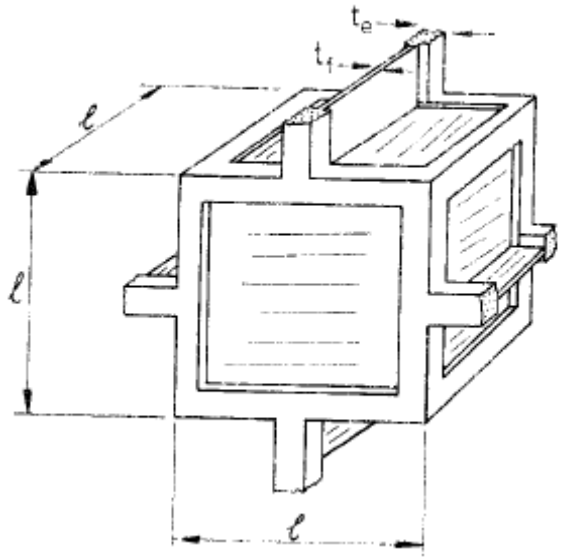

Figure 7.17: Cubic model for the closed-cell foam, showing the edge length *l* and thickness *t* (Gibson and Ashby, 1999)

8. Experiment two - Method

8.1 Apparatus

The vertical and fore-and-aft forces were measured using a 12-channels Kistler force platform (model 9281B) with an aluminium top plate. The force platform has four force transducers for each of the three orthogonal directions x, y and z. The four vertical force transducers have closely matched sensitivity, so their can be signals summed and amplified by a Kistler 5001 amplifier. Same procedure was adopted for the fore-and-aft force signal. The force plate was secured to a rigid seat with a rigid plywood backrest. The rigid seat was attached to the platform of a six-axis hydraulic motion simulator vibrator in the laboratories of the Human Factors Research Unit at the Institute of Sound and Vibration Research (Figure 8.1). The fore-and-aft stiffness of the backrest was tested with one subject by comparing the seat base and the backrest acceleration spectra. Differences did not exceed the 10% at frequencies between 0 and 25 Hz. It is believed that the backrest, due its geometry, is much rigid in the vertical direction: vertical stiffness was not checked. The vertical and fore-and-aft accelerations at the seat base were measured using two Silicon Design 2260-002 accelerometers. The vertical and fore-and-aft accelerations at the seat human interface were measured using a 'SAE pad' with tri-axial embedded Entran ECGS-240D accelerometers. Both of the accelerometers have a maximal cross-talk of 3%.

The force and acceleration signals were amplified and low-pass filtered (3-pole Butterworth, 50-Hz cut-off frequency) by Fylde signal conditioning before being acquired to computer at 512 samples/second via a National Instrument NI-USB-6251 DAQ, controlled by HVLab Matlab Toolbox software.

The signal from the fore-and-aft direction accelerometer embedded in the 'SAE pad', after amplification via Fylde signal conditioner, was monitored in real time through a digital display, in order to check the alignment of the accelerometer respect to the horizontal direction. Piezo-resistive accelerometers are sensitive to the gravitational field. The 'SAE pad' x-axis accelerometer output reading was set to zero when pad was resting on the seat without any subject on. In this condition, it is reasonable assuming that the 'SAE pad' is aligned to the horizontal direction. Any quasi-static tilting of the accelerometer results into acceleration output that is dependent on the gravitational acceleration g and on the sine of the tilt angle θ. A tolerance of $\pm 0.5g$ was set, meaning that the pad angular misalignment tolerance was $\theta = asin(\pm 0.5/g) = \pm 3°$. The acceleration value given by the accelerometer before and after each stimulus was checked in order to make sure that the accelerometer was not tilted respect to the horizontal. If the reading from the accelerometer was not in the tolerance range the subject was asked to adjust his

positioning respect to the ‘SAE pad’ until the reading was inside the tolerance range. Usually, placing the ‘SAE pad’ under the ischial tuberosities ensured a good alignment.

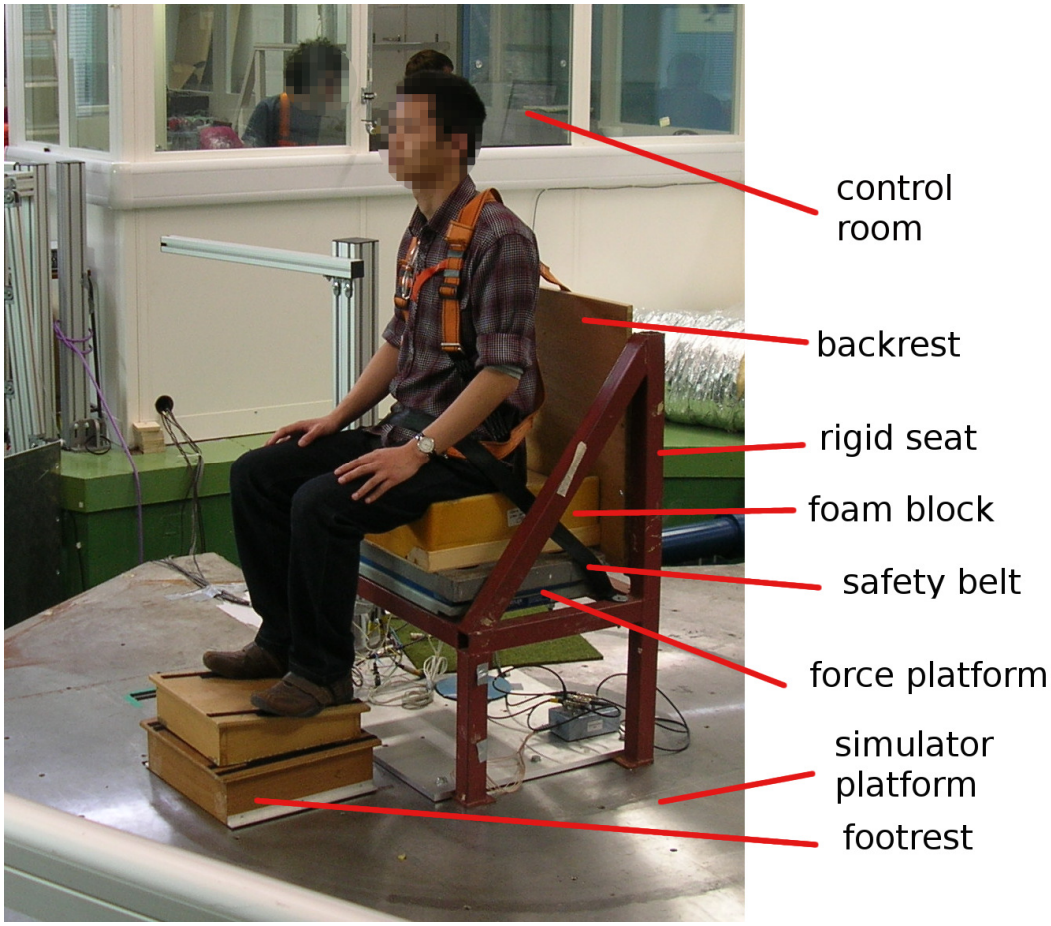

Figure 1: experimental setup

Two blocks (‘hard’ and ‘soft’ foam) of polyurethane foams suitable for automotive seats were selected from a larger sample so as to represent different dynamic characteristics (Table 8.1).

Table 8.1: Foam properties.

Dynamic stiffness	Composition	Density (kg/m^3)	Maximum thickness (mm)	Weight (kg)
soft	MDI	75	80	1.05
hard	MDI	75	80	0.93

The upper flat surface of each foam block was 400 mm wide by 450 mm deep. The lower surfaces of the foams were flat, apart from a 40-mm reduction in thickness over 60-mm wide strips on both sides. The foams (with no covers) were supported on a wooden base (weighing 2.1 kg) resting on the aluminium plate secured to the force platform. During the tests the SAE-pad was placed at the centre of the foam block.

In order to reduce the influence of viscoelastic deflection on foam characteristics, subjects sat on the foam blocks for three minutes before commencing the test.

8.2 Experimental design

Fifteen male subjects participated in the study. Their ages, standing weights, statures, and hip breadths were measured as described by Pheasant (1988) (see Table 8.2). The sitting weights for each subject were measured with a weighting scale with and without backrest contact. When measuring the sitting weight, the sitting posture was the same as in the dynamic tests (same footrest height and backrest distance).

Table 8.2: Subjects characteristics

	age	**weight**	**stature**	**hip breadth**	**sitting weight**	**s. weight (backrest ON)**	**weight ratio**	**weight ratio (backrest ON)**
	(yr)	(kg)	(cm)	(cm)	(kg)	(kg)	(-)	(-)
median	28	79	173	38	63	58	0.77	0.74
min	23	48	165	30	34	35	0.72	0.69
max	42	108	195	42	80	74	0.84	0.77
range	19	60	30	12	46	39	0.12	0.08

The subjects were instructed to sit in two postures: (i) one erect posture with no backrest contact ('backrest OFF'); (ii) one posture with backrest contact limited to the upper part of the back ('backrest ON'). In both postures lower legs were vertical and hands on the laps. A footrest supported on the moving platform of the vibrator was adjusted in height so as to maintain the uncompressed cushion surface 400 mm above the feet. The sitting posture is dependent on the distance between the seat-buttock contact area and the backrest. This distance was controlled by keeping the distance between the 'SAE pad' and the vertical backrest constant. Since the pad was positioned at the centre of the seat, and the seat was contiguous to the backrest, the distance was equal to half the length of the seat, i.e. 225 mm.

The eight possible combinations of 90 seconds vertical and fore-and-aft Gaussian random acceleration stimuli (0 to 25 Hz frequency range) at 0, 0.25 and 1.0 ms^{-2} r.m.s. magnitudes were used in the experiment. Combinations of stimuli, seating and associated measurements are presented in Table 8.3. The order of presenting the six seating conditions was randomised, as well as the order of presenting the vibration

stimulus with each seat. The total duration of the experiment was about 90 minutes. The experiment was approved by the Human Experimentation Safety and Ethics Committee of the Institute of Sound and Vibration Research.

Table 8.3: combinations of stimuli, seating and associated measurements

Seating	Backrest	Stimuli (ms^{-2} r.m.s.)	Calculated functions
Soft foam	ON	z = 0.25, x = 0 z = 1, x = 0 z = 0, x = 0.25 z = 0, x = 1 z = 0.25, x = 0.25 z = 0.25, x = 1 z = 1, x = 0.25 z = 1, x = 1	Seat transmissibility: vertical, fore-and-aft and cross-axis Human body apparent mass: vertical and fore-and-aft
	OFF	z = 0.25, x = 0 z = 1, x = 0 z = 0, x = 0.25 z = 0, x = 1 z = 0.25, x = 0.25 z = 0.25, x = 1 z = 1, x = 0.25 z = 1, x = 1	Seat transmissibility: vertical, fore-and-aft and cross-axis Human body apparent mass: vertical and fore-and-aft
Hard foam	OFF	z = 0.25, x = 0 z = 1, x = 0 z = 0, x = 0.25 z = 0, x = 1 z = 0.25, x = 0.25 z = 0.25, x = 1 z = 1, x = 0.25 z = 1, x = 1	Seat transmissibility: vertical, fore-and-aft and cross-axis Human body apparent mass: vertical and fore-and-aft
	ON	z = 0, x = 0.25 z = 0, x = 1	Seat transmissibility: fore-and-aft Human body apparent mass: fore-and-aft
Rigid seat	ON	z = 0, x = 0.25 z = 0, x = 1	Human body apparent mass: fore-and-aft
	OFF	z = 0, x = 0.25 z = 0, x = 1	Human body apparent mass: fore-and-aft

8.3 Analysis

When generating the vibration inputs (via HVLab Matlab Toolbox) signals presented some correlation. Pairs of least correlated x and z direction inputs were chosen among a set of one hundred stimuli. Signals were then played on the 6-axis simulator and equalised until the time domain error between the desired motion and the shaker response measured on the platform was less than the 5% r.m.s. Correlation between real

inputs, after equalization on the shaker, has been checked at 0.25 Hz resolution (it has to be noticed that spectral resolution affects the results, generally a coarser spectral resolution gives lower average coherency values), since the simulator can show cross-coupling between motion axes. In all the test conditions having dual-axis input, the average coherency throughout the whole 0-25 Hz spectrum had a maximum of $\gamma^2_{12}(f)$ =0.027. The maximum values of coherency were not systematically found at specific frequencies, apart from a very low frequency component (less than 1 Hz) probably due to simulator cross-coupling. If the maximum of coherency was searched in the frequency range from 0 to 25 Hz, the maximum value was $\gamma^2_{12}(f)$ =0.61, whereas if was searched from 1 to 25 Hz, the maximum value was $\gamma^2_{12}(f)$ =0.13. Considering the very low level of correlation between the inputs $\gamma^2_{12}\approx 0$, a SISO (single-input-single-output) model could have been used (Bendat, 1980). Anyway it was noticed that using a general two-input-out output model (Bendat, 1980) improved coherency through the whole spectrum.

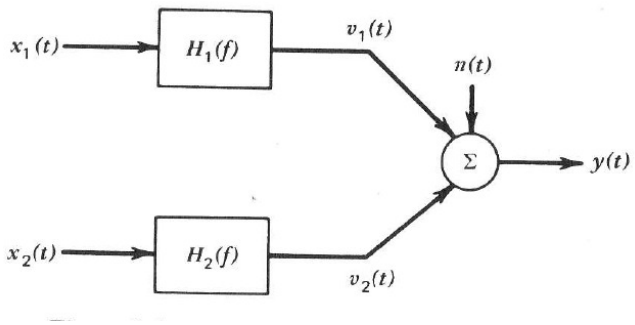

Figure 2: two-input model (Bendat, 2000)

8.3.1 MIMO model for optimum frequency response

The optimum frequency response functions $H_1(f)$ and $H_2(f)$ are calculated as (frequency dependency is omitted for notation simplicity) (Bendat, 2000):

$$H_1 = \frac{S_{22}S_{1y} - S_{12}S_{2y}}{S_{11}S_{22} - |S_{12}|^2} = \frac{S_{1Y}\left[1 - \dfrac{S_{12}S_{2Y}}{S_{22}S_{1y}}\right]}{S_{11}\left[1 - \gamma^2_{12}\right]}$$

$$H_2 = \frac{S_{11}S_{2y} - S_{21}S_{1y}}{S_{11}S_{22} - |S_{12}|^2} = \frac{S_{2Y}\left[1 - \dfrac{S_{21}S_{1Y}}{S_{11}S_{2y}}\right]}{S_{22}\left[1 - \gamma^2_{12}\right]}$$

where S_{ii} are double sided power spectral densities and S_{ij} are cross-sided spectral densities. γ^2_{ij} are coherency functions associated to the cross-sided spectral densities. Coherency function between inputs and output are calculates as:

$$\gamma^2_{1y} = \frac{\left|H_1 S_{11} + H_2 S_{12}\right|^2}{S_{11} S_{yy}}$$

$$\gamma^2_{2y} = \frac{\left|H_2 S_{22} + H_1 S_{21}\right|^2}{S_{22} S_{yy}}$$

Multiple coherence function is defined as the ratio of the ideal predicted linear output spectrum S_{vv} divided by the total measured output spectrum (Bendat, 1980).

$$\gamma^2_{y:x} = \frac{S_{vv}}{S_{yy}} = \frac{S_{yy} - S_{nn}}{S_{yy}} = 1 - \frac{S_{nn}}{S_{yy}}$$

where S_{nn} is the spectrum of the noise. Multiple coherency function can also be defined as the ratio of output measured spectrum $S_{yy}(f)$ due to the inputs $x_1(t)$ and $x_2(t)$.

Inputs and outputs of the above model are substituted with forces and accelerations measured time histories in order to calculate optimum linear systems representing seat transmissibility, human body apparent mass and seat dynamic stiffness. Apparent mass on soft seat in fore-and-aft direction was calculated with the same method used in experiment one for vertical direction. Mass cancellation for the mass of the aluminium plate above the force cells and mass of the seat was performed in time domain.

Table 8.4: input and output for the calculated optimum frequency response functions

optimum frequency response function $H_1(f)$	**input $x_1(t)$**	**input $x_2(t)$**	**output $y(t)$**	**optimum frequency response function $H_2(f)$**
Seat z to z (vertical) in-line transmissibility $H_{zz}(f)$	Seat base vertical acceleration $a_{z1}(t)$	Seat base fore-and-aft acceleration $a_{x1}(t)$	Seat pan vertical acceleration $a_{z2}(t)$	Seat x to z cross-axis transmissibility $H_{xz}(f)$
Seat x to x (fore-and-aft) in-line transmissibility $H_{xx}(f)$	Seat base fore-and-aft acceleration $a_{x1}(t)$	Seat base vertical acceleration $a_{z1}(t)$	Seat pan fore-and-aft acceleration $a_{x2}(t)$	Seat z to x cross-axis transmissibility $H_{zx}(f)$
Human body soft seat fore-and-aft apparent mass $AM_{xx}(f)$	Seat pan fore-and-aft acceleration $a_{x2}(t)$	Seat pan vertical acceleration $a_{z2}(t)$	Seat pan fore-and-aft net force $F_{x2}(t)=F_{x.measured}(t)-(m_{seat}-m_{plate})a_{x1}(t)$	not calculated
Human body fore-and-aft apparent mass $AM_{xx}(f)$ on rigid seat	Seat base fore-and-aft acceleration $a_{x1}(t)$	Seat base vertical acceleration $a_{z1}(t)$	Seat pan fore-and-aft net force $F_{x1}(t)=F_{x.measured}(t)-m_{plate}\,a_{x1}(t)$	not calculated
Seat fore-and-aft dynamic stiffness $S_{xx}(f)$ *(calculated from seat apparent mass $\omega^2 M_{xx}(f)$)*	$\Delta a_x(t)=a_{x2}(t)-a_{x1}(t)$	Seat pan vertical acceleration $a_{z2}(t)$	Seat pan fore-and-aft net force $F_{x2}(t)=F_{x.measured}(t)-(m_{seat}-m_{plate})\,a_{x1}(t)$	not calculated

Seat vertical dynamic stiffness $S_{zz}(f)$ *(calculated from seat apparent mass* $\omega^2 M_{zz}(f)$*)*	$\Delta a_z(t)=a_{z2}(t)-a_{z1}(t)$	Seat pan fore-and-aft acceleration $a_{z2}(t)$	Seat pan fore-and-aft net force $F_{z2}(t)=F_{z,measured}(t)-(m_{seat}-m_{plate})\,a_{z1}(t)$	not calculated

8.3.2 Conditioned analysis

Conditioned analysis (Bendat, 1980) can be used to remove the linear effects of an input on system optimum frequency responses. A two-inputs-single-output model can be transformed into a single-input-single-output model by removing the linear effects of an input from both the other input and the output. For a system such the one in Figure 8.2, it is possible to study the linear relation between $x_1(t)$ and $y(t)$ when all correlated effects of $x_2(t)$ are removed from the problem by transforming the system into the one in Figure 8.3.

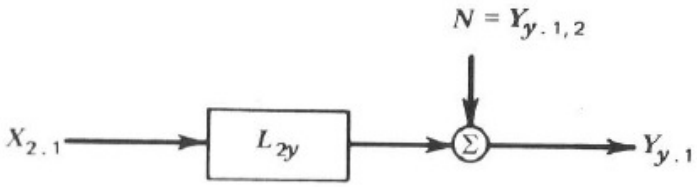

Figure 8.3: two input-one output system conditioned analysis

$X_{2.1}(f)$ and $Y_{y.1}(f)$ are the Fourier transforms of, respectively, the input $x_2(t)$ and the output $y(t)$ when the linear effect of $x_1(t)$ are removed. $L_{2y}(f)$ is the optimum linear system to predict $Y_{y.1}(f)$ from $X_{2.1}(f)$

$$L_{2y} = \frac{S_{2y.1}}{S_{22.1}} = \frac{S_{2y} - S_{21}\dfrac{S_{1y}}{S_{11}}}{S_{22}\left(1-\gamma^2_{12}\right)}$$

For an comprehensive treatise on conditioned analysis the reader should refer to (Bendat, 1980).

In the present research, conditioned analysis will be used to study the non-linear effects of an input while keeping the other input at a constant magnitude. For instance, let's consider the test having dual axis input (z = 0.25, x = 0 ms^{-2} r.m.s.) and (z = 0.25, x = 0.25 ms^{-2} r.m.s.). If we compare the vertical transmissibilities $H_{zz}(f)$ of the two test, changes can arise from: (i) linear effects of x vibration input contributing to z output spectrum S_{yy}; (ii) nonlinear effects of x vibration input on the output spectrum.

To study the linear contribution of x vibration to vertical vibration out, test (z = 0.25, x = 0.25 ms^{-2} r.m.s.) has to be considered. Referring to Figure 8.2, given $x_1(t) = x_{input}(t)$, $x_2(t) = z_{input}(t)$, $y(t) = z_{output}(t)$, the optimum frequency response system $H_2(f)$ represents the

vertical seat transmissibility, i.e. the amount of vibration transmitted from the seat base to the seat pan at each frequency. $H_1(f)$ represents the amount of x vibration linearly transmitted to the vertical seat pan acceleration. The reason for x vibration transmitted is a linear cross-coupling and can be attributed to the human body or/and the seat.

To study the nonlinear contribution of x_{input} = 0.25 ms^{-2} r.m.s. vibration to vertical transmissibility, vertical transmissibility in tests (z = 0.25, x = 0 ms^{-2} r.m.s.) and (z = 0.25, x = 0.25 ms^{-2} r.m.s.) have to be compared. Linear effects of x_{input} on z_{output} are removed by means of conditioned analysis. Referring to Figure 3, $X_{2.1}(f)$ and $Y_{y.1}(f)$ will be z_{input} and z_{output} when linear effects of x_{input} are removed from both. If any significant nonlinear effect of x_{input} exists, it can be seen by comparing conditioned vertical seat transmissibilities L_{2y} of the tests (z = 0.25, x = 0 ms^{-2} r.m.s.) with the one of test (z = 0.25, x = 0.25 ms^{-2} r.m.s.).

9. Experiment two - Results

9.1.1 Fore-and-aft transmissibility - Iinter-subject variability

Individual fore-and-aft transmissibility curves for the 15 subjects generally show a low frequency peak in the range of 0.5 - 0.75 Hz in the case of 'backrest OFF' condition. It is not possible to identify this peak in all the subjects. A second peak of resonance clearly appears in the range of 2 to 6 Hz. In the 'backrest ON' condition, only one peak appears in the range of 3 to 7 Hz. In both 'backrest ON' and 'backrest OFF' conditions, the transmissibility drops to a value of about 0.8 in the range of 4 to 9 Hz, and then increases linearly with frequency, usually exceeding unity at 25 Hz.

In order to test the significance of the effect of vibration magnitude, rigid backrest and seat dynamic stiffness on fore-and-aft transmissibility, *Wilcoxon matched pairs signed rank* non-parametric statistical test (Siegel, 1988) was performed on four fore-and-aft transmissibility parameters: (i) second resonance frequency; (ii) magnitude of the second resonance; (iii) transmissibility at 12.5; (iv) transmissibility at 25 Hz (respectively f_r, $H(f_r)$, $H(12.5)$, $H(25)$). Significance level is set at $\alpha = 0.05$.

SEAT values were calculated for the fore-and-aft transmissibility of foams, using weightings suggested in (ISO 2631-1, 1997). Values were pretty close to unity, with small variability.

Table 9.1: SEAT values for the fore-and-aft seat transmissibility

condition	median	maximum	minimum
soft 0.25 ms^{-2} r.m.s. backrest OFF	1.03	1.07	1.01
soft 1.0 ms^{-2} r.m.s. backrest OFF	1.02	1.06	0.97
hard 0.25 ms^{-2} r.m.s. backrest OFF	1.09	1.11	1.03
hard 1.0 ms^{-2} r.m.s. backrest OFF	1.08	1.12	1.00
soft 0.25 ms^{-2} r.m.s. backrest ON	1.02	1.06	0.99
soft 1 ms^{-2} r.m.s. backrest ON	1.00	1.04	0.95
hard 0.25 ms^{-2} r.m.s. backrest ON	1.07	1.12	1.06
hard 1 ms^{-2} r.m.s. backrest ON	1.07	1.13	1.05

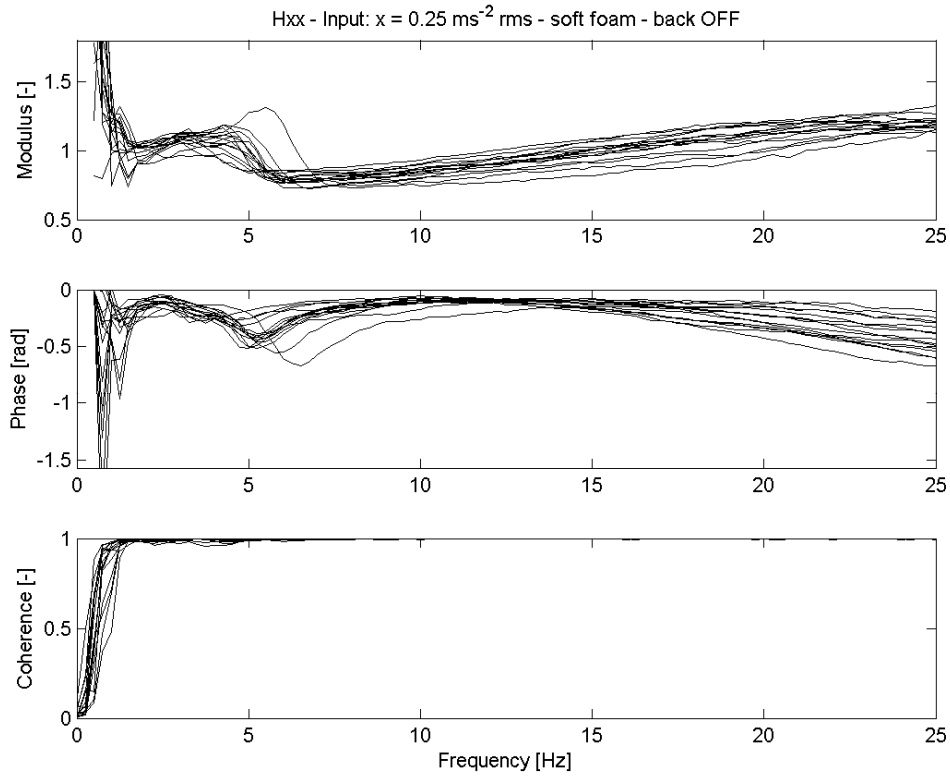

Figure 9.1: seat fore-and-aft transmissibility for the 15 subjects

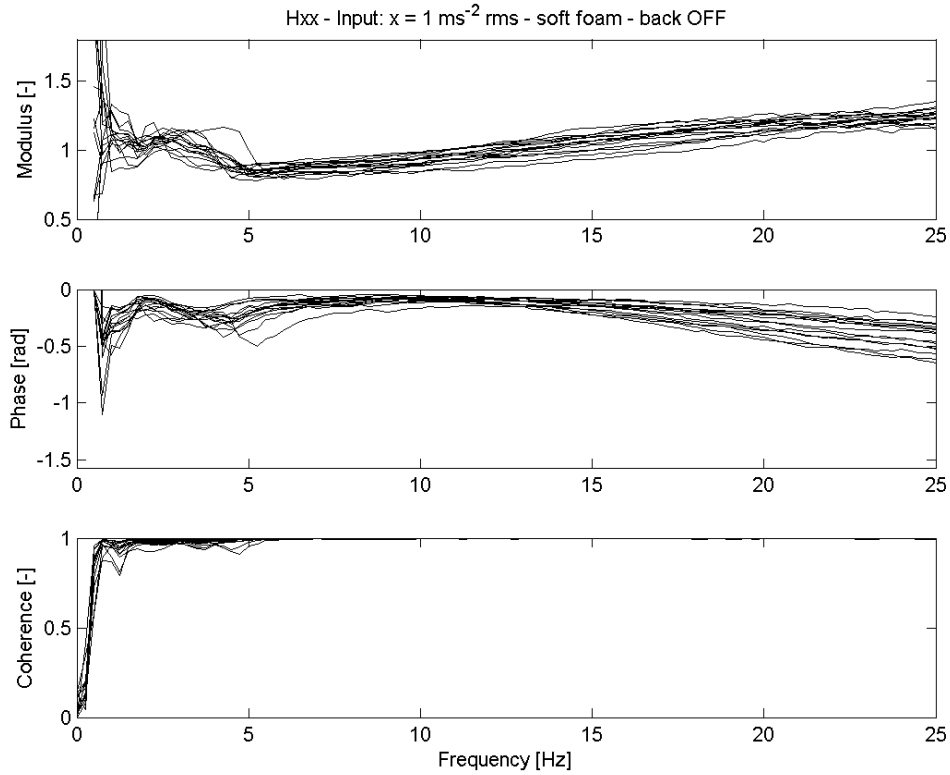

Figure 9.2: seat fore-and-aft transmissibility for the 15 subjects

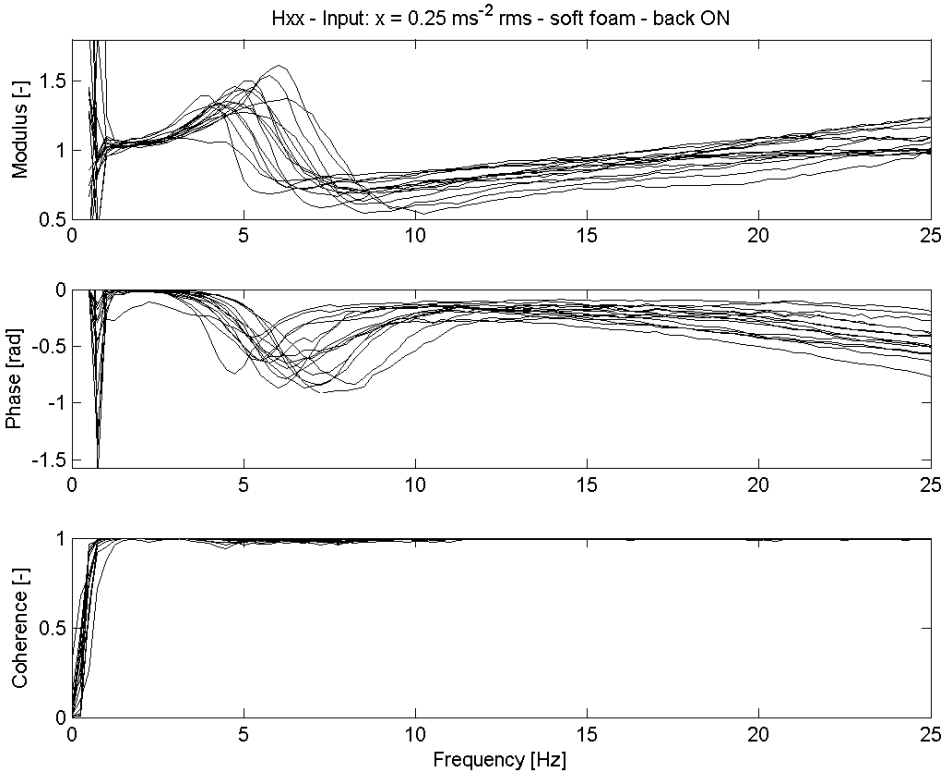

Figure 9.3: seat fore-and-aft transmissibility for the 15 subjects

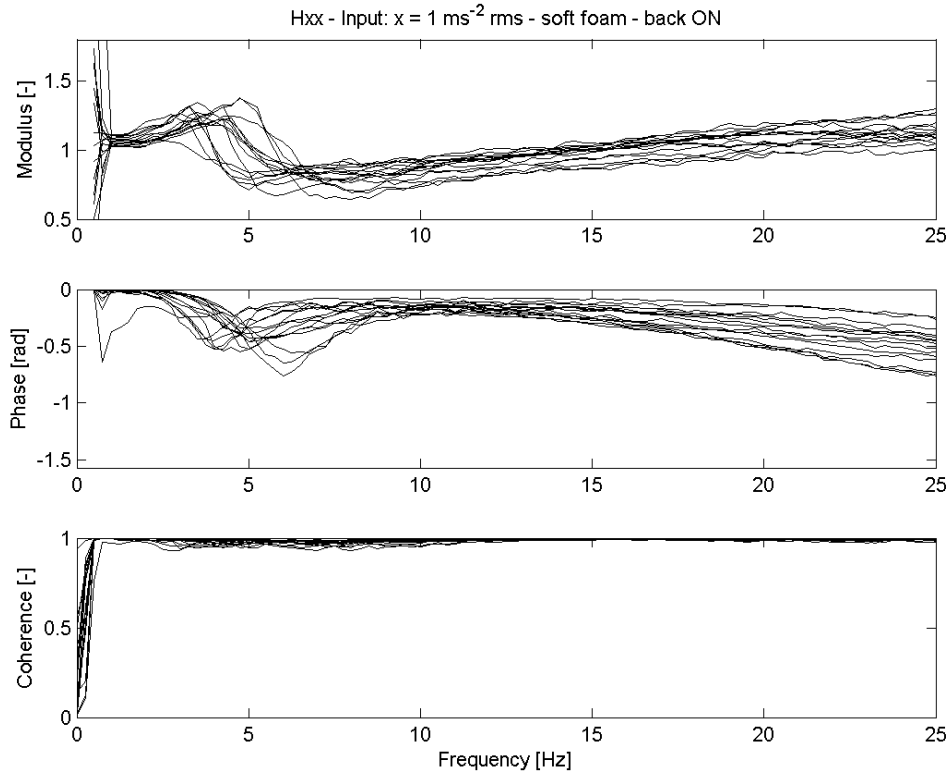

Figure 9.4: seat fore-and-aft transmissibility for the 15 subjects

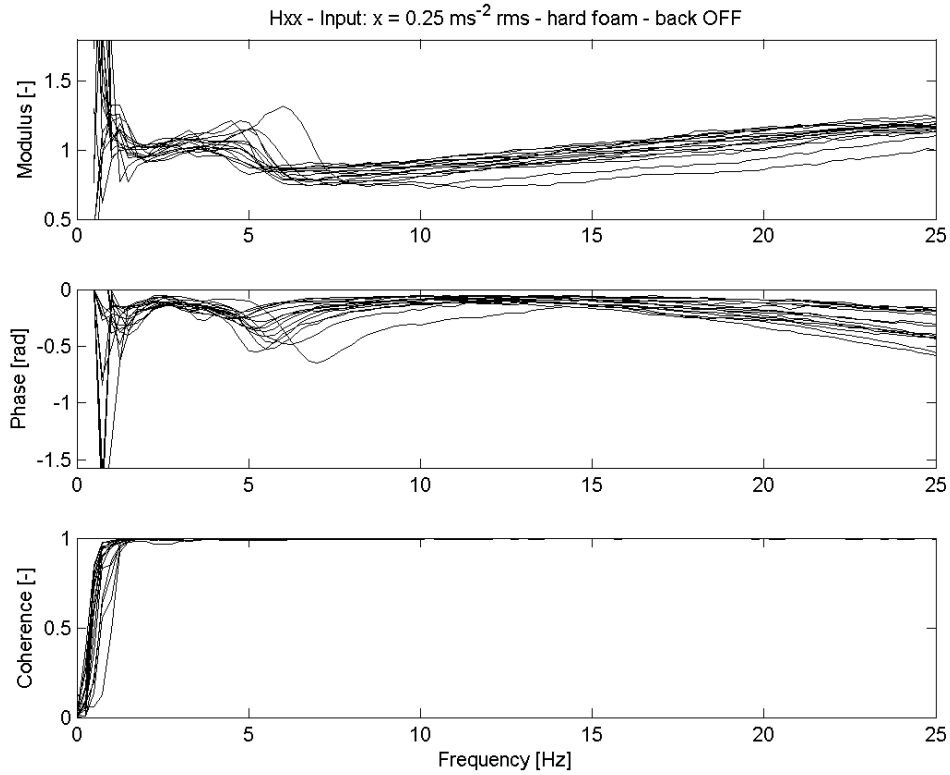

Figure 9.5: seat fore-and-aft transmissibility for the 15 subjects

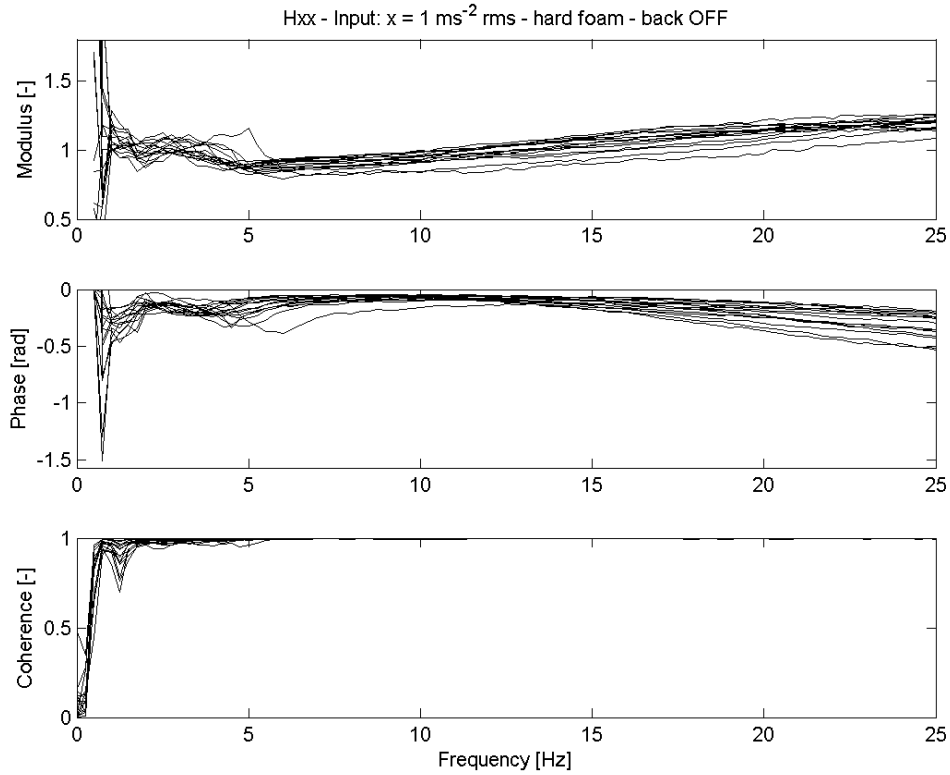

Figure 9.6: seat fore-and-aft transmissibility for the 15 subjects

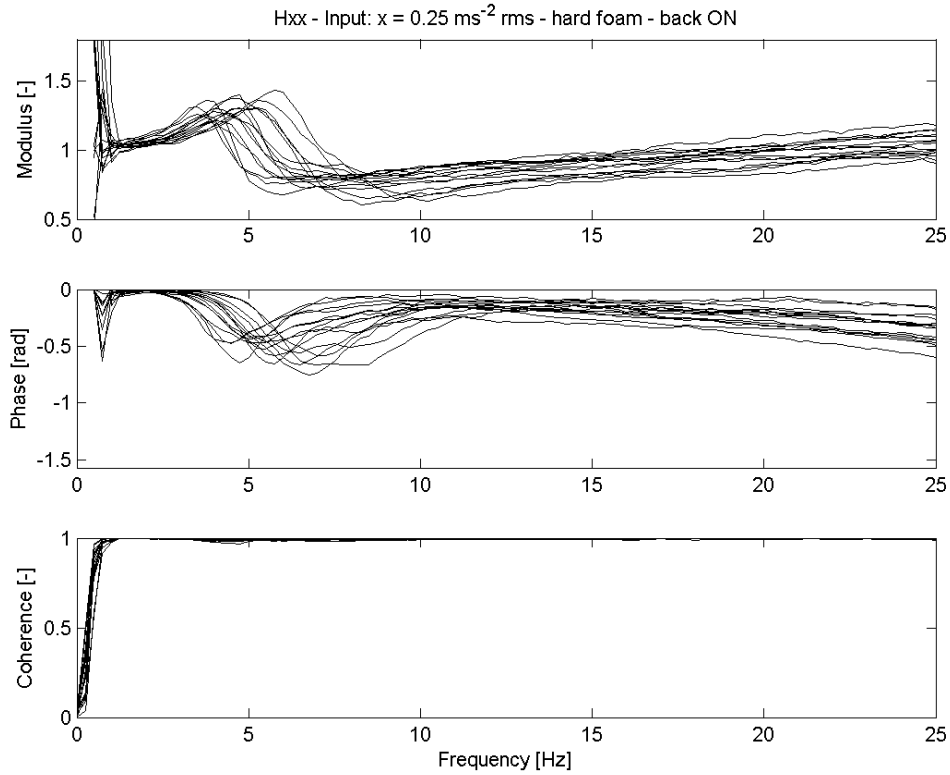

Figure 9.7: seat fore-and-aft transmissibility for the 15 subjects

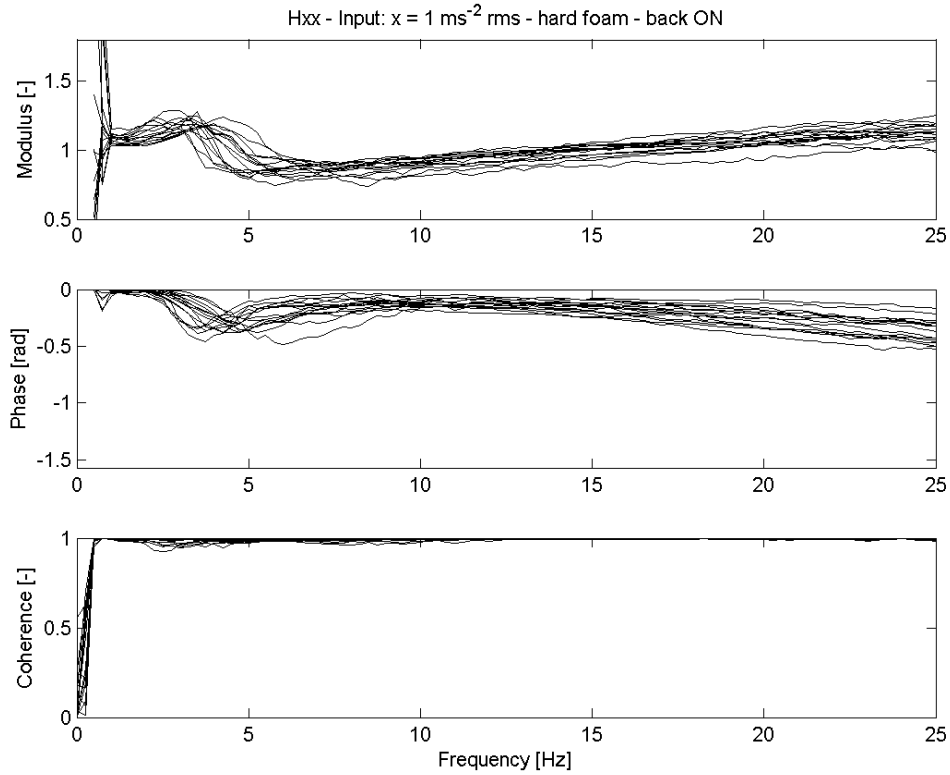

Figure 9.8: seat fore-and-aft transmissibility for the 15 subjects

9.1.2 Fore-and-aft transmissibility - Effect of magnitude

Figures 9.9 to 9.12 show the effect of seat stiffness on fore-and-aft transmissibility median curves. The first peak of resonance clearly appears at about 0.75 Hz, while the second seems to be smeared out by the statistical process. When increasing the magnitude of the acceleration input from 0.25 to 1 ms^{-2} r.m.s., the second peak decreases in magnitude and shifts towards lower frequencies. The resonance frequency f_r is identified as the maximum of the absolute value of transmissibility in the range of 2 to 6 Hz with a spectral resolution of 0.125 Hz. $H(f_r)$ is the modulus of transmissibility at the frequency f_r. Effects of vibration magnitude on the first resonance are not analysed, as this peak is not clearly visible in all the individual data and its magnitude and frequency are generally dependent on the chosen spectral resolution. Results reported in Table 9.2 show that an increase in vibration magnitude provokes a reduction in resonance frequency f_r ($p < 0.05$), for both the 'backrest ON' and 'backrest OFF' conditions. An increase in vibration magnitude decreases the transmissibility at resonance for the hard foam ($p < 0.05$) and for the soft foam in the 'backrest ON' condition, while increasing acceleration magnitude increases *H(12.5)*

and *H(25)*, in both the hard and soft foam ($p < 0.05$) in the 'backrest ON' and 'backrest OFF' conditions.

Table 9.2: Statistical significance of the effect of magnitude on fore-and-aft seat transmissibility (Wilcoxon matched pairs signed rank test)

effect of vibration magnitude	**condition**		**Condition**	**significance level *p***
fr	soft 0.25 ms^{-2} r.m.s. backrest OFF	>	soft 1 ms^{-2} r.m.s. backrest OFF	**.001**
	hard 0.25 ms^{-2} r.m.s. backrest OFF	>	hard 1 ms^{-2} r.m.s. backrest OFF	**.001**
	soft 0.25 ms^{-2} r.m.s. backrest ON	>	soft 1 ms^{-2} r.m.s. backrest ON	**.001**
	hard 0.25 ms^{-2} r.m.s. backrest ON	>	hard 1 ms^{-2} r.m.s. backrest ON	**.001**
H(fr)	soft 0.25 ms^{-2} r.m.s. backrest OFF	>	soft 1 ms^{-2} r.m.s. backrest OFF	**.102**
	hard 0.25 ms^{-2} r.m.s. backrest OFF	>	hard 1 ms^{-2} r.m.s. backrest OFF	**.013**
	soft 0.25 ms^{-2} r.m.s. backrest ON	>	soft 1 ms^{-2} r.m.s. backrest ON	**.001**
	hard 0.25 ms^{-2} r.m.s. backrest ON	>	hard 1 ms^{-2} r.m.s. backrest ON	**.001**
H(12.5)	soft 0.25 ms^{-2} r.m.s. backrest OFF	<	soft 1 ms^{-2} r.m.s. backrest OFF	**.001**
	hard 0.25 ms^{-2} r.m.s. backrest OFF	<	hard 1 ms^{-2} r.m.s. backrest OFF	**.001**
	soft 0.25 ms^{-2} r.m.s. backrest ON	<	soft 1 ms^{-2} r.m.s. backrest ON	**.001**
	hard 0.25 ms^{-2} r.m.s. backrest ON	<	hard 1 ms^{-2} r.m.s. backrest ON	**.001**
H(25)	soft 0.25 ms^{-2} r.m.s. backrest OFF	<	soft 1 ms^{-2} r.m.s. backrest OFF	**.001**
	hard 0.25 ms^{-2} r.m.s. backrest OFF	<	hard 1 ms^{-2} r.m.s. backrest OFF	**.001**
	soft 0.25 ms^{-2} r.m.s. backrest ON	<	soft 1 ms^{-2} r.m.s. backrest ON	**.012**
	hard 0.25 ms^{-2} r.m.s. backrest ON	<	hard 1 ms^{-2} r.m.s. backrest ON	**.001**

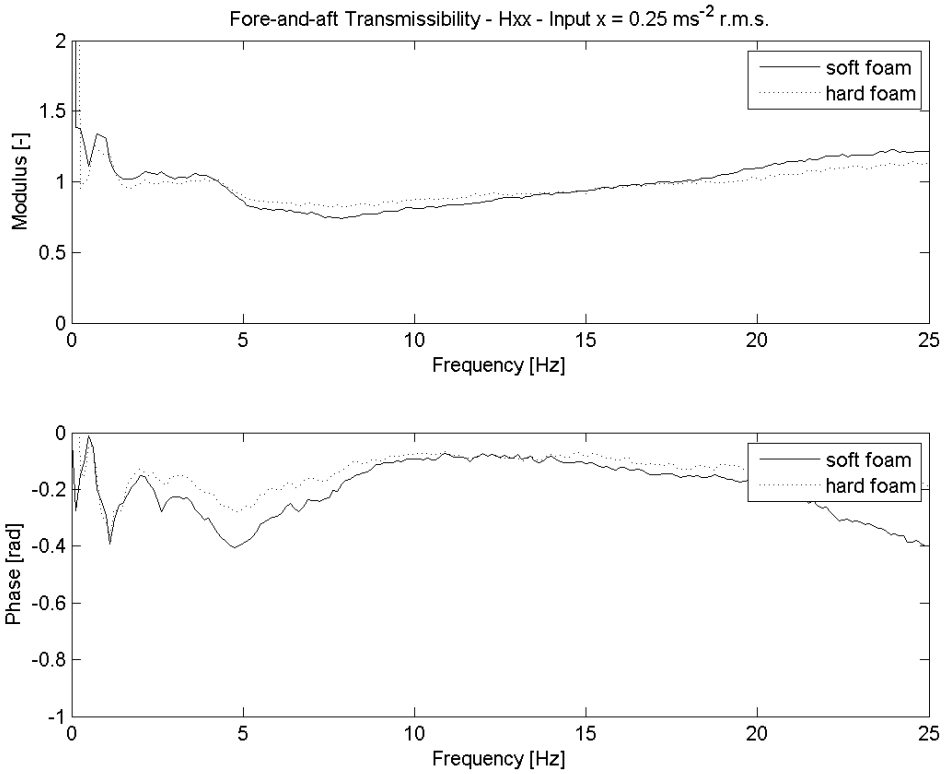

Figure 9.9: seat fore-and-aft median transmissibility

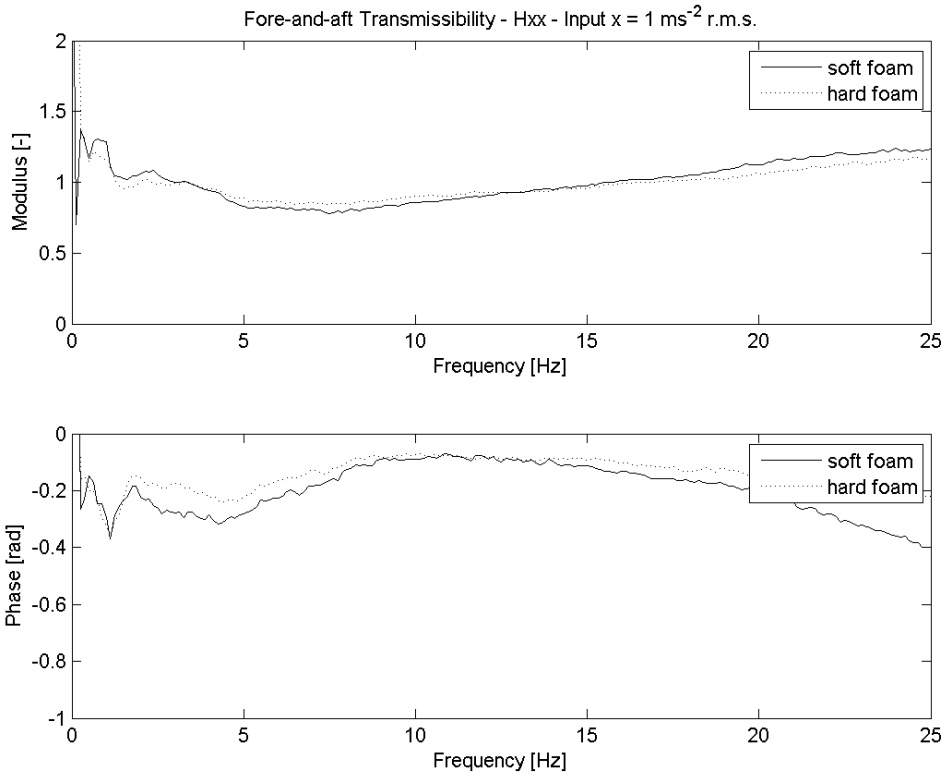

Figure 9.10: seat fore-and-aft median transmissibility

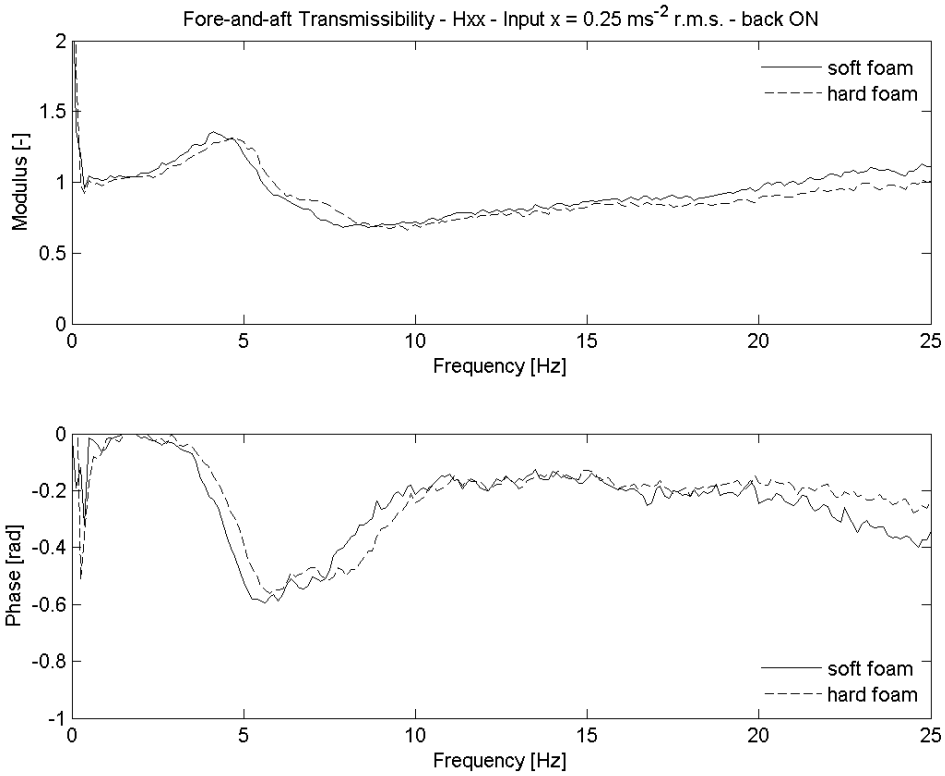

Figure 9.11: seat fore-and-aft median transmissibility

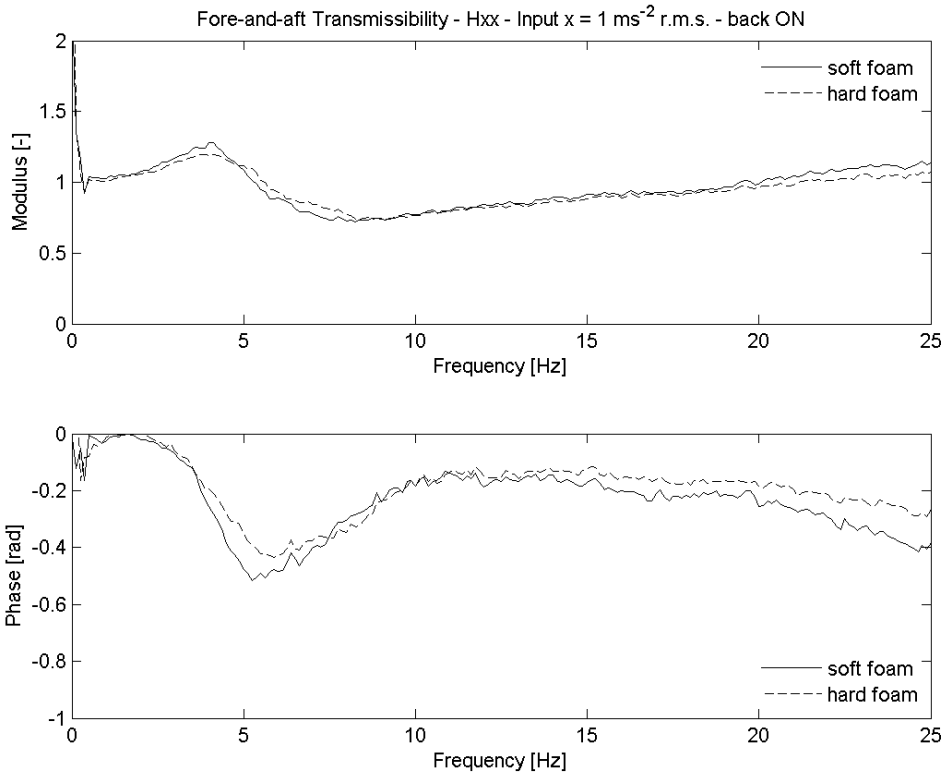

Figure 9.12: seat fore-and-aft median transmissibility

9.1.3 Fore-and-aft transmissibility - Effect of a rigid backrest

Figures 9.13 and 9.14 show the effect of the rigid vertical backrest on median transmissibility with the two levels of vibration magnitude. The presence of the backrest removed the first peak of resonance and increases the transmissibility at resonance, while decreasing the transmissibility at higher frequencies. The backrest enhanced the effect of vibration magnitude. The presence of a backrest reduced the transmissibility at frequencies above 7 Hz, even though the difference was relatively small.

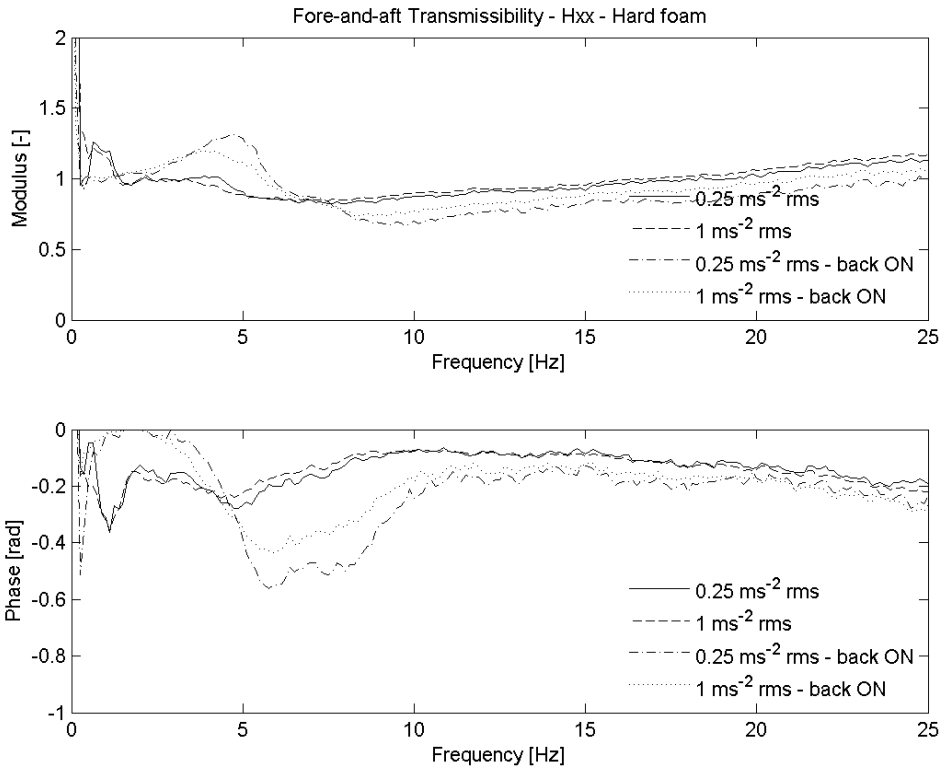

Figure 9.13: seat fore-and-aft median transmissibility

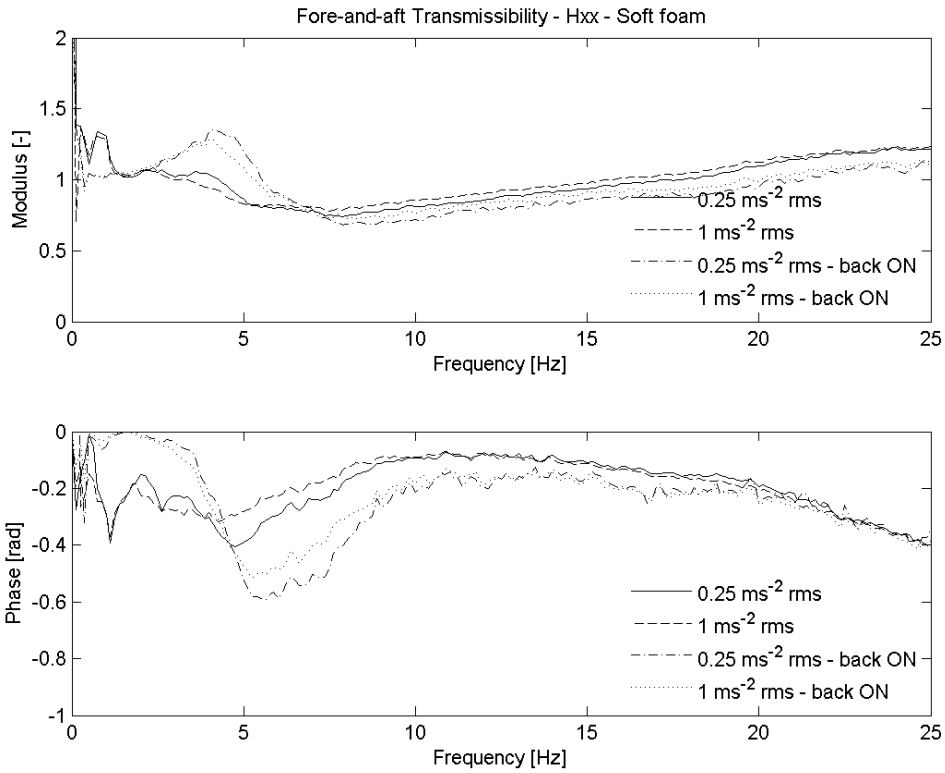

Figure 9.14: seat fore-and-aft transmissibility medians

Results in of the Wilcoxon test are reported in Table 9.3. It can be seen that, given the same magnitude, the resonance frequency, f_r, is higher in the 'backrest ON' than in the 'backrest OFF' condition ($p < 0.05$). Table 9.3 shows that the use of a rigid backrest increases the transmissibility at resonance ($p < 0.05$) and decreases the transmissibility at 12.5 and 25 Hz ($p < 0.05$).

Table 9.3: Statistical significance of the effect of a rigid backrest on fore-and-aft seat transmissibility (Wilcoxon matched pairs signed rank test)

effect of rigid backrest	condition		Condition	significance level *p*
fr	soft 0.25 ms^{-2} r.m.s. backrest OFF	>	soft 1 ms^{-2} r.m.s. backrest OFF	**.001**
	hard 0.25 ms^{-2} r.m.s. backrest OFF	>	hard 1 ms^{-2} r.m.s. backrest OFF	**.001**
	soft 0.25 ms^{-2} r.m.s. backrest ON	>	soft 1 ms^{-2} r.m.s. backrest ON	**.001**
	hard 0.25 ms^{-2} r.m.s. backrest ON	>	hard 1 ms^{-2} r.m.s. backrest ON	**.001**
H(fr)	soft 0.25 ms^{-2} r.m.s. backrest ON	>	soft 0.25 ms^{-2} r.m.s. backrest OFF	**.001**
	hard 0.25 ms^{-2} r.m.s. backrest ON	>	hard 0.25 ms^{-2} r.m.s. backrest OFF	**.001**
	soft 1 ms^{-2} r.m.s. backrest ON	>	soft 1 ms^{-2} r.m.s. backrest OFF	**.001**
	hard 1 ms^{-2} r.m.s. backrest ON	>	hard 1 ms^{-2} r.m.s. backrest OFF	**.001**
H(12.5)	soft 0.25 ms^{-2} r.m.s. backrest ON	<	soft 0.25 ms^{-2} r.m.s. backrest OFF	**.001**
	hard 0.25 ms^{-2} r.m.s. backrest ON	<	hard 0.25 ms^{-2} r.m.s. backrest OFF	**.003**
	soft 1 ms^{-2} r.m.s. backrest ON	<	soft 1 ms^{-2} r.m.s. backrest OFF	**.001**
	hard 1 ms^{-2} r.m.s. backrest ON	<	hard 1 ms^{-2} r.m.s. backrest OFF	**.008**
H(25)	soft 0.25 ms^{-2} r.m.s. backrest ON	<	soft 0.25 ms^{-2} r.m.s. backrest OFF	**0.001**
	hard 0.25 ms^{-2} r.m.s. backrest ON	<	hard 0.25 ms^{-2} r.m.s. backrest OFF	**.001**
	soft 1 ms^{-2} r.m.s. backrest ON	<	soft 1 ms^{-2} r.m.s. backrest OFF	**.001**
	hard 1 ms^{-2} r.m.s. backrest ON	<	hard 1 ms^{-2} r.m.s. backrest OFF	**.001**

9.1.4 Fore-and-aft transmissibility - Effect of foam stiffness

The effect of foam stiffness seems to be marginal: the differences in median transmissibility never exceeded the 15% and they are usually less than 10%. The harder foam gives lower transmissibility at frequencies below 5 Hz and higher that 15 Hz. Table 9.4 shows no significant effect of foam composition on resonance frequency f_r was found ($p > 0.05$), while it had a significant effect on the modulus of transmissibility at resonance, but not in the low magnitude 'backrest OFF' condition. Foam stiffness had a significant effect ($p < 0.05$) in the 'backrest OFF' conditions: harder foam gave lower *H(12.5)* and *H(25)*. 'Backrest ON' transmissibility at 12.5 Hz was influenced by foam composition only in the low magnitude case ($p < 0.05$). There was no effect of foam composition on 25 Hz transmissibility for the 'backrest ON' condition ($p > 0.05$).

Table 9.4: Statistical significance of the effect of foam stiffness on fore-and-aft seat transmissibility (Wilcoxon matched pairs signed rank test)

effect of foam stiffness	**condition**		**Condition**	**significance level *p***
fr	soft 0.25 ms^{-2} r.m.s. backrest OFF	>	hard 0.25 ms^{-2} r.m.s. backrest OFF	.100
	soft 1 ms^{-2} r.m.s. backrest OFF	>	hard 1 ms^{-2} r.m.s. backrest OFF	.083
	soft 0.25 ms^{-2} r.m.s. backrest ON	>	hard 0.25 ms^{-2} r.m.s. backrest ON	.053
	soft 1 ms^{-2} r.m.s. backrest ON	>	hard 1 ms^{-2} r.m.s. backrest ON	.150
H(fr)	soft 0.25 ms^{-2} r.m.s. backrest OFF	>	hard 0.25 ms^{-2} r.m.s. backrest OFF	.312
	soft 1 ms^{-2} r.m.s. backrest OFF	>	hard 1 ms^{-2} r.m.s. backrest OFF	**.002**
	soft 0.25 ms^{-2} r.m.s. backrest ON	>	hard 0.25 ms^{-2} r.m.s. backrest ON	**.008**
	soft 1 ms^{-2} r.m.s. backrest ON	>	hard 1 ms^{-2} r.m.s. backrest ON	**.023**
H(12.5)	soft 0.25 ms^{-2} r.m.s. backrest OFF	>	hard 0.25 ms^{-2} r.m.s. backrest OFF	**.003**
	soft 1 ms^{-2} r.m.s. backrest OFF	>	hard 1 ms^{-2} r.m.s. backrest OFF	**.021**
	soft 0.25 ms^{-2} r.m.s. backrest ON	>	hard 0.25 ms^{-2} r.m.s. backrest ON	**.005**
	soft 1 ms^{-2} r.m.s. backrest ON	>	hard 1 ms^{-2} r.m.s. backrest ON	.062
H(25)	soft 0.25 ms^{-2} r.m.s. backrest OFF	>	hard 0.25 ms^{-2} r.m.s. backrest OFF	**.003**
	soft 1 ms^{-2} r.m.s. backrest OFF	>	hard 1 ms^{-2} r.m.s. backrest OFF	**.001**
	soft 0.25 ms^{-2} r.m.s. backrest ON	>	hard 0.25 ms^{-2} r.m.s. backrest ON	.115
	soft 1 ms^{-2} r.m.s. backrest ON	>	hard 1 ms^{-2} r.m.s. backrest ON	.690

Table 9.5: Individual values of the second resonance frequency, the transmissibility at resonance and at 12.5 and 25 Hz for all the test conditions.

	subject	1	2	3	4	5	6	7	8	9	10	11	12	13	14	15
soft 0.25 ms^{-2} r.m.s.	f_r	3.13	2.38	1.75	2.75	2.63	3.13	4.38	3.63	5	3.88	2.5	3.75	3.88	2.63	2.13
	$H(f_r)$	1.04	1.1	0.98	1.16	1.12	1.11	1.16	1.19	1.33	1.12	1.12	1.21	1.18	1.14	1.07
	H(12.5Hz)	0.97	0.93	1.04	0.93	1.01	0.97	0.97	0.93	0.78	0.93	0.87	0.94	0.85	0.94	0.89
	H(25Hz)	1.19	1.33	1.21	1.15	1.24	1.13	1.13	1.18	1.11	1.18	1.21	1.25	1.18	1.22	1.21
soft 1 ms^{-2} r.m.s.	f_r	4.38	3.75	3.38	4.38	3.63	3.5	4	4.63	5.63	4.75	2.38	5.13	5.75	4.63	4.13
	$H(f_r)$	1.28	1.35	1.43	1.47	1.34	1.33	1.36	1.55	1.63	1.45	1.11	1.56	1.38	1.45	1.36
	H(12.5Hz)	0.77	0.84	0.9	0.76	0.89	0.93	0.85	0.85	0.66	0.84	0.89	0.81	0.72	0.83	0.8
	H(25Hz)	0.98	1.22	1.09	0.95	1.22	0.98	1	0.99	0.96	1.17	1.24	0.99	1.06	1.07	1.11
soft 0.25 ms^{-2} r.m.s. backrest ON	f_r	2	1.88	1.75	2.38	2	1.75	2.38	2.88	4.13	2.13	1.75	2	2.75	2	2.38
	$H(f_r)$	1.01	1.02	1.21	1.17	1.05	1.11	1.09	1.17	1.21	1.07	1.11	1.15	1.16	1.16	1.11
	H(12.5Hz)	1.05	1	1.06	1.02	1.09	1.03	1.08	1.01	0.9	1	0.96	1.02	0.92	1.05	0.98
	H(25Hz)	1.28	1.34	1.26	1.16	1.3	1.23	1.21	1.16	1.2	1.22	1.31	1.26	1.26	1.28	1.24
soft 1 ms^{-2} r.m.s. backrest ON	f_r	2.88	2.75	2.75	4.13	2.38	2.25	3.5	3.63	4.13	3	1.75	3.75	4	3.13	3.75
	$H(f_r)$	1.22	1.34	1.34	1.41	1.29	1.3	1.29	1.35	1.39	1.26	1.1	1.22	1.26	1.37	1.23
	H(12.5Hz)	0.9	0.97	1	0.83	1.02	1.02	0.95	0.96	0.82	0.95	0.97	0.97	0.83	0.95	0.9
	H(25Hz)	1.08	1.25	1.08	1.01	1.05	1.09	1.04	1.03	1.12	1.26	1.3	1.07	1.17	1.21	1.14
hard 0.25 ms^{-2} r.m.s.	f_r	3.13	2.38	3.13	2.75	2.75	3	4.38	4	5.5	3.5	2.38	4.38	4.75	2.5	3.88
	$H(f_r)$	1.04	1.09	1.01	1.15	1.07	1.09	1.17	1.22	1.35	1.02	1.11	1.24	1.17	1.09	1.02
	H(12.5Hz)	0.99	0.96	1.01	0.91	1	0.97	0.94	0.9	0.75	0.95	0.88	0.89	0.8	0.95	0.91
	H(25Hz)	1.15	1.24	1.15	1.13	1.23	1.14	1.15	1.15	1	1.19	1.15	1.2	1.11	1.17	1.13
hard 1 ms^{-2} r.m.s.	f_r	3.63	3.38	3	4	4	3	3.63	4.25	5.38	4.13	3	4.88	4.75	3.38	4.75
	$H(f_r)$	1.29	1.23	1.34	1.39	1.29	1.27	1.31	1.31	1.45	1.42	1.26	1.37	1.32	1.39	1.31
	H(12.5Hz)	0.82	0.95	0.91	0.77	0.92	0.92	0.88	0.86	0.73	0.85	0.92	0.86	0.81	0.91	0.77
	H(25Hz)	0.96	1.12	1	0.98	1.2	0.98	1.04	0.88	0.94	1.1	1.14	1.07	1.06	1.1	1
hard 0.25 ms^{-2} r.m.s. backrest ON	f_r	2.13	2.13	2.38	2	1.88	2.5	2.38	2.88	4.5	2.38	1.75	2.38	3.13	1.88	2.13
	$H(f_r)$	1.01	1.01	1	1.1	1.03	1.11	1.07	1.12	1.18	1.02	1.08	1.16	1.08	1.15	1.04
	H(12.5Hz)	1.04	0.99	1.07	1.01	1.06	1.04	1.04	1.01	0.86	1.01	0.95	0.98	0.91	1.05	0.94
	H(25Hz)	1.22	1.28	1.2	1.15	1.25	1.2	1.15	1.14	1.09	1.22	1.24	1.21	1.17	1.26	1.21
hard 1 ms^{-2} r.m.s. backrest ON	f_r	2.38	3	2.5	3	2.88	2.5	2.88	3.25	4.13	3	2.5	3.5	3	2.38	3.63
	$H(f_r)$	1.27	1.24	1.26	1.24	1.15	1.27	1.23	1.18	1.27	1.31	1.23	1.21	1.2	1.31	1.18
	H(12.5Hz)	0.93	1.03	1	0.95	1	1	0.95	0.97	0.84	0.97	0.99	0.98	0.91	0.98	0.87
	H(25Hz)	1.09	1.17	1.07	1.14	1.19	1.04	1.13	0.98	1.06	1.19	1.24	1.12	1.18	1.17	1.12

9.2 Fore-and-aft apparent mass - Effect of backrest, seating and vibration magnitude

Apparent masses on hard, soft and rigid seats have similar shapes, showing large inter-subject variability. In the 'backrest OFF', low magnitude test, three vibration modes were apparent in the frequency range 0–7 Hz. The first vibration mode was at about 0.7 Hz. The second vibration mode was at about 2-3 Hz, while the third appeared in the region of 5 to 7 Hz. In the high magnitude test (1 ms^{-2} r.m.s.) there were two peaks appearing. They seemed to be the first and second peak of the low magnitude test that shifted towards lower frequencies. The third peak seemed to

disappear when increasing magnitude of vibration. The phase plots also suggests the presence of three resonances. Coherence functions had values close to unity in the range from 0.5 to 20 Hz. Median curves showed two main resonance peaks: one distinct at about 1 Hz and one, probably due to the existence of different highly damped modes, in the range of 3-5 Hz. When increasing the input level to 1 ms^{-2} r.m.s. resonance frequencies shifted towards lower frequencies, as in the case of a softening nonlinear system. At both magnitudes, the moduli on the rigid seat were bigger. The median apparent mass on the hard foam did not show the second peak of resonance, which is probably smeared out by the statistical process.

In the 'backrest ON' condition, there was one main resonance, whose peak was in the range 2-7 Hz. Individual data suggested the possible presence of other resonances close to the main one, but they were difficult to identify because the modes are highly damped. The main peak shifted towards lower frequencies when increasing the vibration magnitude. Phase plots suggest that the human body behaves like a single degree-of-freedom system. Coherency functions have values close to unity in the range from 0.5 to 23 Hz and drop just before 25 Hz.

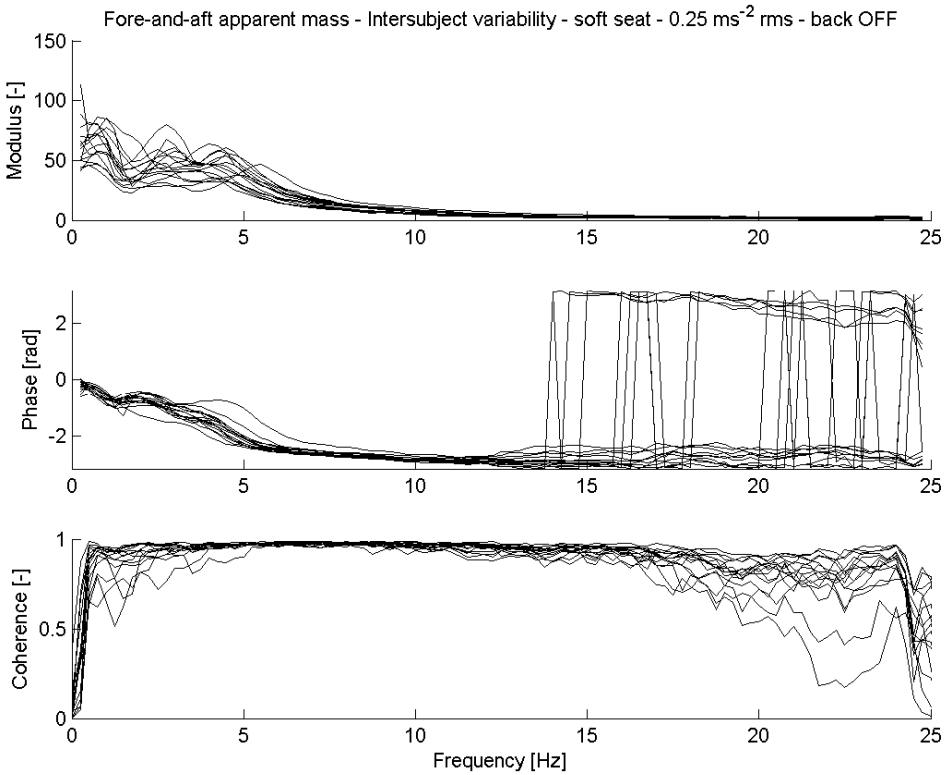

Figure 9.15: fore-and-aft apparent mass inter-subject variability

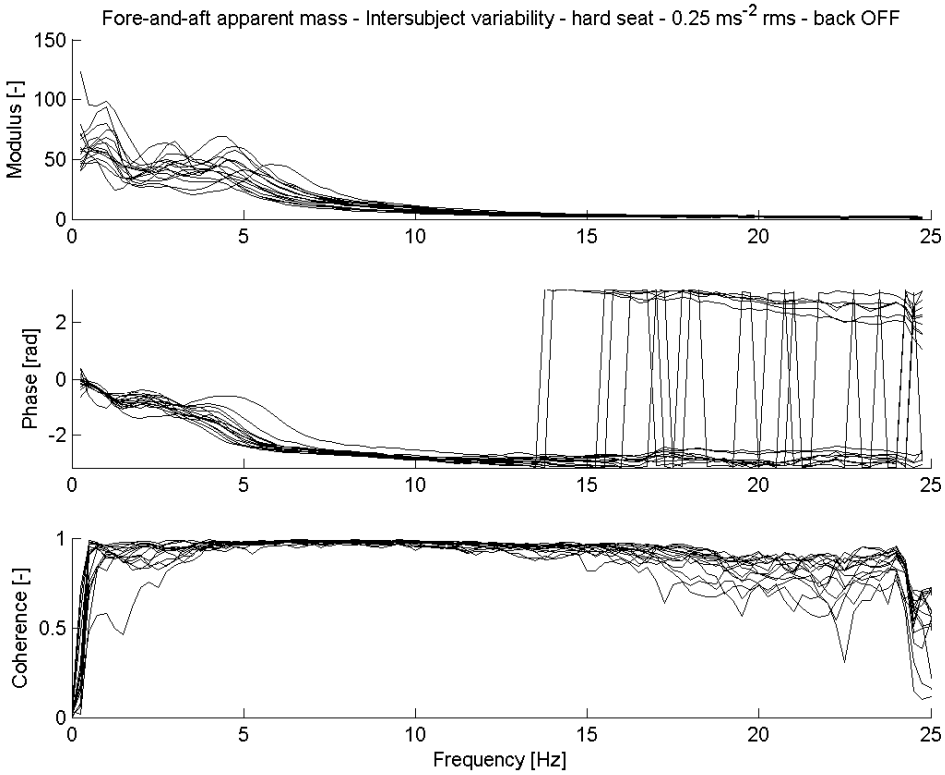

Figure 9.16: fore-and-aft apparent mass inter-subject variability

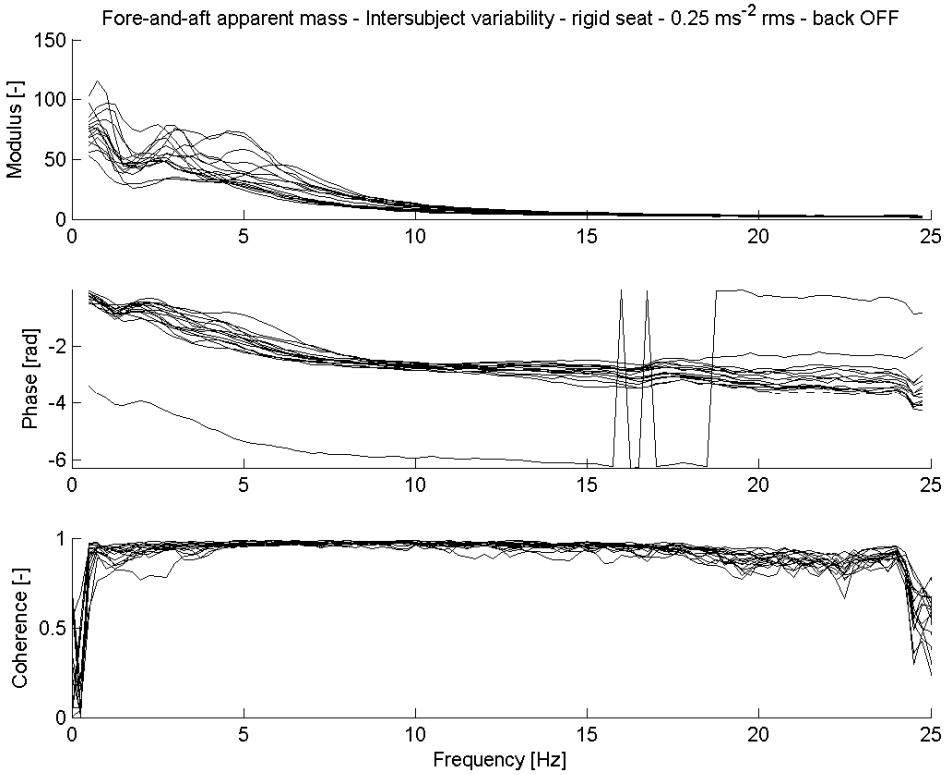

Figure 9.17: fore-and-aft apparent mass inter-subject variability

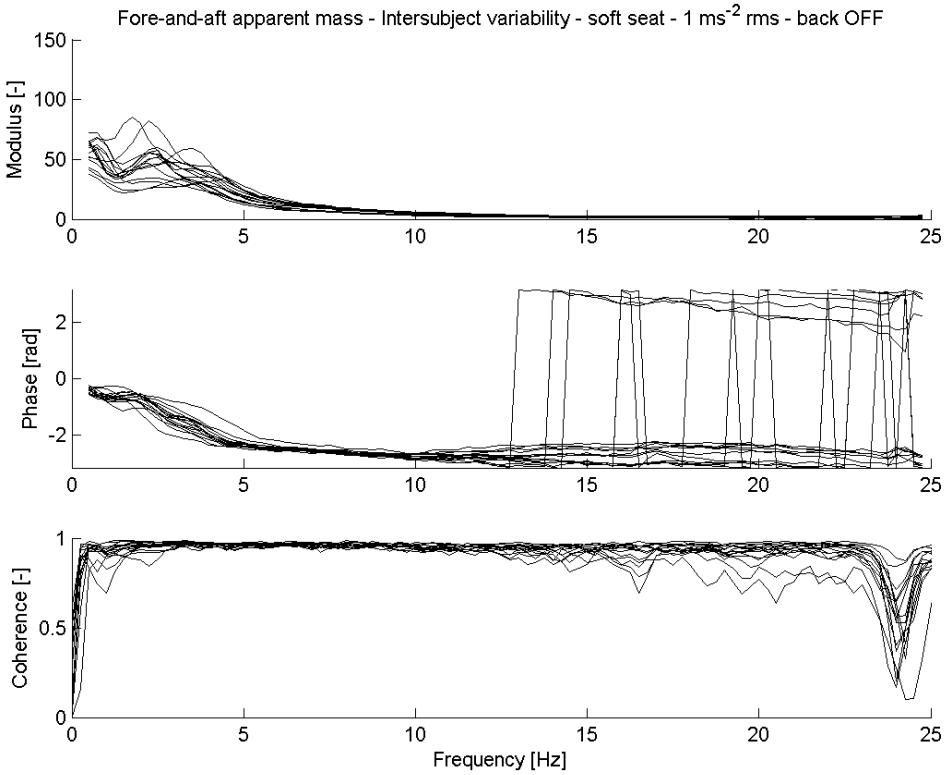

Figure 9.18: fore-and-aft apparent mass inter-subject variability

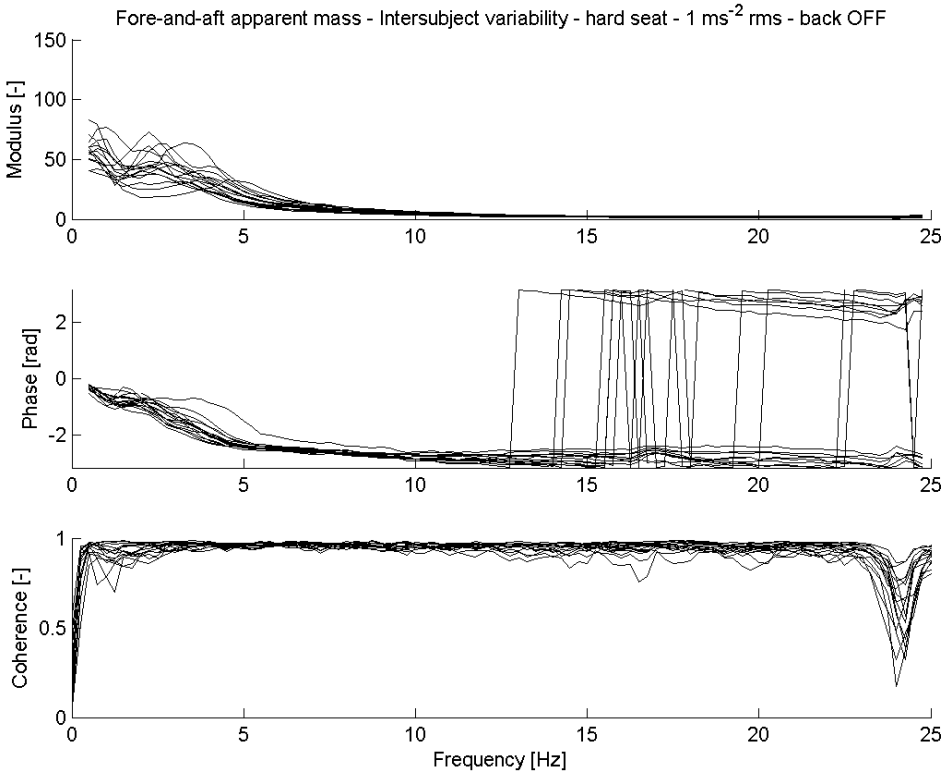

Figure 9.19: fore-and-aft apparent mass inter-subject variability

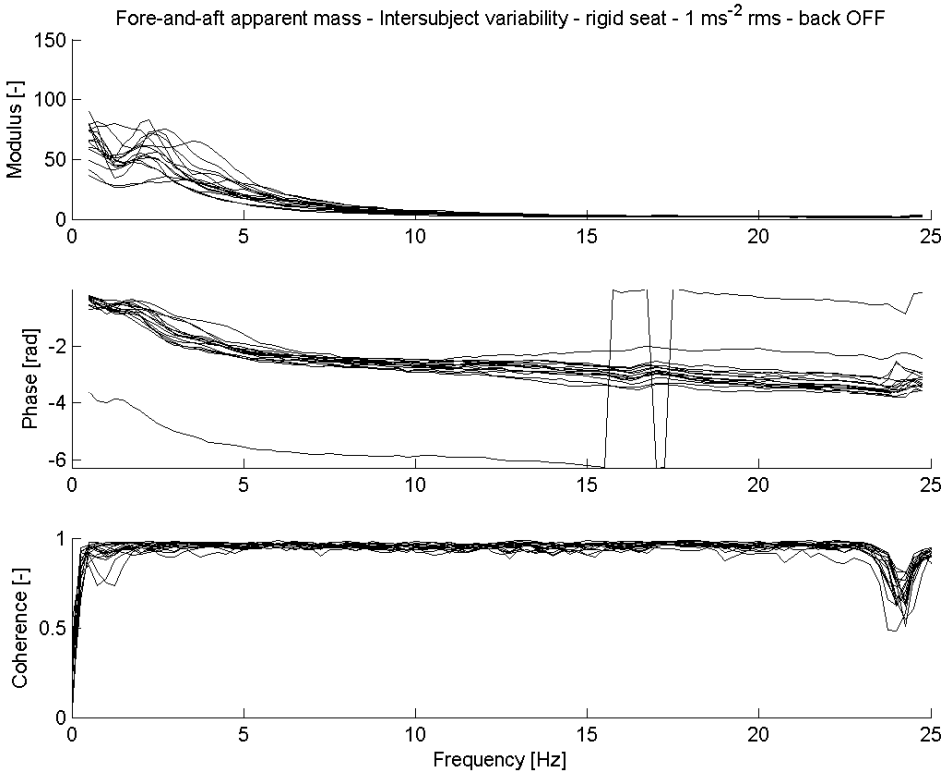

Figure 9.20: fore-and-aft apparent mass inter-subject variability

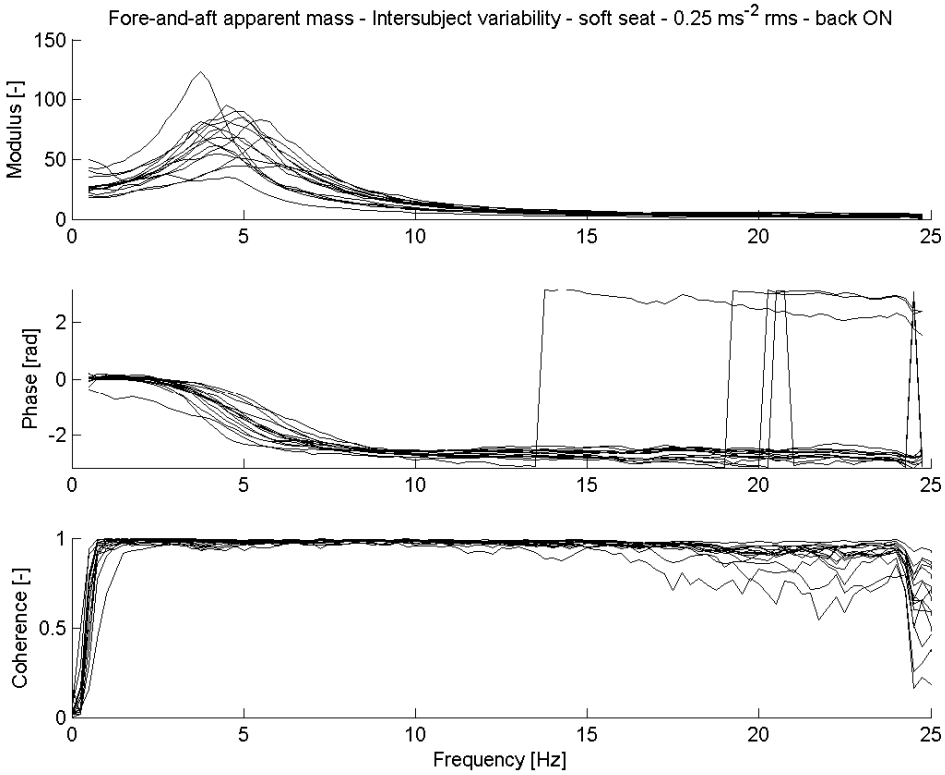

Figure 9.21: fore-and-aft apparent mass inter-subject variability

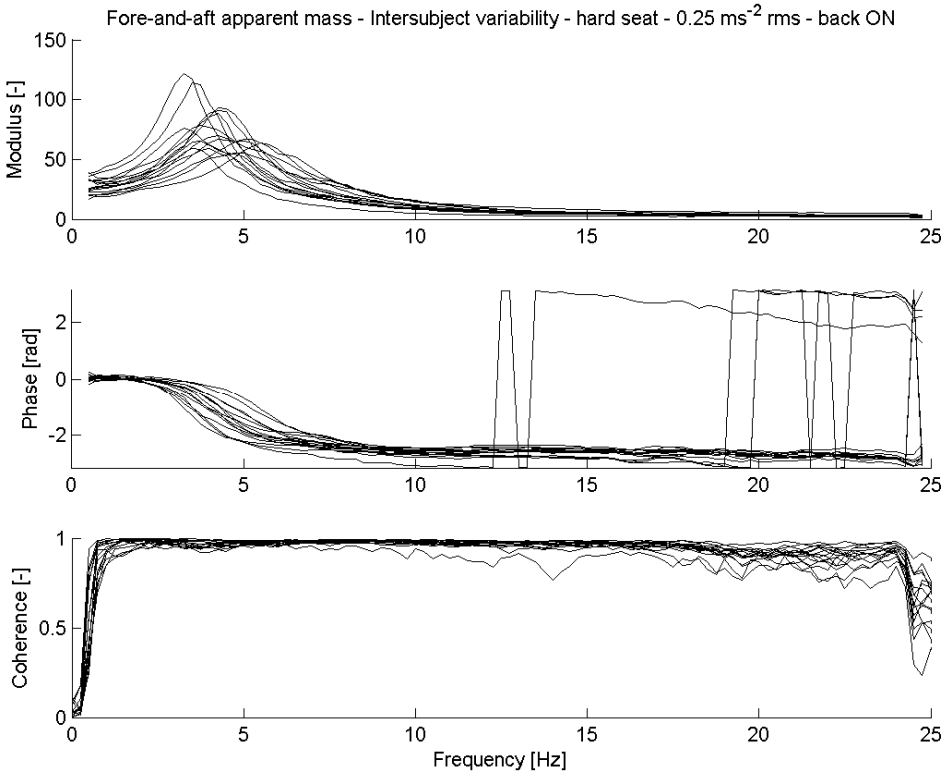

Figure 9.22: fore-and-aft apparent mass inter-subject variability

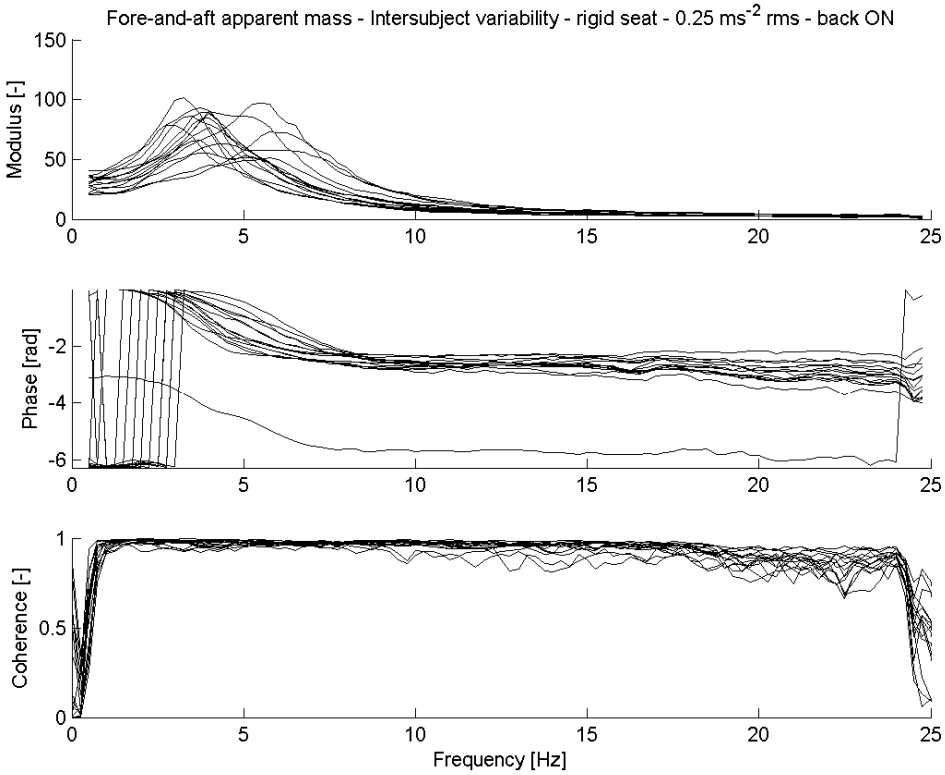

Figure 9.23: fore-and-aft apparent mass inter-subject variability

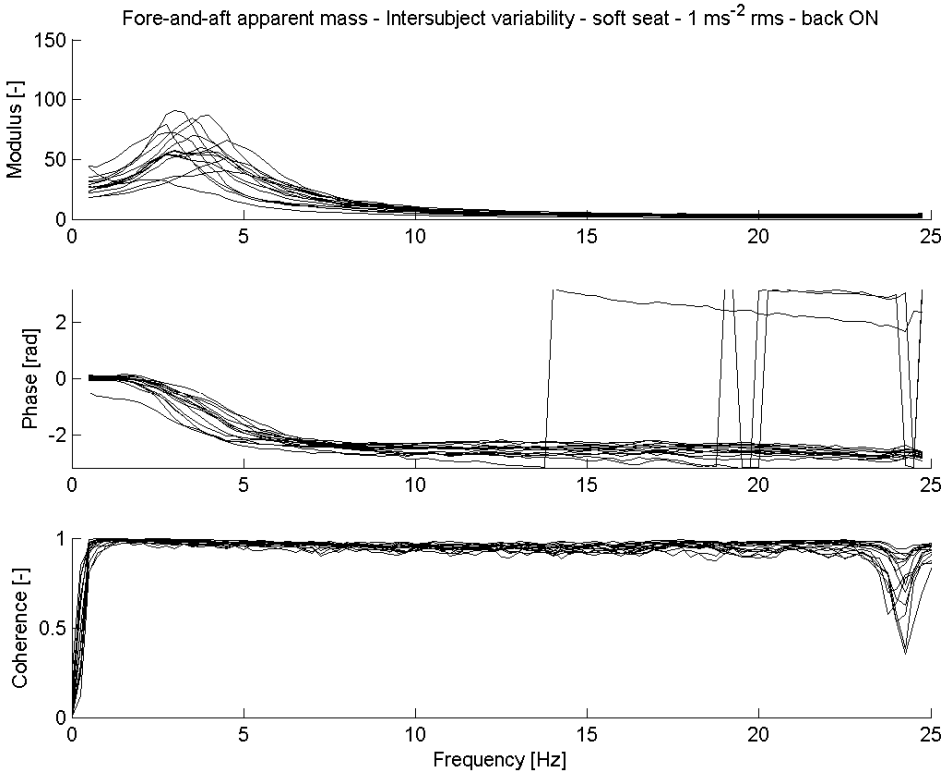

Figure 9.24: fore-and-aft apparent mass inter-subject variability

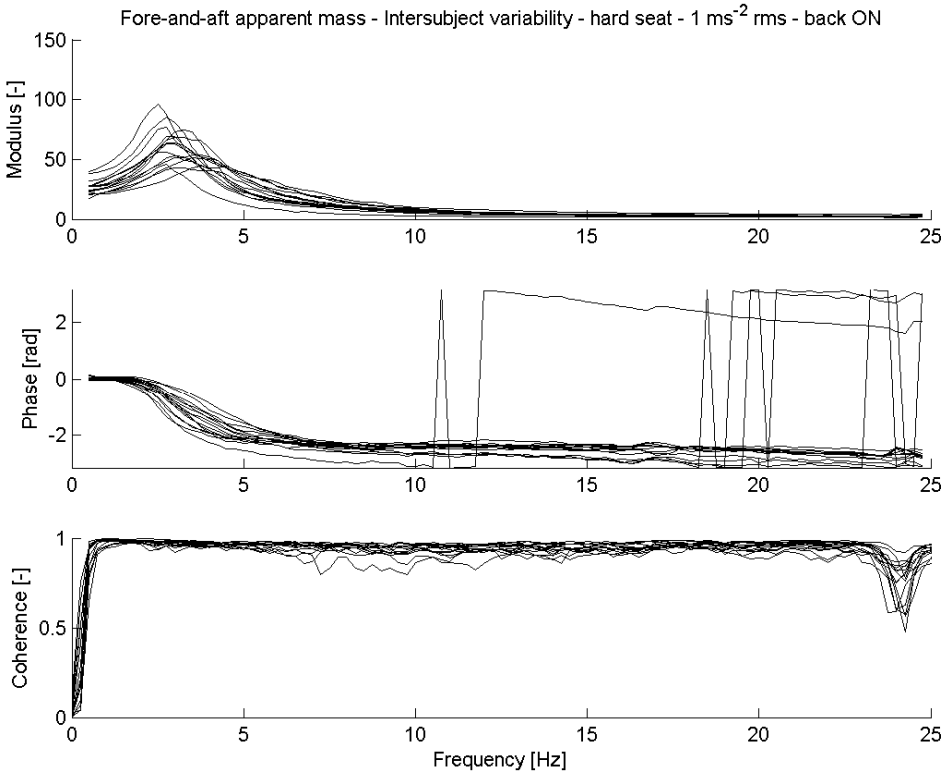

Figure 9.25: fore-and-aft apparent mass inter-subject variability

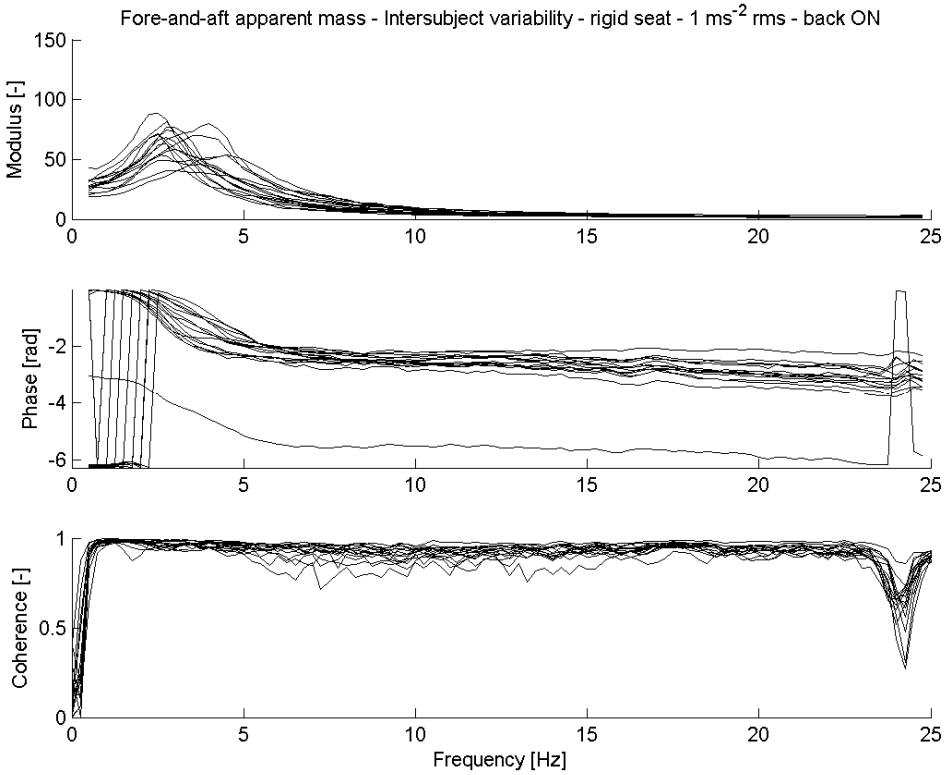

Figure 9.26: fore-and-aft apparent mass inter-subject variability

Statistical test are carried on the 'backrest ON' condition only, because of the difficulty in identifying peaks and tracking them through the different tests in the 'backrest OFF' case. Due to data acquisition problems, the results of subject no. 11 are removed from the test, which is therefore performed on the remaining 14 subjects. *Wilcoxon matched pairs signed rank* non-parametric statistical test (Siegel, 1988) is performed on the main resonance frequency to test the effect of seating condition on the resonance frequency of the apparent mass. Results are presented in Table 9.6: in bold significant tests.

Table 9.6: Wilcoxon test on fore-and-aft apparent mass resonance frequency

vibration magnitude	0.25 ms^{-2} rms			1 ms^{-2} rms		
seat	soft vs. rigid	hard vs. rigid	hard vs. soft	soft vs. rigid	hard vs. rigid	hard vs. soft
Significance (2-tailed)	**.032**	.964	**.007**	**.037**	.179	.096
	>	-	**<**	**>**	-	-

Wilcoxon test was also performed on the value of apparent mass at resonance. No significance ($p > 0.05$) was obtained in any of the tests.

Table 9.7: Wilcoxon test on fore-and-aft apparent mass modulus at resonance

vibration magnitude	0.25 ms^{-2} rms			1 ms^{-2} rms		
seat	soft vs. rigid	hard vs. rigid	hard vs. soft	soft vs. rigid	hard vs. rigid	hard vs. soft
Significance (2-tailed)	.397	.975	.551	.875	.433	.363
	-	-	-	-	-	-

The effect of vibration magnitude on the fore-and-aft human body apparent mass is tested via Wilcoxon non-parametric test, confronting the test at 0.25 and 1 ms^{-2}. Higher magnitude gave lower values of resonance frequency, consistent with a softening behaviour, and lower apparent mass at resonance, suggesting an increase in human body damping.

Table 9.8: Wilcoxon test on fore-and-aft apparent mass resonance frequency: effect of magnitude

seat	rigid	hard	soft
Significance (2-tailed)	0.001	0.001	0.001

Table 9.9: Wilcoxon test on fore-and-aft apparent mass modulus at resonance: effect of magnitude

seat	rigid	hard	soft
Significance (2-tailed)	0.001	0.003	0.001

9.3.1 Linear effects of fore-and-aft vibration at the seat base on vertical vibration at the seat pan

This section investigates whether the spectrum of vertical, z, vibration $G_{zz}(f)$ on the seat pan is affected by the addition of vibration in fore-and-aft, x, direction. A general two-input-one-output model that takes into account the correlation between inputs is used (Bendat, 1980). Figure 9.27 shows the z to z and x to z transmissibility inter-quartile ranges when adding 0.25 ms^{-2} rms x-axis vibration to 0.25 ms^{-2} rms z-axis vibration and associated median coherencies. The plots represent linear relationships between input x and z vibration and the total vertical output spectrum $G_{zz}(f)$. Partial coherency functions represent the part of the output spectrum due to the specific input (Bendat, 1980). The contribution of x-axis vibration to $G_{zz}(f)$ is minimal. Same remarks can be applied to the case of 1 ms^{-2} rms x-axis vibration added to 1.0 ms^{-2} rms z-axis vibration (Figure 9.28) and for the harder foam (not reported). Multiple coherency functions are close to unity, showing that the noise to signal ratio in the measurements or the non-linear contribution of x to z vibration was. A different scenario is encountered when adding 1 ms^{-2} r.m.s. x-axis vibration to 0.25 ms^{-2} r.m.s. z-axis vibration. The contribution of z vibration to the z output spectrum G_{zz} is prevalent at low frequencies, while the x vibration is more important at high frequencies, since z to z transmissibility at high frequencies is fairly low. Figure 9.30 shows that the x vibration becomes even more dominant when adding backrest contact, which represents another input in x direction. All the x to z curves have a peak at about 5 Hz (that might correspond with the main resonance frequency of the vertical and cross-axis human body apparent mass), while then they are almost constant for frequencies for 7 to 25 Hz. Considering the fairly low effect of cross-coupling and the possibility of the results being biased from accelerometers misalignment and cross-talk, no statistical analyses are performed.

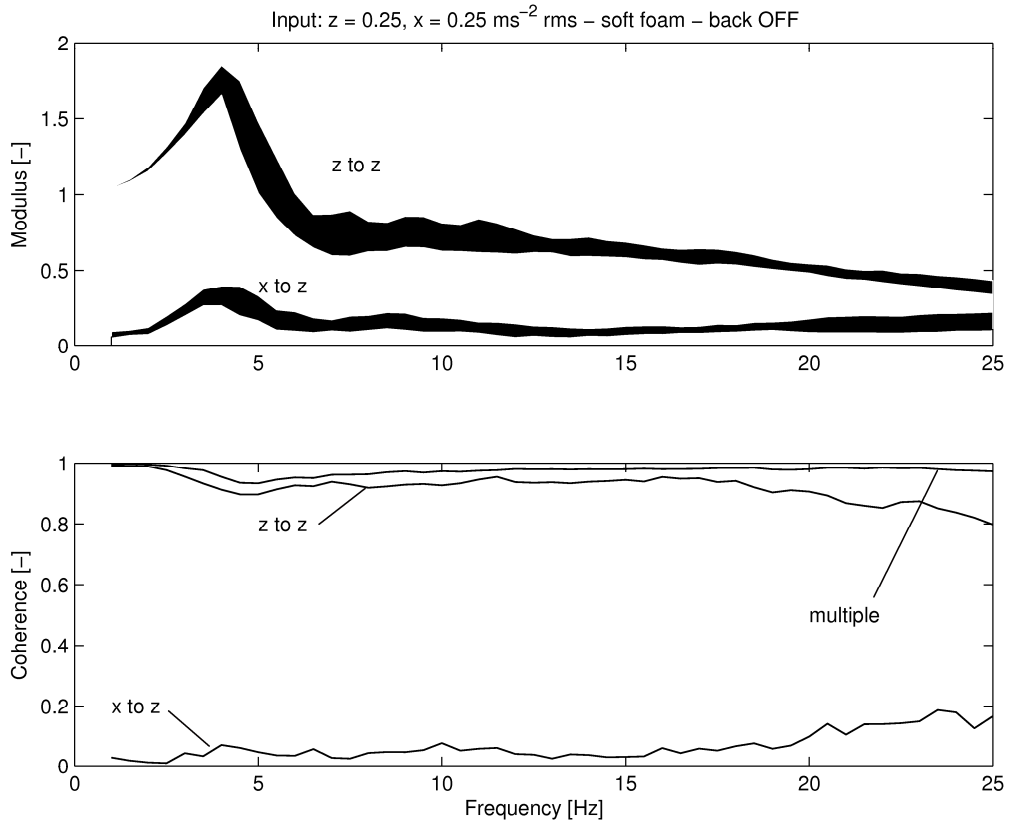

Figure 9.27: transmissibility inter-quartile range and coherence median for vertical and cross-axis x to z seat transmissibility

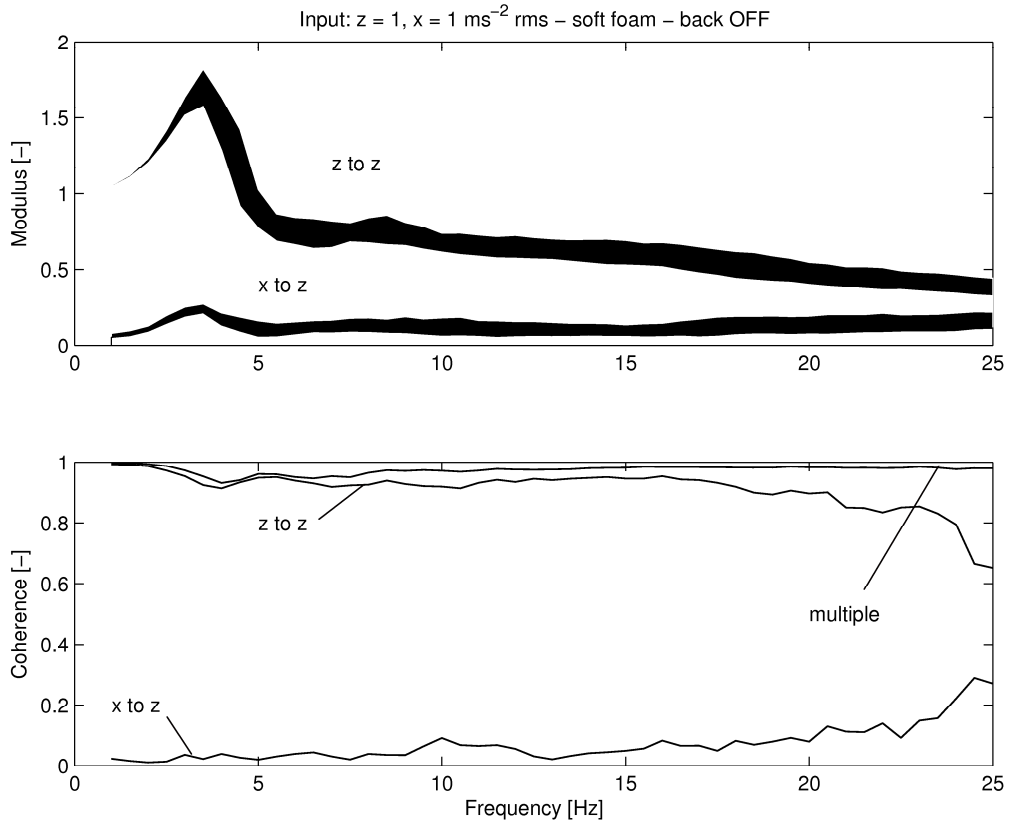

Figure 9.28: transmissibility inter-quartile range and coherence median for vertical and cross-axis x to z seat transmissibility

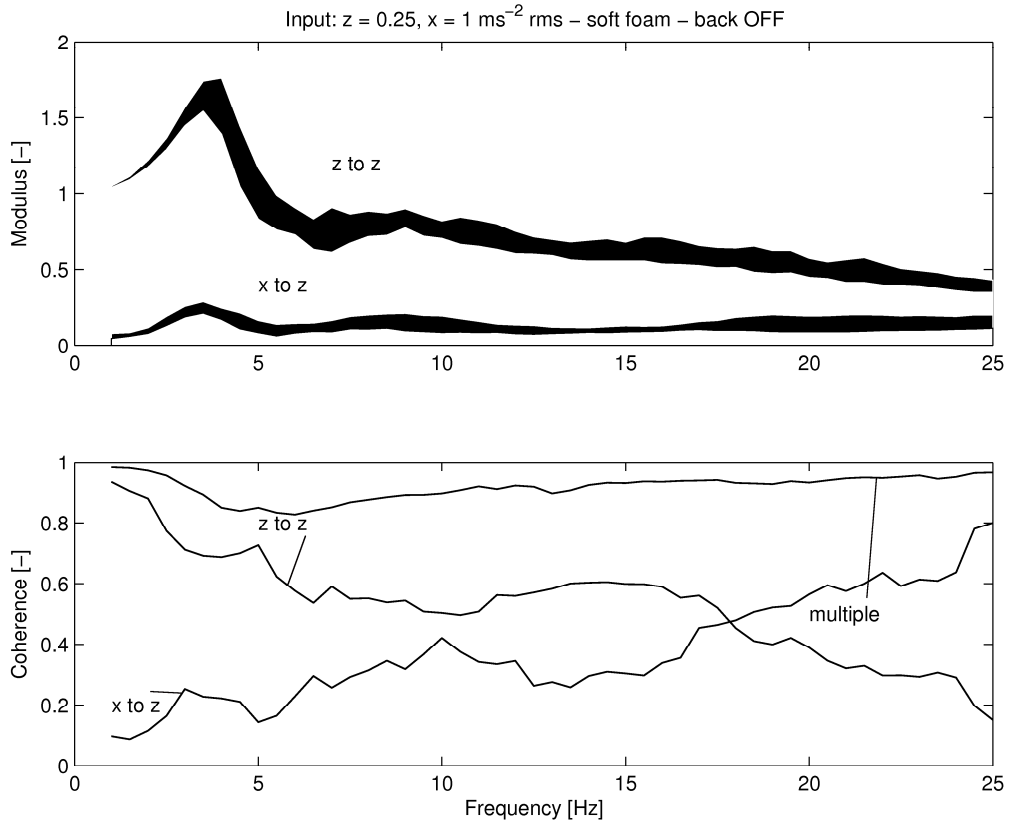

Figure 9.29: transmissibility inter-quartile range and coherence median for vertical and cross-axis x to z seat transmissibility

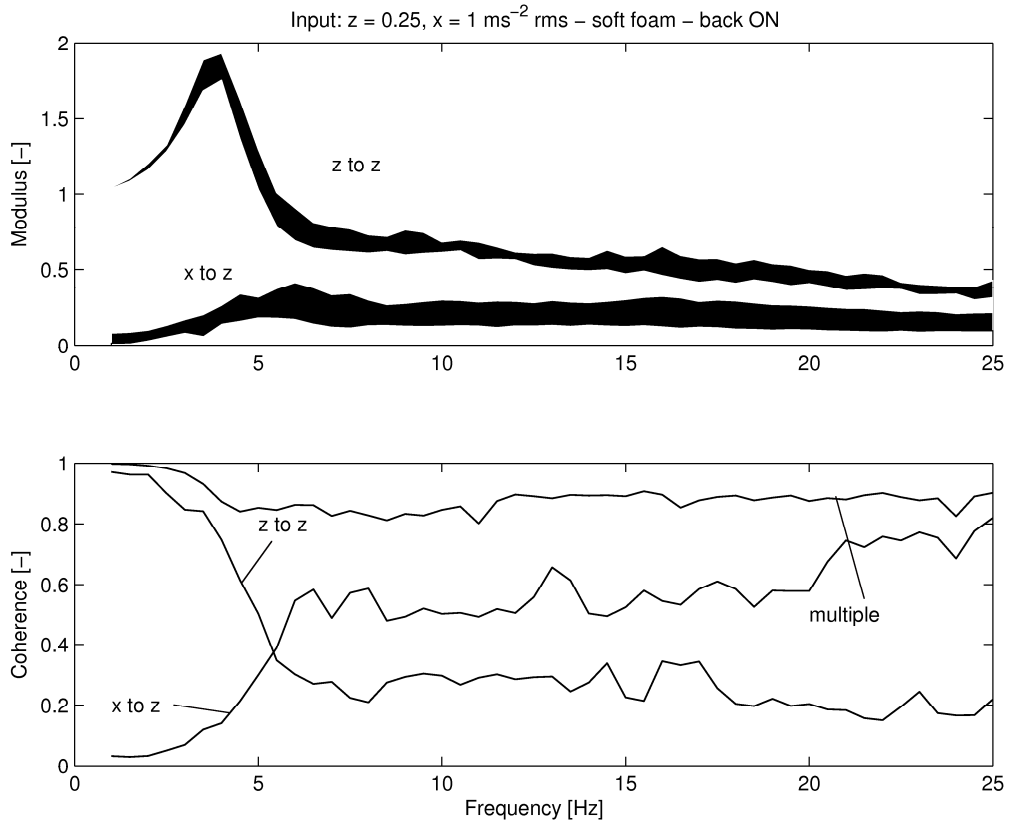

Figure 9.30: transmissibility inter-quartile range and coherence median for vertical and cross-axis x to z seat transmissibility

9.3.2 Linear effects of vertical vibration at the seat base on fore-and-aft vibration at the seat pan

This section investigates whether the spectrum of the fore-and-aft vibration $G_{xx}(f)$ on the seat pan is affected by the addition of vibration in vertical, z, direction. A general two-input-one-output model is used, taking into account the correlation between inputs (Bendat, 1980). Figures 9.31 to 9.34 show the linear relationships between x and z input vibration and the total x output spectrum $G_{xx}(f)$. Figure 9.31 shows the x to x and z to x-axis transmissibility inter-quartile ranges for the 15 subjects when adding 0.25 ms^{-2} rms z vibration to 0.25 ms^{-2} rms x vibration. Effects of z vibration on x output are minimal. Same results were found for the same stimulus on the hard foam and also when adding 1 ms^{-2} rms z vibration to 1 ms^{-2} rms x vibration for the soft and hard foam. The results are different when adding 1 ms^{-2} r.m.s. vertical vibration to 0.25 ms^{-2} rms fore-and-aft vibration, which thing is likely to happen in real transport environments. As shown in Figure 9.32 the z input can contribute to up to the 50% of the x output at frequencies about 4 Hz. No high frequency component is encountered in this case (if

compared with the x = 1, z = 0.25 ms^{-2} r.m.s. test in the previous paragraph). The same effect is present, although is less evident, in the hard foam (Figure 9.33). The 'backrest ON' condition gave similar results to the 'backrest OFF' one in the case of equal magnitude in the vertical and horizontal axes (x = 0.25, z = 0.25 and x = 1, z = 1 ms^{-2} r.m.s.). In the case of x = 0.25, z = 1 ms^{-2} r.m.s., 'backrest ON', the contribution of z input to x axis was of about the 30% at frequencies higher than 5 Hz.

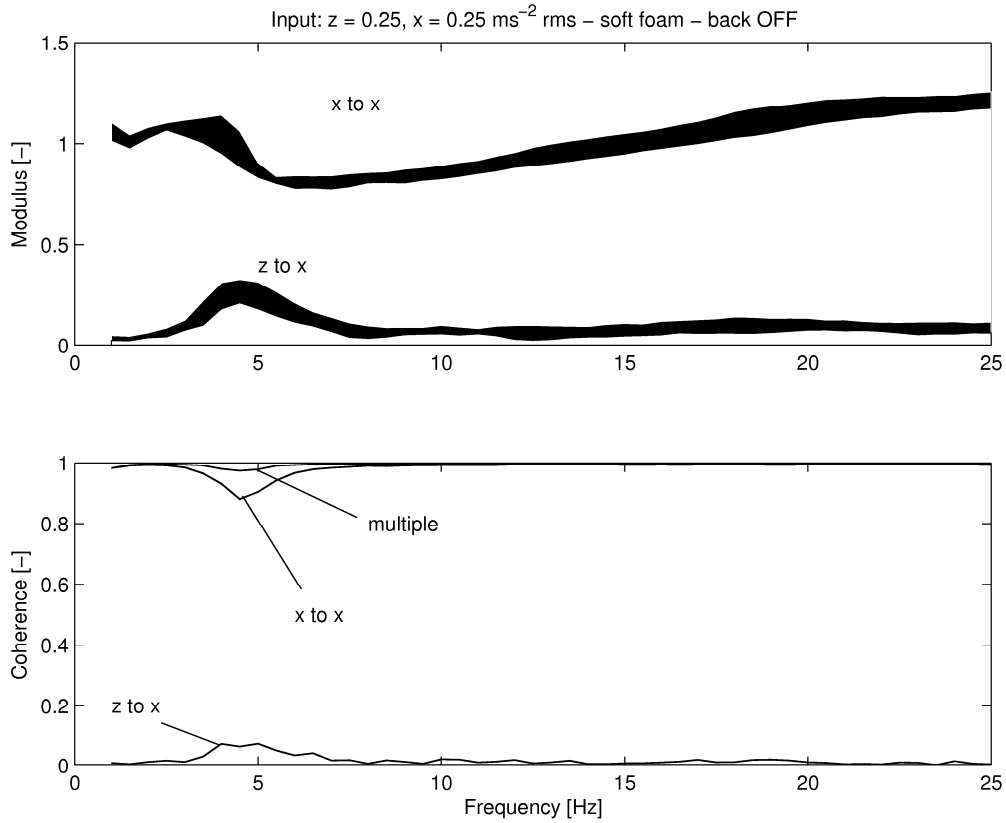

Figure 9.31: transmissibility inter-quartile range and coherence median for fore-and-aft and cross-axis z to x seat transmissibility

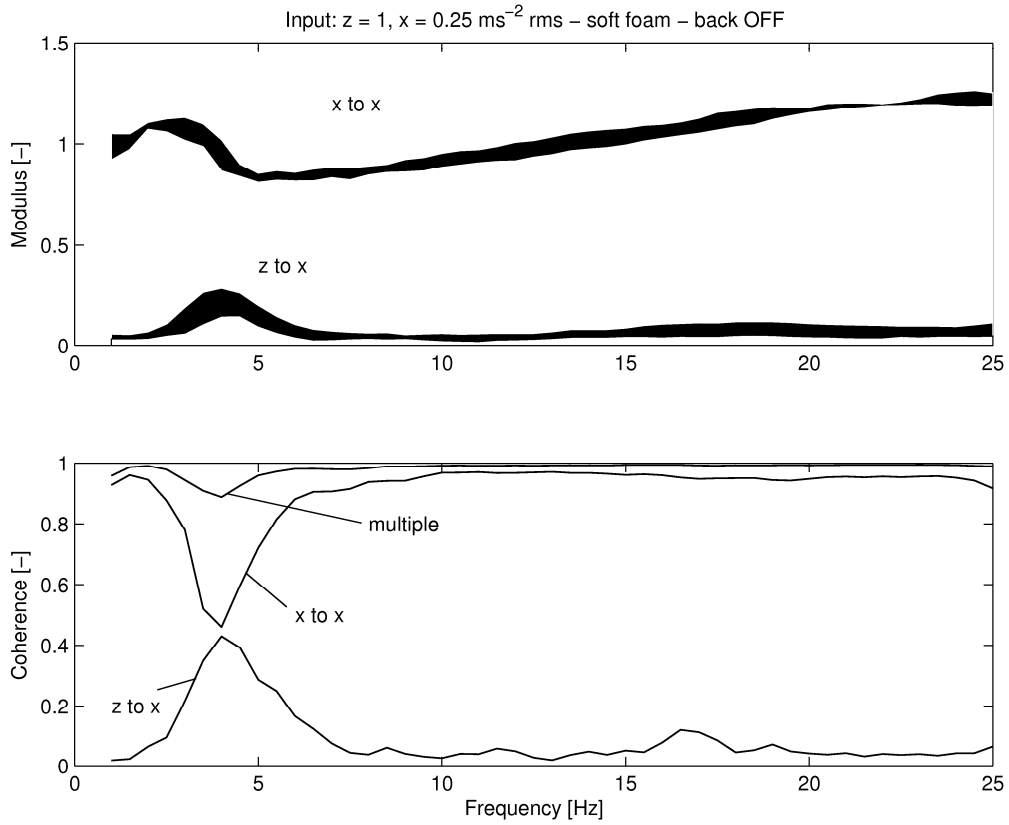

Figure 9.32: transmissibility inter-quartile range and coherence median for fore-and-aft and cross-axis z to x seat transmissibility

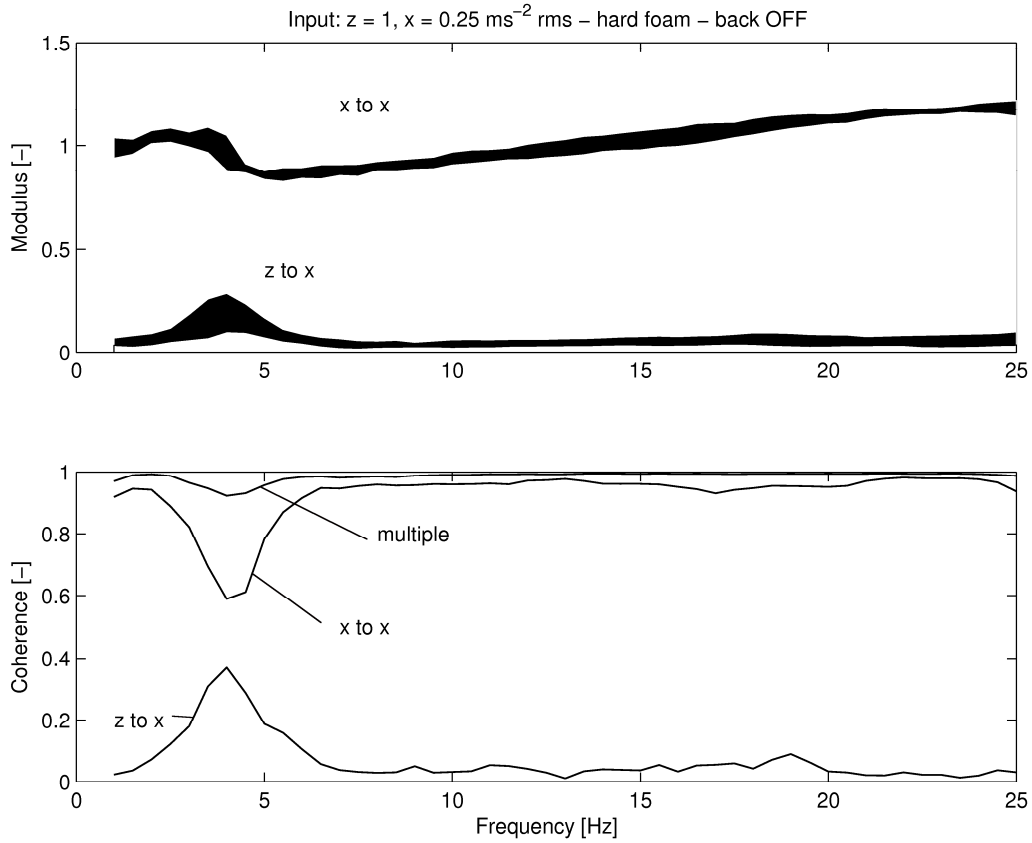

Figure 9.33: transmissibility inter-quartile range and coherence median for fore-and-aft and cross-axis z to x seat transmissibility

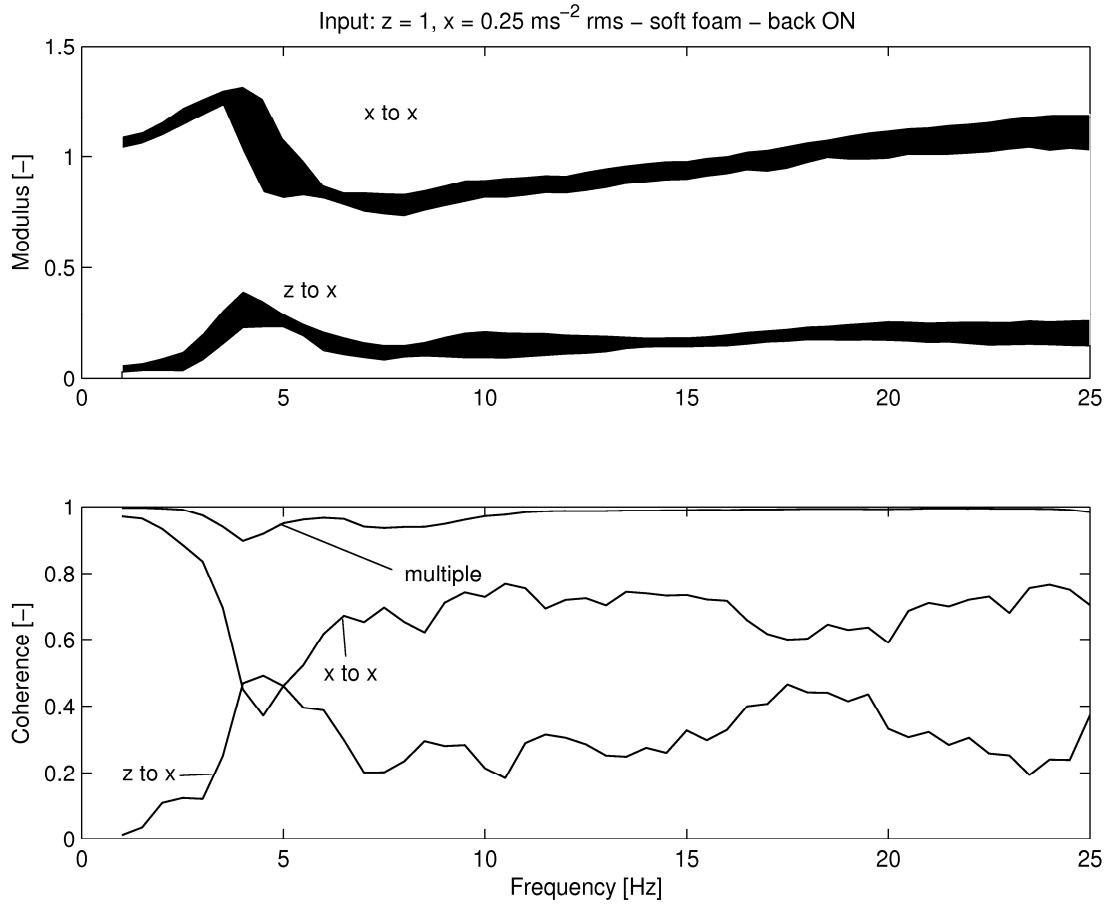

Figure 9.34: transmissibility inter-quartile range and coherence median for fore-and-aft and cross-axis z to x seat transmissibility

9.3.3 Non-linear effects of vertical vibration on in-line fore-and-aft transmissibility

This section investigates the non-linear effects of dual-axis vibration on fore-and-aft transmissibility. Linear effects, which are treated in 9.3.1 are removed by means of conditioned analysis (Bendat, 1980). Any significant changes in x transmissibility are due to nonlinearities in human body and polyurethane foam, since any linear effects of fore-and-aft vibration are removed (see 8.4.2). In this case, $x_1(t)$ is the vertical vibration, $x_2(t)$ and $y(t)$ are, respectively, the fore-and-aft input and output. Median curves show that fore-and-aft input vibration magnitude affects fore-and-aft transmissibility as seen in section 9.1.2. The addition of vertical vibration seems to affect fore-and-aft seat transmissibility, as it can be noticed by comparing median transmissibility curves of tests having the same x and different z inputs.

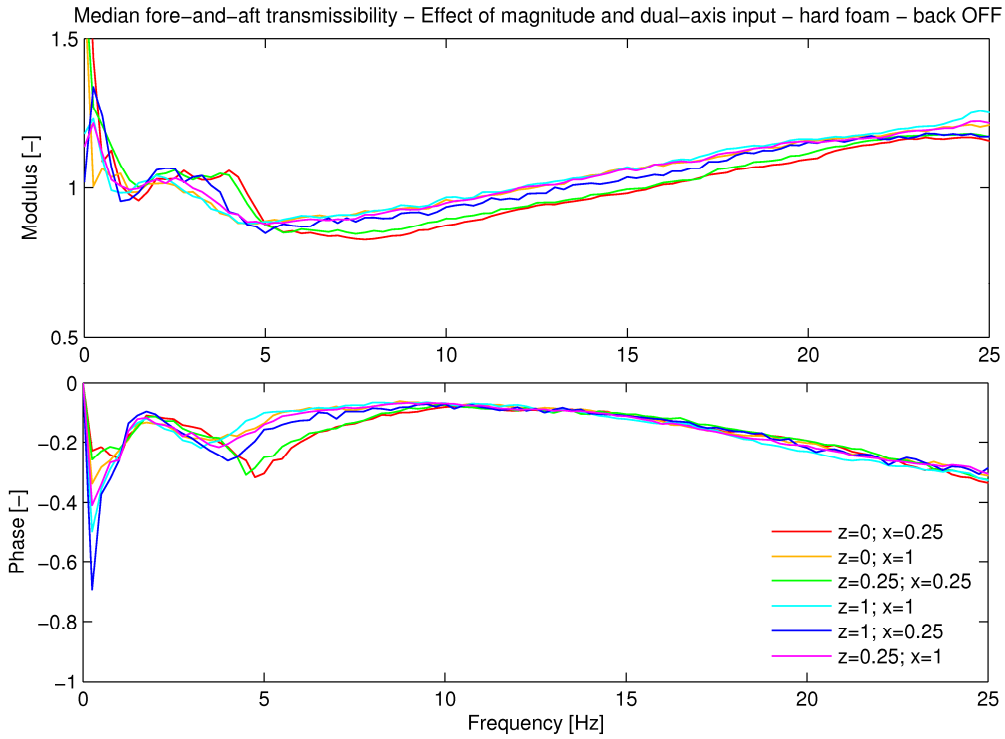

Figure 9.35: values in the legend are in ms^{-2} r.m.s.

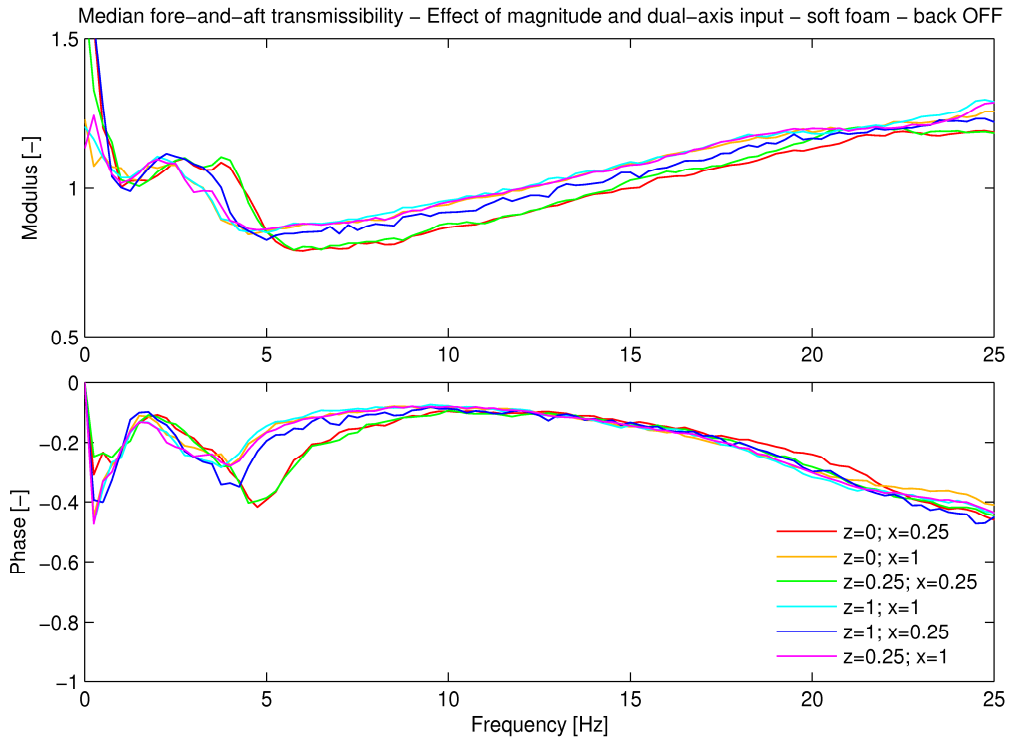

Figure 9.36: values in the legend are in ms^{-2} r.m.s.

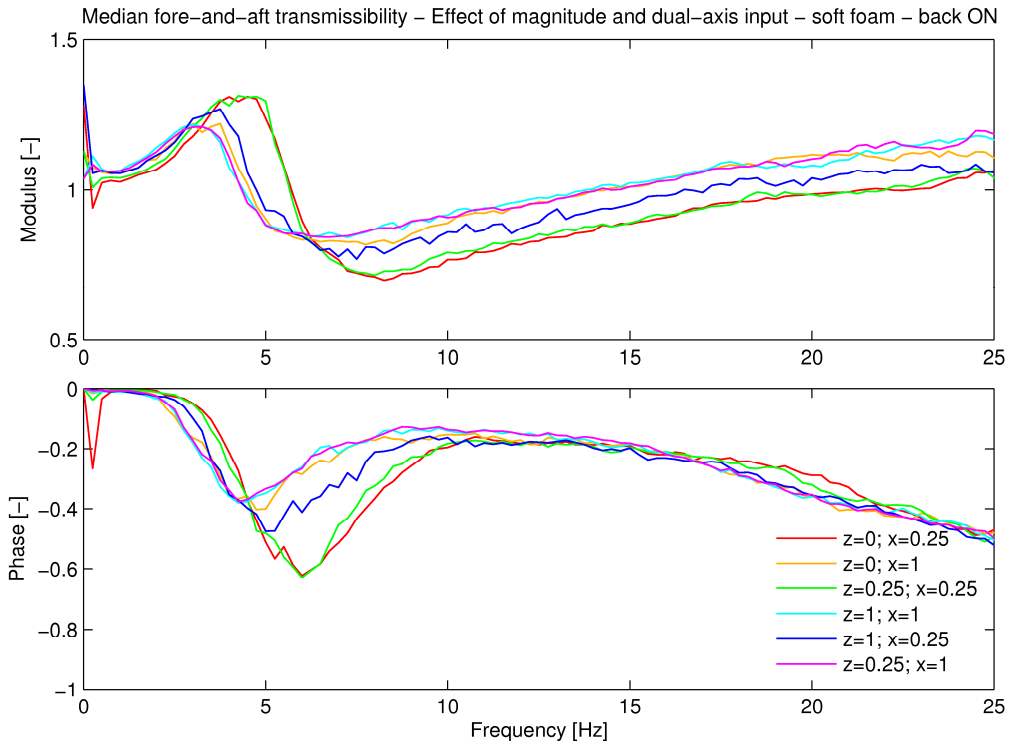

Figure 9.37: values in the legend are in ms^{-2} r.m.s.

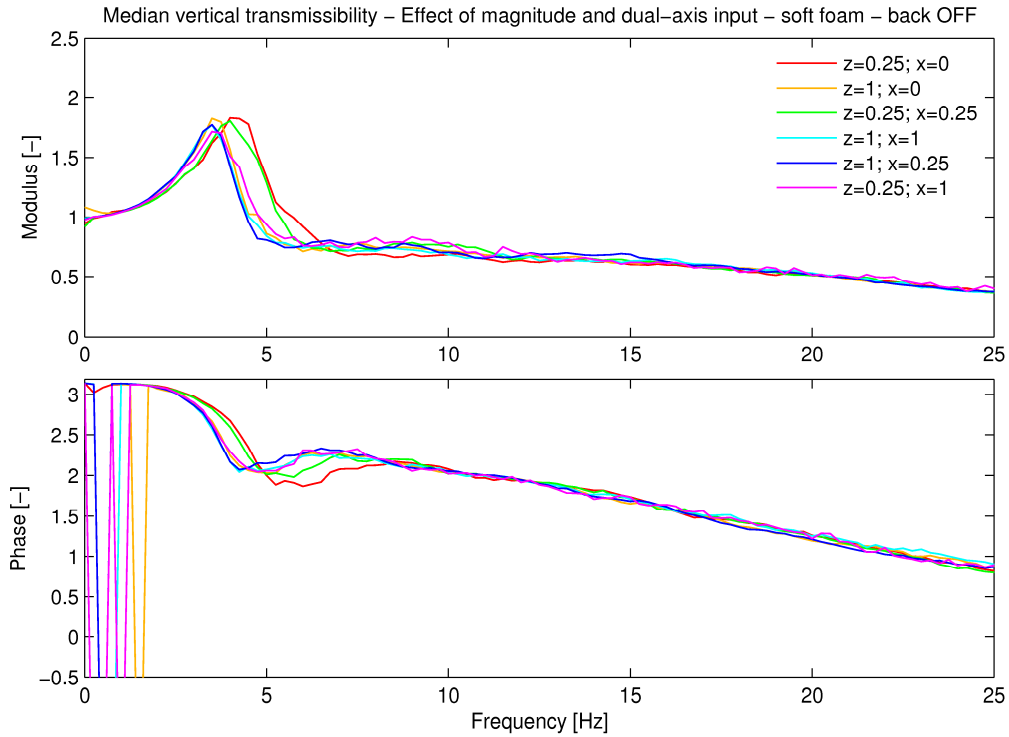

Figure 9.38: values in the legend are in ms^{-2} r.m.s.

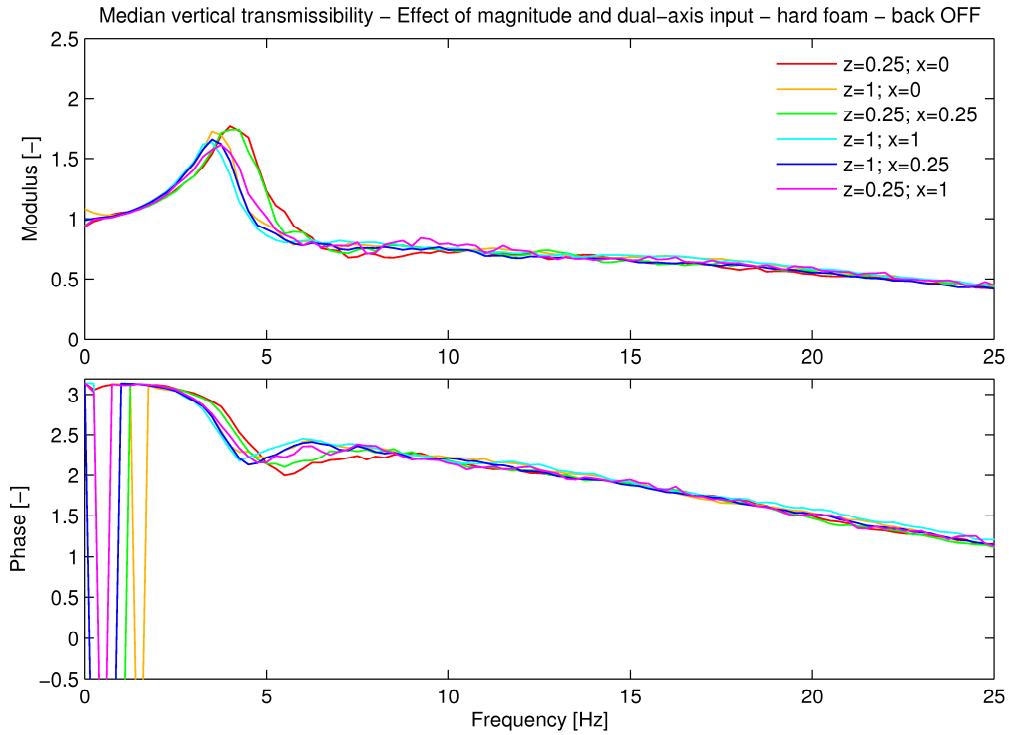

Figure 9.39: values in the legend are in ms^{-2} r.m.s.

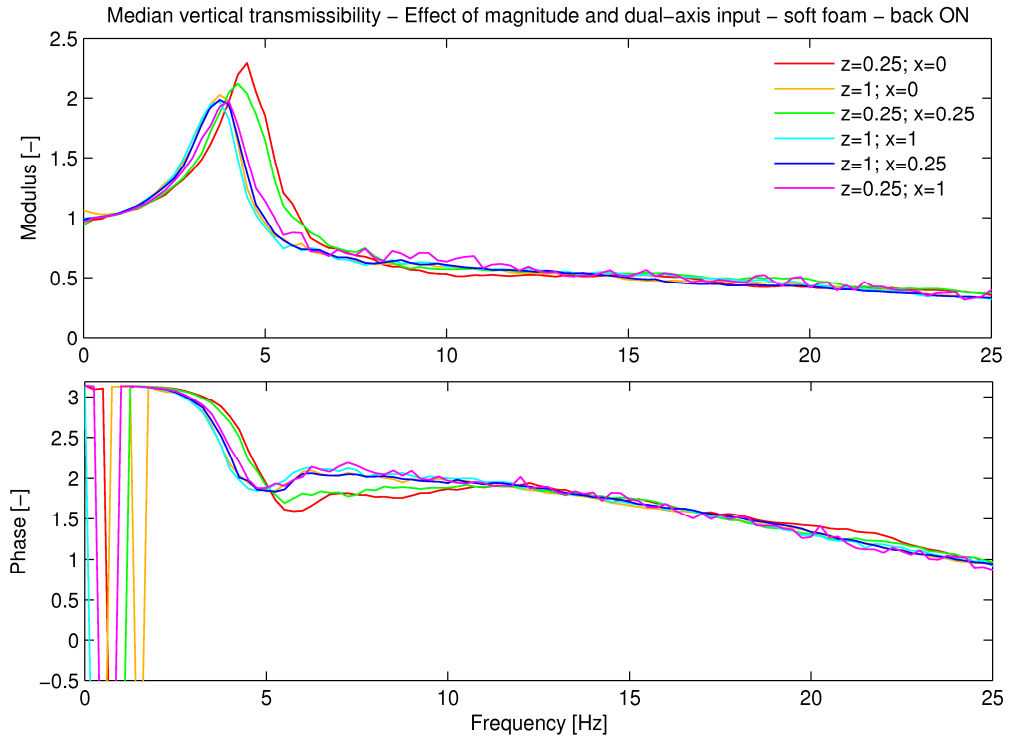

Figure 9.40: values in the legend are in ms^{-2} r.m.s.

The effects of simultaneous vertical vibration on the in-line fore-and-aft transmissibility, $H_{xx(f)}$, are investigated by means of *Friedman two way analysis of variance* and *Wilcoxon matched pairs signed rank* non-parametric statistical tests (Siegel, 1988). Four parameters are chosen to investigate the nonlinearity of the seat-human system: (i) frequency and (ii) magnitude of the second resonance and on the values of (iii) transmissibility at 12.5 and (iv) at 25 Hz (respectively f_r, $H(f_r)$, $H(12.5)$, $H(25)$).

Table 9.10: effect of magnitude and dual-axis vibration input (values in ms^{-2}) on fore-and-aft seat transmissibility f_r and $H(f_r)$ (Wilcoxon p values: in bold significant tests)

		soft foam		soft foam backrest ON		Hard foam	
Stimuli	**overall magnitude**	**fr**	**H(fr)**	**fr**	**H(fr)**	**Fr**	**H(fr)**
[ms^{-2} r.m.s.]	**[ms^{-2} r.m.s.]**	**[Hz]**	**[-]**	**[Hz]**	**[-]**	**[Hz]**	**[-]**
z=0; x =0.25	**0.25**	-	-	-	-	<	-
vs	vs						
z=0.25; x = 0.25	**0.5**	0.719	0.496	0.385	0.394	**0.004**	0.57
z=0; x =0.25	**0.25**	>	-	>	>	>	-
vs	vs						
z=1; x = 0.25	**1.25**	0.22	0.394	**0.001**	**0.003**	**0.001**	0.57
z=0.25; x =1	**1.25**	-	-	-	>	-	-
vs	vs						
z=0; x = 1	**1**	0.691	0.46	0.329	**0.008**	0.552	0.1
z=0; x =1	**1**	-	-	>	>	-	-
vs	vs						
z=1; x = 1	**2**	0.478	0.496	0.38	**0.023**	0.176	0.173
z=0.25; x =0.25	**0.5**	>	-	>	>	-	-
vs	vs						
z=1; x = 0.25	**1.25**	0.12	0.427	**0.001**	**0.012**	0.209	0.532

Table 9.11: effect of magnitude and dual-axis vibration input (values in ms^{-2}) on fore-and-aft seat transmissibility *H(12.5)* and *H(25)* (Wilcoxon *p* values: in bold significant tests)

		soft foam		soft foam backrest ON		hard foam	
stimuli	**overall magnitude**	**H(12.5)**	**H(25)**	**H(12.5)**	**H(25)**	**H(12.5)**	**H(25)**
[ms^{-2} r.m.s.]	**[ms^{-2} r.m.s.]**	**[Hz]**	**[Hz]**	**[Hz]**	**[Hz]**	**[Hz]**	**[Hz]**
z=0; x =0.25 vs **z=0.25; x = 0.25**	**0.25** vs **0.5**	- 0.691	- 0.955	- 0.691	- 0.256	< **0.008**	- 0.125
z=0; x =0.25 vs **z=1; x = 0.25**	**0.25** vs **1.25**	< **0.001**	< 0.27	< **0.001**	- 0.053	< **0.001**	> 0.061
z=0.25; x =1 vs **z=0; x = 1**	**1.25** vs **1**	- 0.363	< **0.001**	- 0.363	< **0.001**	- 0.281	< **0.009**
z=0; x =1 vs **z=1; x = 1**	**1** vs **2**	< **0.008**	< **0.001**	< **0.008**	< **0.004**	- 0.173	< **0.001**
z=0.25; x =0.25 vs **z=1; x = 0.25**	**0.5** vs **1.25**	< **0.001**	< **0.017**	< **0.001**	< **0.001**	< **0.001**	- 0.69

Testing (z=0; x=0.25 ms^{-2} r.m.s.) vs. (z=0.25; x=0.25 ms^{-2} r.m.s.) shows that adding 0.25 ms^{-2} r.m.s. vertical vibration had a significant effect only on f_r and *H(12.5)* of the hard foam ($p < 0.05$). When adding z=1 ms^{-2} r.m.s. to (z=0; x =0.25), the 'backrest ON' test become significant ($p < 0.05$). The effect of adding vibration in perpendicular direction is to reduce the resonance frequency f_r and to increase the transmissibility at resonance $H(f_r)$.

Table 9.12 quantifies the differences in horizontal transmissibility due to nonlinearity calculated across some combination of vertical and horizontal motion. It has to be considered that the spectral resolution of the analysis in 0.125 Hz. The shift in resonance frequency, *Δfr*, has a median of 1.25 Hz for the 'backrest OFF' conditions and of 1.38 for the 'backrest ON' condition. The transmissibility at resonance median shift is the 8% for the 'backrest OFF' conditions and the 17% for the backrest on condition. Subjects showing highest nonlinearity had a shift in resonance frequency higher than 2 Hz and a shift in transmissibility in resonance up to the 34% of the vibration input.

Table 9.12: Differences in fore-and-aft transmissibility f_r and $H(f_r)$ across all the tests

	soft foam		soft foam backrest ON		hard foam	
	Δfr	**ΔH(fr)**	**Δfr**	**ΔH(fr)**	**Δfr**	**ΔH(fr)**
median	1.25	0.08	1.38	0.17	1.25	0.08
max	2.13	0.27	2.63	0.34	2.00	0.23
min	0.63	0.02	1.00	0.03	0.38	0.03

9.3.4 Non-linear effects of fore-and-aft vibration on vertical in-line transmissibility

This section investigates the non-linear effects of dual-axis vibration on vertical transmissibility. Linear effects, which are treated in section 9.3.2 are removed by means of conditioned analysis (see 8.4.2). In this case $x_1(t)$ is the fore-and-aft I vibration, $x_2(t)$ and $y(t)$ are, respectively, the vertical input and output.

The addition of horizontal vibration seems to affect vertical seat transmissibility as well, as it can be noticed by comparing tests with the same vertical input. Any significant changes in vertical transmissibility are due to nonlinearities in human body and polyurethane foam, since any linear effects of fore-and-aft vibration are removed from vertical input and output by means of conditioned analysis. *Friedman two way analysis of variance* and *Wilcoxon matched pairs signed rank* are performed on three parameters: (i) main resonance frequency f_{r1}, i.e. the frequency of maximum transmissibility; (ii) the value of transmissibility at the main resonance, $H(f_{r1})$. Results are presented in Table 9.13 and 9.14.

Wilcoxon test (z=0.25; x=0) vs. (z=0.25; x=0.25) shows that adding x=0.25 ms^{-2} r.m.s. had a significant effect on soft foam f_r and $H(f_r)$ and on hard foam f_r ($p < 0.05$). Test (z=0.25; x=0) vs. (z=0.25; x=1) shows that also the 'backrest ON' vertical transmissibility can be influenced by fore-and-aft vibration, but it requires an higher level of fore-and-aft vibration.

Table 9.13: effect of magnitude and dual-axis vibration input (values in ms^{-2}) on vertical seat transmissibility f_r and $H(f_r)$ (Wilcoxon p values: in bold significant tests)

		soft foam		soft foam backrest ON		hard foam	
		fr_1	$H(fr_1)$	fr_1	$H(fr_1)$	fr_1	$H(fr_1)$
z=0.25; x =0 vs **z=0.25; x = 0.25**	0.25 vs 0.5	> **0.048**	> **0.006**	- 0.385	- 0.394	< **0.004**	- 0.57
z=0.25; x =0 vs **z=0.25; x = 1**	0.25 vs 1.25	> **0.007**	> **0.008**	> **0.001**	> **0.003**	> **0.001**	- 0.57
z=1; x =0 vs **z=1; x = 0.25**	1 vs 1.25	- 0.185	> **0.02**	- 0.329	> **0.008**	- 0.552	- 0.1
z=1; x =0 vs **z=1; x = 1**	1 vs 2	> **0.002**	> **0.008**	> 0.38	> **0.023**	- 0.176	- 0.173
z=0.25; x =0.25 vs **z=0.25; x = 1**	0.5 vs 1.25	> **0.001**	> **0.0036**	> **0.001**	> **0.012**	- 0.209	- 0.532
z=1; x =0.25 vs **z=1; x =1**	1.25 vs 2	- 0.08	0.776	- 0.128	- 0.46	- 0.835	- 0.221

Table 9.14: Differences in vertical transmissibility f_r and $H(f_r)$ across all the tests

	soft foam		soft foam backrest ON		hard foam	
	Δfr	**ΔH(fr)**	**Δfr**	**ΔH(fr)**	**Δfr**	**ΔH(fr)**
median	0.75	0.26	0.75	0.36	0.94	0.24
max	1.13	0.48	1.00	0.68	1.37	0.30
min	0.63	0.12	0.50	0.21	0.38	0.11

Table 9.14 quantifies the effects of nonlinearity on vertical transmissibility calculated across al the possible combination of vertical and horizontal motion. The spectral resolution of the analysis is 0.125 Hz. The shift in resonance frequency, *Δfr*, has a median of 0.75 Hz for the soft foam, and of 0.96 Hz for the hard foam. The transmissibility at resonance median shift is of about 25% for the 'backrest OFF' conditions and 36% for the backrest on condition. Subjects showing highest nonlinearity had a shift in resonance frequency higher than 2 Hz and a shift in transmissibility in resonance up to the 34% of the vibration input.

9.4.1 Comparison between foam dynamic stiffness in vertical and horizontal direction

Damped accelerometers have been used in the second experiment. Those accelerometers introduce phase distortion, giving a systematic error that in the imaginary part of the dynamic stiffness (see Appendix A). Therefore, in this section, we will deal only with the value of the real part of seat dynamic stiffness at a specific frequency. The values of coherency function of the seat apparent mass (from whom

seat dynamic stiffness is measured) are particularly high at about 5 Hz in all the conditions, so the value $k = Re(S(f))$, f = 5 Hz, will be used to test the relationship between vertical, k_z, and fore-and-aft, k_x, foam dynamic stiffness.

Wilcoxon matched pairs signed rank test (Siegel, 1988) is carried on the individual values of k_z and k_x in the conditions with horizontal vibration only (0.25 and 1.0 r.m.s. 'backrest OFF'). All the tests gave high significance ($p < 0.002$). The shear stiffness at 5 Hz, k_x, was significantly bigger than the one in compression, k_z. Table 9.15 shows median, maximum and minimum of the ratio k_z/k_x. Values of k_z/k_x greater than one have been measured in just one subject.

Table 9.15: values for the ratio between vertical and fore-and-aft seat stiffness

	soft foam 0.25 ms^{-2} r.m.s.	soft foam 0.25 ms^{-2} r.m.s. backrest ON	soft foam 1.0 ms^{-2} r.m.s.	soft foam 1.0 ms^{-2} r.m.s. backrest ON	hard foam 0.25 ms^{-2} r.m.s.	hard foam 1.0 ms^{-2} r.m.s.
median	0.81	0.66	0.72	0.56	0.77	0.68
min	0.56	0.48	0.52	0.34	0.47	0.46
max	1.11	0.80	0.95	0.75	1.20	1.02
range	0.54	0.33	0.43	0.40	0.73	0.56
interquartile range	0.22	0.07	0.18	0.16	0.17	0.31

Correlation between k_x, k_z, k_x/k_z, subjects' hip breadth and sitting weight (with or without backrest) is tested with the Spearman rank-order correlation coefficient. Results are reported in Table 9.16

Table 9.16: Spearman rank-order correlation coefficients and associated p values for correlation between seat stiffness and subject characteristics

	soft foam 0.25 ms^{-2} r.m.s.	soft foam 0.25 ms^{-2} r.m.s. backrest ON	soft foam 1.0 ms^{-2} r.m.s.	soft foam 1.0 ms^{-2} r.m.s. backrest ON	hard foam 0.25 ms^{-2} r.m.s.	hard foam 1.0 ms^{-2} r.m.s.
kx - kz	.593*	.786*	.489	.675**	.318	.436
	.020	.001	.064	.006	.248	.104
kz – hip breadth	.742*	.625*	.615*	.595*	.686**	.611*
	.002	.013	.015	.019	.005	.016
kz – seated weight*	.587*	.640*	.564*	.583*	.583*	.571*
	.021	.010	.029	.023	.022	.026
kx – hip breadth	.622*	.512	.598*	.528	.528	.717*
	.013	.051	.018	.043	.043	.003
kx – seated weight*	.649*	.570*	.583*	.606*	.526*	.744**
	.009	.026	.022	.017	.044	.001
kz/kx – hip breadth	.370	.330	.122	.057	.379	.038
	.175	.229	.666	.841	.164	.893
kz/kx – seated weight*	.262	.253	.118	-.047	.173	.006
	.345	.362	.675	.869	.538	.982

*seated weight is measured in both backrest ON and backrest OFF conditions

Both k_x, k_z show correlation with the human body variables ($p < 0.05$) apart for k_x with hip breadth in the case of soft foam, 0.25 ms^{-2} r.m.s. vibration input with backrest ($p > 0.05$, α=0.051). Hard foam does not show any correlation between k_x and k_z ($p > 0.05$). Soft foam k_x and k_z are correlated in all tests ($p < 0.05$) but in the 1.0 ms^{-2} r.m.s.

vibration input without backrest ($p > 0.05$). The ratio between k_z and k_x isn't correlated with hip breadth or sitting weight.

9.4.2 Fore-and-aft dynamic stiffness: effect of magnitude

The effect of vibration magnitude on k_x is investigated by means of Wilcoxon matched pairs signed rank test (Siegel, 1988). Individual values of k_x in 0.25 and 1 ms^{-2} r.m.s. test are compared in order to test the presence of softening effect in the foam stiffness. As showed in Table 9.17, vibration magnitude had a significant softening effect on both hard and soft foam, in the 'backrest ON' and 'backrest OFF' conditions.

Table 9.17: Wilcoxon test for effect of vibration magnitude on foam stiffness (0.25 vs 1.0 ms^{-2}). Higher magnitude gave lower value of stiffness (softening)

foam	soft	hard	soft backrest ON	hard backrest OFF
Significance (2-tailed)	0.001	0.002	0.008	0.003

9.4.3 Effect of dual-axis input on seat dynamic stiffness

Table 9.18: effect of dual axis input on vertical foam dynamic stiffness

		soft	soft backrest ON	hard
z=0.25; x =0 vs **z=0.25; x = 0.25**	0.25 vs 0.5	.570	**0.001**	.650
z=0.25; x =0 vs **z=0.25; x = 1**	0.25 vs 1.25	**.001**	**0.001**	**0.005**
z=1; x =0 vs **z=1; x = 0.25**	1 vs 1.25	0.140	0.570	**0.031**
z=1; x =0 vs **z=1; x = 1**	1 vs 2	.394	1	**0.027**
z=0.25; x =0.25 vs **z=0.25; x = 1**	0.5 vs 1.25	**0.001**	**0.011**	**0.001**
z=1; x =0.25 vs **z=1; x =1**	1.25 vs 2	0.156	**0.036**	0.865

Table 9.19: effect of dual axis input on fore-and-aft foam dynamic stiffness

		soft	soft backrest ON	hard
z=0; x =0.25 vs **z=0.25; x = 0.25**	**0.25** vs **0.5**	**0.023**	0.125	**0.047**
z=0; x =0.25 vs **z=1; x = 0.25**	**0.25** vs **1.25**	**0.015**	**0.012**	**0.003**
z=0.25; x =1 vs **z=0; x = 1**	**1.25** vs **1**	0.140	0.334	0.053
z=0; x =1 vs **z=1; x = 1**	**1** vs **2**	1.00	0.733	0.650
z=0.25; x =0.25 vs **z=1; x = 0.25**	**0.5** vs **1.25**	**0.001**	**0.003**	**0.001**

10. Discussion

10.1.1 Fore-and-aft transmissibility - Inter-subject variability

Individual fore-and-aft transmissibility curves for the 15 subjects show a general agreement with literature, although none of literature measurements of transmissibility was done in similar experimental conditions.

The 'backrest OFF' transmissibility, showed a low frequency peak that is most likely associated with the low frequency resonance due to rocking of the upper human body in fore-and-aft directions (e.g. Fairley and Griffin, 1990; Nawayseh and Griffin, 2005; Mandapuram et al., 2005). The low frequency peak could not be identified in all the 15 subjects, probably due to the lack of energy at frequencies lower than 0.5-0.75 Hz as showed by the very low values of the coherence function. Fairley and Griffin (1984) used a suspended seat without a backrest and measured transmissibility of the seat without suspension and without backrest contact. They did not report a low frequency peak in the transmissibility, but the frequency range in that study was 1 to 10 Hz range.

The 'backrest ON' fore-and-aft transmissibility curves are similar to those reported by Smith and Smith (2008) and by Qiu and Griffin (2004), who used a real car seat in a field and in a laboratory experiment. The main resonance peak was probably due to the same process giving the second resonance in the 'backrest OFF' condition, but with an apparent increase in stiffness (slightly higher resonance frequency and transmissibility at resonance). Transmissibilities in (Smith and Smith, 2008) and in (Qiu and Griffin, 2008) seem to report a slightly lower resonance frequency and a higher transmissibility modulus at resonance. Reasons for this discrepancies can be: (i) in the presence of a compliant backrest, which alters the seat base vibration; (ii) the different inclination of the seat pan surface; (iii) the inclination and shape of the backrest, that is likely to support the upper body differently from the rigid vertical backrest used in the present study; (iv) the differences between the seats.

Transmissibility curves in both 'backrest ON' and 'backrest OFF' conditions show a trend for an increase for frequencies higher than 5-8 Hz. This seems to reveal the presence of a second resonance peak at frequency higher than the maximum of this study, as showed in researches with a broader frequency range (e.g. Qiu and Griffin, 2004; Smith and Smith, 2005).

Seat values in Table 9.1 suggest the poor insulating properties of polyurethane squabs in fore-and-aft direction. Similar results were found by Griffin (1978) for different car seats.

The ride experienced on a soft seat is quite similar to the one at the base of the seat, at least for the dynamic range of the present study.

10.1.2 Fore-and-aft transmissibility - Effect of vibration magnitude

Fore-and-aft seat transmissibilities are reported, to the author knowledge, only by Qiu and Griffin (2004). Findings in the present study and in (Qiu and Griffin, 2004) are similar: reduction of main resonance frequency and modulus at resonance and increase of transmissibility at higher frequencies (Table 9.2). The seat-human system is a softening nonlinear system with increasing vibration magnitude, as for the vertical seat transmissibility (e.g. Fairley and Griffin, 1986).

10.1.3 Fore-and-aft transmissibility - Effect of a rigid backrest

As showed in (Fairley and Griffin, 1990; Fleury and Mistrot, 2006), the upper human body in fore-and-aft direction exhibited a low frequency resonance. The backrest represents a constraint for the rocking motion and so the first peak of resonance disappears. It is unclear if the increased fore-and-aft transmissibility in due to real fore-and-aft motion, or is due to the pitching of the 'SAE pad' transducer giving an output due to the sensitivity of the x-axis piezoresistive accelerometer to g-acceleration. The increase of resonance frequency and modulus at resonance is consistent with the increase of stiffness in the human body due to the backrest support (e.g. Fairley and Griffin, 1990). The backrest seems to enhance the effect of vibration magnitude on transmissibility. This can be due to the presence of a second vibration input to the human body.

10.1.4 Fore-and-aft transmissibility - Effect of foam stiffness

Foam stiffness affects the transmissibility modulus at resonance more than the resonance frequency or the transmissibility at high frequencies: it seems that the differences in damping between the two foams play a more significant role. In order to better understand the role of foam stiffness, modelling and subsequent sensitivity tests should be carried out. In any case, differences between the two foam transmissibility are rather small, especially if we consider the sensitivity of the human body to vibration at frequencies higher than 4 Hz and the higher importance of the backrest vibration.

10.2 Fore-and-aft apparent mass: effect of backrest, seating and vibration magnitude

Apparent mass curves on rigid and soft seat, with backrest unsupported, are quite similar to those reported in (Nawayseh and Griffin, 2003), with three peaks appearing in the low magnitude test. Mansfield and Lundström (1999) reported two peaks in the apparent mass, but the frequency range of their experiment did not allow to identify the first, low frequency, peak. By another hand, Fairley and Griffin (1990) reported two peaks, at about 0.7 Hz and the second at about 2-3 Hz, which are probably coincident with the first and

second peak of the present study, but not the third. As discussed in (Nawayseh and Griffin, 2005), this is probably due to the relatively high magnitude of the vibration input (minimum of 0.5 ms^{-2} r.m.s.). In fact, in this study, as well as in (Nawayseh and Griffin, 2005) and in (Mandapuram et al., 2005), the increase in vibration magnitude affected the visibility of the third mode of vibration. Mandapuram et al. (2005) suggested that the reason for vibration modes disappearing could be the different subjects muscle tension between the low and high magnitude tests.

The effect of a rigid backrest is to remove the first resonance mode and to increase the frequency and modulus of the second: results are similar to those reported in (Fairley and Griffin, 1990), (Mandapuram et. al, 2005) and in (Fleury and Mistrot, 2006) for only one subject.

Differences between the fore-and-aft apparent masses on hard and soft seat are difficult to discuss, in the light of lack of literature. Stein et al. (2008) data can not be compared to those in the present study, as explained in Section 1.2. Fleury and Mistrot (2006) measured one subject apparent mass on a soft seat with a method similar to the present study. In (Fleury and Mistrot, 2006) the first peak of resonance in the apparent mass with backrest unsupported does not appear clearly, probably because the presence of a steering wheel provided a constraint to the rocking motion of the upper body. Results are compared more easily with those regarding the effect of seating on the human body apparent mass in vertical direction reported in the previous section of this thesis. No statistical tests are performed on the vibration modes resonance frequencies in the 'backrest OFF' case. Median curves show that the apparent mass on a rigid seat looks less damped than the one on the soft seat, with behaviour similar to the one in vertical direction. In the 'backrest ON' condition, differently from the results of the vertical apparent mass, there are some differences in the resonance frequency between soft and hard seat and between soft and rigid seat. No differences between hard and rigid seat. Anyway those differences are quite small, with the soft seat giving a higher resonance frequency. Reasons for this stiffening are not easily found. It could be that the compliance of the seat gave larger motion at the buttocks and more reaction of the legs with consequent stiffening.

The effects of vibration magnitude were investigated only in the backrest ON condition. Softening effect appears clearly, as in the case of vertical vibration. Furthermore, there is a clear reduction in the modulus of the apparent mass at resonance. Results are in

agreement with (Fairley and Griffin, 1990), (Nawayseh and Griffin, 2005), and (Mandapuram et al., 2005).

The drop in apparent mass coherency functions at about 25Hz can be attributed to a pitching mode in the simulator that could cause a difference between the input at the seat base and the input at the backrest: a SISO model could not be the most appropriate.

10.3.1 Linear effects of fore-and-aft vibration at the seat base on vertical vibration at the seat pan

When the magnitude of z and x-axis vibration are comparable, effects of fore-and-aft vibration to vertical vibration on the seat pan are low, as showed by Fairley (1983) for a conventional seat with backrest and by Smith et al. (2008) for a suspended seat, despite (i) the differences in seat composition (foam and springs), (ii) and posture (foam backrest contact in (Fairley, 1983)), (iii) the presence of undesired pitch motion and (iv) the use of a different measuring device (SIT-BAR) and (v) the possible tilting of transducer in (Fairley, 1983) respect to the vertical and horizontal directions.

When the fore-and-aft vibration magnitude was substantially higher than the one in vertical direction (z = 0.25, x = 1 ms^{-2} r.m.s.), the contribution of x vibration to vertical seat pan vibration increased in a linear trend with frequency, as showed by partial coherence functions in Figure 9.29. Anyway, as addressed by Fairley (1983), the significance of cross-axis motion has to be considered relatively to the magnitude of vertical vibration. At 20 Hz, the amount of vertical vibration is quite low (due to the properties of the cushion): the contribution of fore-and-aft vibration to vertical discomfort is consequently low. Furthermore, it is not common to find vibrating environments with such a ratio between vertical and fore-and-aft vibration magnitudes. The multiple coherence function has values of about 0.9, with a decrease respect to the case (z = 0.25, x = 1 ms^{-2} r.m.s.). It should be investigated whether other unwanted motion occurring in the vibrator (such as pitching) was contributing to vertical vibration at the seat pan. With the vibration input (z = 0.25, x = 1 ms^{-2} r.m.s.) and the backrest contact, the contribution of fore-and-aft motion to vertical vibration becomes dominant at frequencies higher than 6 Hz. Reason for this effect be researched in the different dynamic response of the human body (with the backrest increasing the cross-coupling) or in the opportunity of considering a MIMO model with the backrest vibration input.

10.3.2 Linear effects of vertical vibration at the seat base on fore-and-aft vibration at the seat pan

No past literature presented such transmissibility measurements. Results are quite similar to those in 4.3.1. The amount of vertical vibration is almost zero in the cases in which vertical and fore-and-aft vibration have the same magnitude. When the r.m.s. magnitude of vertical vibration is four times higher than the fore-and-aft, there is z to x transfer of motion only at about 5 Hz, which corresponds to the main resonance of the human body in vertical direction. It is believed that the human body at resonance gives a combination of motion in the vertical and fore-and-aft axes (Mansfield and Griffin, 2000). It is not possible to determine whether the motion of the body at resonance gave translational fore-and-aft vibration, or pitching of the accelerometer which resulted in an output of the x-axis accelerometer due to its sensitivity to g-acceleration. As seen in 4.3.1, the backrest contact increases the amount of cross-axis vibration. It should be investigated whether this effect could be of any significance in real seats.

10.3.3 Non-linear effects of vertical vibration on in-line fore-and-aft transmissibility

Nonlinear effects were expected in the light of studies such as (Hinz et al., 2006; Mansfield and Maeda, 2006; Qiu and Griffin, 2010): the apparent mass with dual-axis input contributed to the significance of some tests. Results in 9.4.3, seem to suggest that also the dynamic stiffness could contribute to nonlinearity in seat transmissibility. The soft foam transmissibility did not give any significance, even if there was a reduction in stiffness, as shown in Table 9.19. This means that the role of the foam in determining fore-and-aft transmissibility was less important than the human body's. Hinz et al. showed no significant effect of the multi-axis vibration on the fore-and-aft apparent mass. If we consider the results of the previous experiment, showing that the main contribution to nonlinearity is given by the human body, this can explain the lack of significance of some tests.

Tests having x = 0.25 ms^{-2} r.m.s. show, overall, higher significance than those with x = 1.0 ms^{-2} r.m.s., This could be due to a 'saturation' effect in nonlinearity, meaning that non-linearity could be sensitive to overall vibration and, reached a certain level of vibration, the mechanism does not happen anymore.

10.3.4 Non-linear effects of vertical vibration on in-line fore-and-aft transmissibility

Results seem clearer than in the case of fore-and-aft transmissibility, probably due to the different shape of the transmissibility curves that show a neat peak of resonance. Reasons for this can be searched in the substantial differences of the seat-human systems in the two directions. As showed in (Hinz et al., 2006; Table 4) there is no significant effect of multi-axis vibration on fore-and-aft apparent mass (or, at least, on its

resonance frequency). Test with z = 0.25 ms^{-2} r.m.s. were generally more significant that those with z =1 ms^{-2} r.m.s., suggesting that, probably, the high level of vertical vibration saturated the seat-human system giving no nonlinearity.

10.4 Fore-and-aft dynamic stiffness

This is, to the author knowledge, the first attempt of measuring the dynamic stiffness of a seat with a person seating on in the fore-and-aft direction. Results suggest that the determination of the damping is biased the characteristics of the accelerometers. In fact, negative values of damping (not reported) were obtained. Probably also the non perfect alignment of the SAE-pad respect to the accelerometer at the base may have contributed.

Stiffness data show good agreement with those measured in the vertical direction, also in the previous experiment. Effects of vibration magnitude, subject weight and hip breadth are consistent with those in the first part of this study and with those in (Fairley and Griffin, 1986; Wei, 1997).

Results show that the stiffness in fore-and-aft direction is higher than the one in vertical. Formulas for the shear modulus for cellular materials are suggested in (Gibson and Ashby, 1999): shear modulus for a single cell of material is lower than the compressive modulus. This means that, as seen in the case of vertical direction, there are many factors determining the dynamic stiffness of the foam. One reason for the higher stiffness could be the low vibration magnitude 'experienced' by the seat cushion. Having a seat transmissibility close to one in most of the frequency range means that the difference of accelerations (and so of displacements) between the base of the seat and the seat pan are rather small. It is also difficult to quantify the possible error arising from accelerometers misalignment and from the fact that the signal from the force plate is just a sum of the forces at the four corners: single-point mechanical impedance (stiffness) of a system which has a very complex 3D motion was measured.

11. Conclusions

The vertical and fore-and-aft apparent masses of the human body supported on a foam cushion have a similar resonance frequency as when supported on a rigid surface. The apparent mass at resonance was slightly less when supported by foam, suggesting increased body damping due to either the changed contact conditions or nonlinearity associated with the change in vibration magnitude caused by the seat transmissibility. In vertical direction, an apparent increase in body damping was consistent with increased apparent mass at 20 Hz when sitting on the foam. Fore-and-aft apparent mass is strongly dependent on the use of a backrest.

Both the human body and the foam exhibited nonlinear softening behaviour, resulting in changes in transmissibility with changes in vibration magnitude. Nonlinearity in fore-and-aft transmissibility is less pronounced than those in vertical.

The foam elastic stiffness in vertical and fore-and-aft directions showed a nonlinear dependence on vibration magnitude. The foam energy loss parameters in vertical direction were not dependent on vibration magnitude. Foams were found to be stiffer in horizontal than in vertical direction.

The principal contribution to the nonlinearity in vertical transmissibility can be ascribed to nonlinearity in the human body, with only a minor contribution from nonlinearity in the foam.

Correlations between the dynamic properties of the foam and subject weight and hip breadth reveal the complexity of foam behaviour, and differences between foams. It seems that subject weight and contact area can alter the dynamic stiffness of seat foam, in both vertical and fore-and-aft directions.

Linear cross-coupling between vertical and fore-and-aft transmissibility was found: a small part of the vertical (or fore-and-aft) vibration at the seat base contributes to fore-and-aft (or vertical) vibration at the subject-seat interface. Nonlinear cross-coupling was found in seat transmissibility and foam dynamic stiffness: the softening of the seat-subject system in one axis is affected by the vibration in the perpendicular direction.

The author believes that this research increased the current state of knowledge of the dynamics of the seated human body and polyurethane foams and so it represents a step forward in the understanding of the mechanisms involved in the vibration isolation provided by seats.

References

Bendat J. S., Piersol A. G. (1980), *Engineering applications of correlation and spectral analysis*, New York, Wiley-Interscience.

Bendat J.S. and. Piersol A.C (2000), *Random data analysis and measurement procedures*, Wiley-Interscience, 3rd edition

Bluthner R., Seidel H., Hinz B. (2008), *Laboratory study as basis of the development for a seat testing procedure in horizontal directions*, International Journal of Industrial Ergonomics, Volume 38, Issues 5-6, Seating Dynamics, Pages 447-456

Bovenzi M., Pinto I., Stacchini N. (2002), *Low back pain in port machinery operator*, Journal of Sound and Vibration, Volume 253, Issue 1, Pages 3-20

BRITISH STANDARDS INSTITUTION (1987) BS 6841, Measurement and evaluation of human exposure to whole-body mechanical vibration and repeated shock

Conza N.E., Rixen D.J. (2007), *Influence of frequency-dependent properties on system identification: Simulation study on a human pelvis model*, *Journal of Sound and Vibration*, 302: pp. 699-715

Ebe K. (1993), Effect of composition of polyurethane foam on the vibration transmissibility of automotive seats, UK informal group meeting on Human Response to Vibration held at APRE, Ministry of Defence, Farnborough, 20 to 22nd Sept 1993

Fairley T.E. (1983), *The effect of vibration input characteristics on seat transmissibility*, UK informal group meeting on Human Response to Vibration held at NIAB, Silsoe, 14-16 Sept 1983

Fairley T.E. (1984), *Measurements in a vehicle of multi-axis frequency response of a seat*, UK informal group meeting on Human Response to Vibration held at Heriott-Watt University, Edinborough, 21-22 Sept 1984

Fairley T.E. and Griffin M. J. (1989), *The apparent mass of the seated human body: vertical vibration*, Journal of Biomechanics, 22(2): pp. 81-94.

T. Fairley (1986), *Predicting the dynamic performance of seats*, PhD Thesis, University of Southampton

Fairley T.E. and Griffin M.J. (1986), *A test method for predicting seat transmissibility*, in *SAE International Congress and Exposition*, SAE paper 860046: Detroit

Fairley T.E. and Griffin M.J. (1984), *Modelling a seat-person system in the vertical and fore-and-aft axes*, C149/84 iMech 1984

Fairley T.E.and Griffin M.J. (1989), *The apparent mass of the seated human body: Vertical vibration*, Journal of Biomechanics, Volume 22, Issue 2, Pages 81-94

Fairley T.E.and Griffin M.J. (1990), *The apparent mass of the seated human body in the fore-and-aft and lateral directions*, Journal of Sound and Vibration, Volume 139, Issue 2, Pages 299-306

Fleury G., Mistrot P. (2006), *Numerical assessment of fore-and-aft suspension performance to reduce whole-body vibration of wheel loader drivers*, Journal of Sound and Vibration, Volume 298, Issue 3, Special Issue on the Third International Conference on Whole-body Vibration Injuries, Pages 672-687

Gibson L.J, Ashby M.F. (1999), *Cellular Solids: Structure and Properties*, Cambridge University Press; 2 edition

Griffin M.J. (1978), *Evaluation of vehicle vibration and seats*, Applied Ergonomics, 9(1): pp. 15-21

Griffin M.J. (1996), *Handbook of human vibration*, 1996: Academic Press, London

Harris C.M. and Piersol A.G. (2002), *Harris' shock and vibration handbook, 5th edition,* McGraw-Hill

Hilyard N.C. and Cunningham A. (1994), *Low Density Cellular Plastics - Physical basis of behaviour*, Chapman and Hall, London.

Hilyard N.C., Collier P., and Care C.M. (1984), *Influence of the mechanical properties of cellular plastic cushion on materials ride comfort*, in Dynamics in automotive engineering, Cranfield Institute of Technology, 5-6 April 1984.

Hinz B., Rützel S., Blüthner R., Menzel G., Wölfel H.P., Seidel H. (2006), *Apparent mass of seated man - First determination with a soft seat and dynamic seat pressure distributions*, Journal of Sound and Vibration, 298(3): pp. 704-724.

Hinz B., Bluthner R., Menzel G., Rutzel S., Seidel H., Wolfel H.P. (2006), *Apparent mass of seated men--Determination with single- and multi-axis excitations at different magnitudes*, Journal of Sound and Vibration, Volume 298, Issue 3, Special Issue on the Third International Conference on Whole-body Vibration Injuries, Pages 788-809

INTERNATIONAL ORGANIZATION FOR STANDARDIZATION (1997) ISO 2631-1 (E), Mechanical vibration and shock—Evaluation of human exposure to whole-body vibration. Part 1: General requirements

Lewis C.H. and Griffin M.J. (2002), *Evaluating the vibration isolation of soft seat cushions using an active anthropodynamic dummy*, Journal of Sound and Vibration, 253(1): pp. 295-311.

Mandapuram S.C., Rakheja S., Ma S., Demont R.G. And Boileau P. (2005) *Influence of Back Support Conditions on the Apparent Mass of Seated Occupants under Horizontal Vibration,* Ind Health 43, 421-435

Mansfield N.J. and Griffin M.J. (1996), *Vehicle seat dynamics measured withan anthropodynamic dummy and human subjects,* Inter-noise '96, Proceedings of 25th

Anniversary Congress, Liverpool, Book 4, Published: Institute of Acoustics, ISBN: 1-873082 91 6, 1725-1730.

Mansfield N.J. (1998), *Nonlinear dynamic response of the seated person to whole-body vibration*, PhD Thesis, University of Southampton

Mansfield N.J. and Griffin M.J. (2000), *Non-linearities in apparent mass and transmissibility during exposure to whole-body vertical vibration*, Journal of Biomechanics, 33: pp. 933-941.

Mansfield N.J. and Griffin M.J. (2002), *Effects of posture and vibration magnitude on apparent mass and pelvis rotation during exposure to whole-body vertical vibration*, *Journal of Sound and Vibration*, 253(1): pp. 93-107

Mansfield N.J., Holmlund P., Lundström R., Lenzuni P., Nataletti P. (2006), *Effect of vibration magnitude, vibration spectrum and muscle tension on apparent mass and cross axis transfer functions during whole-body vibration exposure*, Journal of biomechanics, volume 39 issue 16 Pages 3062-3070

Mansfield N.J. (2005), *The use of impedance methods (apparent mass, mechanical impedance and absorbed power) for assessment of biomechanical response of the seated person whole-body vibration,* Industrial Health 43, 378-389

Mansfield N.J., Lundström R. (1999), *The apparent mass of the human body exposed to non-orthogonal horizontal vibration*, Journal of biomechanics, volume 32 issue 12 Pages 1269-1278

Mansfield N.J., Maeda S. (2007), *The apparent mass of the seated human exposed to single-axis and multi-axis whole-body vibration*, Journal of biomechanics, volume 40 issue 11 Pages 2543-2551

Muksian R. and Nash C.D. (1976) Jr, *On frequency-dependent damping coefficients in lumped-parameter models of human beings*, Journal of Biomechanics, 9(5): pp. 339-342.

Nawayseh N., Griffin M.J. (2003), *Non-linear dual-axis biodynamic response to vertical whole-body vibration*, Journal of Sound and Vibration, Volume 268, Issue 3, Pages 503-523

Nawayseh N.,Griffin M.J. (2005), *Non-linear dual-axis biodynamic response to fore-and-aft whole-body vibration*, Journal of Sound and Vibration, Volume 282, Issues 3-5, Pages 831-862

Patten W.N. and Pang J. (1998), *Validation of a nonlinear automotive seat cushion vibration model*, Vehicle System Dynamics, 1998, 30: pp. 55-68.

Patten W.N., Sha S., and Mo C. (1998), *A vibration model of open celled polyurethane foam automotive seat cushions*, Journal of Sound and Vibration, 217(1): pp. 145-161.

Pheasant S. and Haslegrave C. (2006), *Bodyspace: anthropometry, ergonomics, and the design of work*, 2006: CRC Press

Qiu Y., Griffin M.J. (2004), *Transmission of vibration to the backrest of a car seat evaluated with multi-input models*, Journal of Sound and Vibration, Volume 274, Issues 1-2, Pages 297-321

Qiu Y., Griffin M.J. (2010), *Biodynamic responses of the seated human body to single-axis and dual-axis vibration*, Industrial Health, Volume 48, Pages 615-627

Siegel S. and Castellan N. (1988), *Nonparametric statistics for the behavioral sciences*, McGraw-Hill New York

Smith S.D. (2008), Dynamic characteristics and human perception of vibration aboard a military propeller aircraft, Journal of Industrial Ergonomics 38, 868-879

Smith S.D., Bowden D.R., Jurcsisn J.C. (2005),MULTIAXIS SEAT CUSHION TRANSMISSIBILITY CHARACTERISTICS

Smith S.D., Smith J.A., Bowden D.R. (2008), *Transmission characteristics of suspension seats in multi-axis vibration environments*, International Journal of Industrial Ergonomics, Volume 38, Issues 5-6, Seating Dynamics,

Stein G.J., Múcka P., Chmúrny R., Hinz B., Blüthner R. (2007), *Measurement and modelling of x-direction apparent mass of the seated human body–cushioned seat system*, Journal of biomechanics, volume 40, issue 7 Pages 1493-1503

Toward M.G.R. (2000), *Use of an anthropodynamic dummy to measure seat transmissibility*, presented at the 35th United Kingdom Meeting on Human Responses to Vibration, held at ISVR, University of Southampton, England, 13-15 September 2000

Wei L. and Griffin M.J. (1997), *The influence of contact area, vibration magnitude and static force of the dynamic stiffness of polyurethane seat foam*, in UK Group meeting on Human Response to Vibration, ISVR, University of Southampton, 17-19 September 1997.

Wei L. and Griffin M.J. (1998b), *Mathematical models for the apparent mass of the seated human body exposed to vertical vibration*, Journal of Sound and Vibration, 212(5): pp. 855-874.

Wei (2000), *Predicting transmissibility of car seats from seat impedance and the apparent mass of the human body,* PhD Thesis, University of Southampton

Wei L. and Griffin M.J. (1998), *The prediction of seat transmissibility from measures of seat impedance*, Journal of Sound and Vibration, 214(1): pp. 121-137.

Whitham E.M. and Griffin M.J. (1977), *Measuring vibration on soft seats*, SAE Paper, 770253

Wu X., Rakheja S., and Boileau P. (1999), *Distribution of human-seat interface pressure on a soft automotive seat under vertical vibration*, *International Journal of Industrial Ergonomics*, 24(5): pp. 545-557

APPENDIX A

Analysis of systematic errors in mechanical impedance measurements.

Assumptions

The following will be a pure mechanical analysis. Everything will be described using lumped linear parameters. The effects due to the electrical part of the data acquisition system are neglected. Even thermal effects on accelerometers are neglected, which is reasonable if we warm up the rig and try to operate always in the same conditions.

Definitions

What is an error in measurement?

Observational error is the difference between a measured value of quantity and its true value (Dodge, Y. (2003), *The Oxford Dictionary of Statistical Terms*). Measurement errors can be divided into two categories: *random* and *systematic errors. Random errors* doe not have any consistent effects across the entire sample. A random error 'pushes' observed scores up or down randomly. This means that if we could see all of the random errors in a distribution they would have to sum to 0, there would be as many negative errors as positive ones. The important property of a random error is that it adds variability to the data but does not affect average performance for the group. Because of this effect, random error is sometimes considered *noise*. The random error (or random variation) is due to factors which we cannot (or do not) control.

Measurement uncertainty describes a region about an observed value of a physical quantity, also called a measurand, which is likely to enclose the true value of that quantity.

* * *

The present analysis was necessary to ensure the validity of the first experiment.

Both human body and foam for seats construction are well known for being nonlinear softening systems. The main idea of first experiment was to measure Dynamic Stiffness of the foam and Apparent Mass of the subject while coupled, in order to better understand they dynamic behaviour.

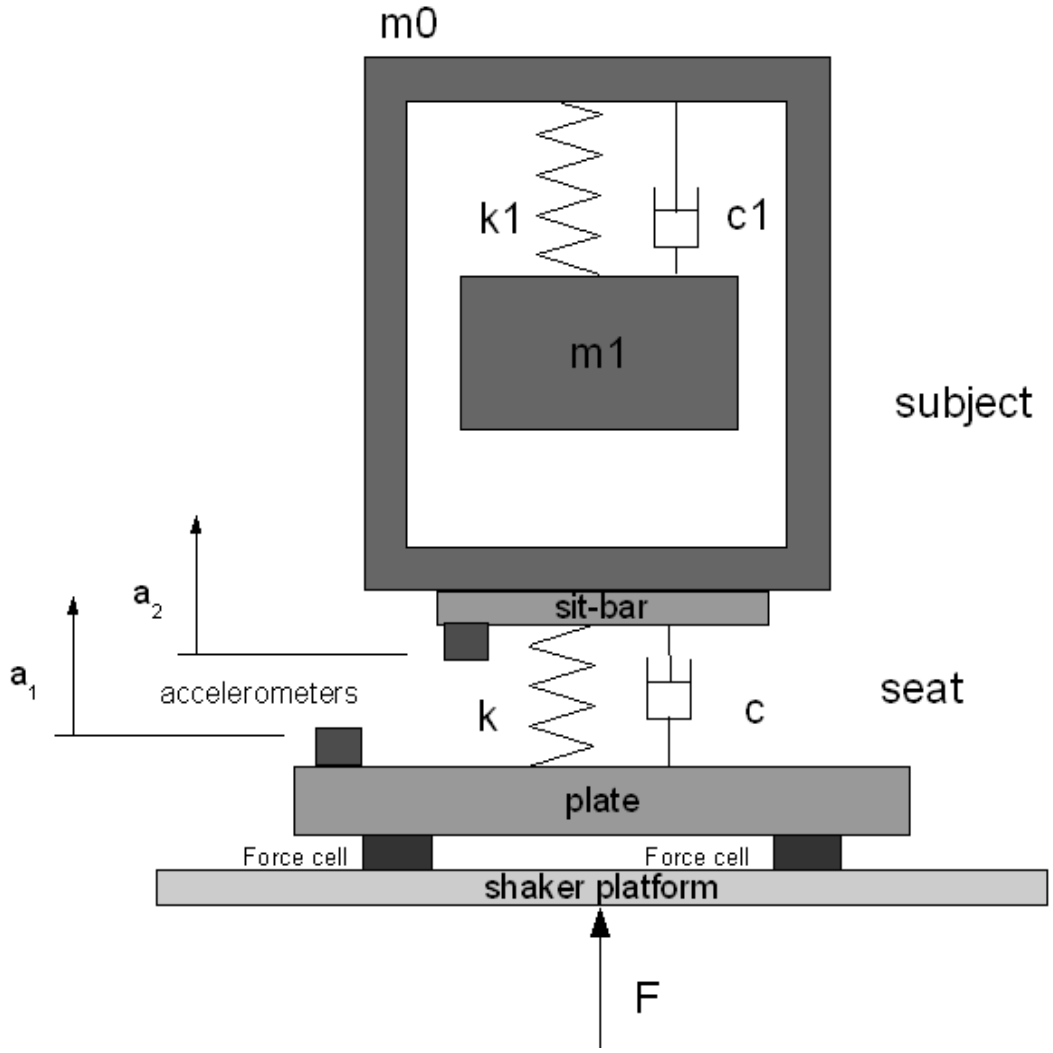

Figure A.1: lumped parameters model of the experimental setup

Dynamic stiffness, *S(ω)*, of the foam, is calculated from the formula:

$$S(\omega) = \frac{\bar{F}(\omega)}{d_{foam}} = \left(\frac{\bar{F}(\omega)}{a_{plate}(\omega) - a_{seat}(\omega)} \right) \omega^2$$

where

$$\bar{F}(t) = F(t) - M_{plate} \times a_{plate}(t)$$

is the net force read by the force cells. Results for the Real Part of S(ω) were coherent with those obtained with the indenter, but the Imaginary Part (which is related to energy loss of the system) dropped toward negative values usually after a certain frequency.

This result was not acceptable, as it implied the foam introducing energy into the system, like an active system.

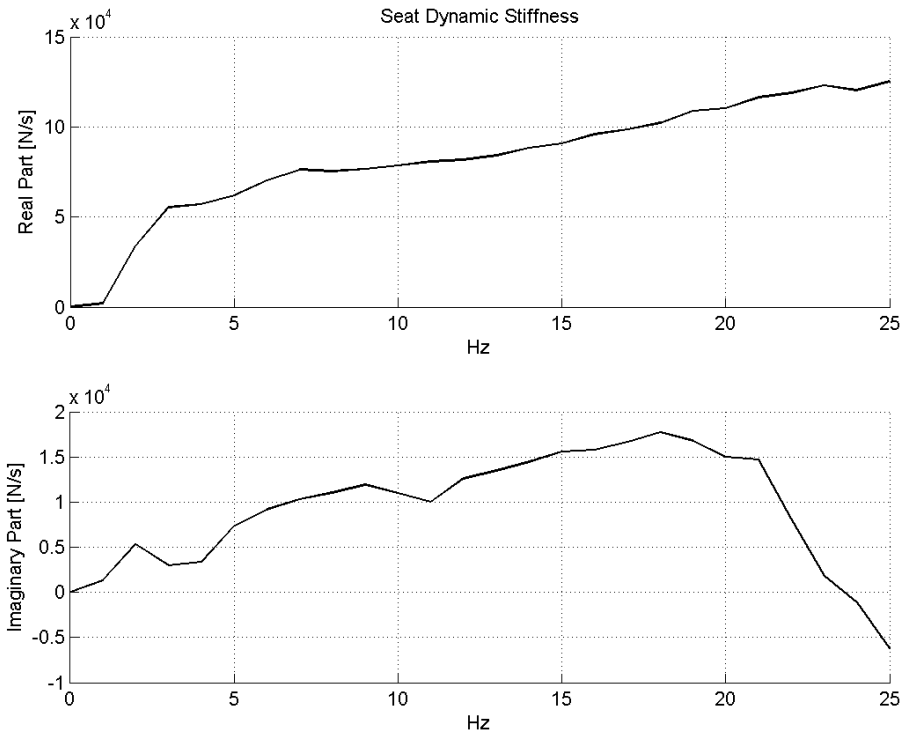

Figure A.2: example of foam dynamic stiffness measurement

This phenomenon can be explained by analysing the response characteristics of the measurement instrumentation. This analysis, as we will see later on, can be applied to other measurements such as the dynamic stiffness measurement with the indenter rig, or human body's *AM(ω)*.

Piezoresistive accelerometers

In the HFRU laboratory, piezoresistive accelerometers are commonly used because they are easy to calibrate and operate, and provide a good response at low frequency and sufficiently good at high frequency. Because of their small dimension they are used for seat transmissibility measurement. For example they are embedded into SAE pads. Piezoresistive accelerometers consist in a moving mass attached to a cantilever. A semiconductor material (a strain gage) is attached to the cantilever so it can read the strain by proportionally changing its resistivity. The behaviour of such devices can be modelled by a single degree-of-freedom oscillating system.

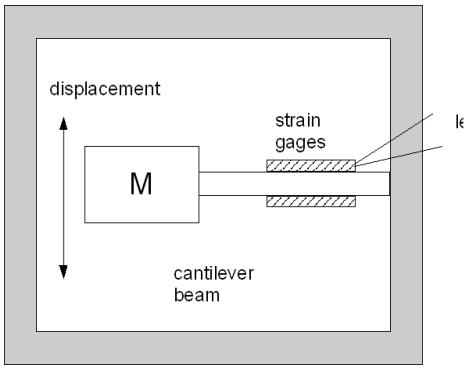

Figure A.3: schematic representation of a piezoresistive accelerometer

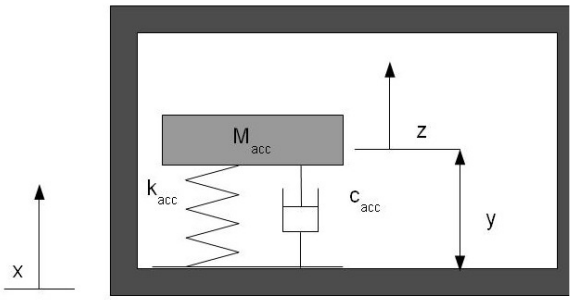

Figure A.4: lumped parameters model of a piezoresistive accelerometer

The voltage output of a piezoresistive accelerometer is therefore proportional to the relative displacement between the moving mass and the case. This means that the measured vibration, *y*, will be to some extent different respect to the vibration of the case, *x* (Figure A.3).

The equation of motion for such system is

$$m\ddot{y} + c\dot{y} + ky = -m\ddot{x}$$

Substituting the oscillating solutions

$$x = \bar{X}e^{\lambda t} \qquad\qquad y = \bar{Y}e^{\lambda t}$$

and

$$c=2zw_n m \qquad\qquad k = mw_n^{\,2} \qquad\qquad W=w/w_n$$

where ω_n is the resonance frequency of the mounted accelerometer and

$$\zeta = \frac{c}{c_c} = \frac{c}{2\omega_n m} = \frac{c}{2\sqrt{km}}$$

is the ratio between damping and critical damping. Rearranging the equation, we obtain

$$\frac{y}{x} = \frac{1-\Omega^2 - i2\zeta\Omega}{\left(1-\Omega^2\right)^2 + \left(2\zeta\Omega\right)^2} = \frac{\ddot{y}}{\ddot{x}} = H_{acc}$$

which is the complex ratio between the output of the accelerometer *x* and the "real" acceleration *y* (again, assuming that all the electrical/electronic part of the measurement system does not affect the data). We can also express it in terms of modulus and phase:

$$\frac{|\ddot{y}|}{|\ddot{x}|} = \frac{1}{\sqrt{\left(1-\Omega^2\right)^2 + \left(2\zeta\Omega\right)^2}} \qquad \tan\varphi = \frac{2\zeta\Omega}{1-\Omega^2}$$

In Figure A.5 is presented the response of two types on piezoresistive accelerometers having natural frequency f_n=*500Hz* and two different damping coefficients: one is an 'undamped' or 'lightly damped' accelerometer (ζ = *0.06*); the other is a 'damped' accelerometer (ζ = *0.7*).

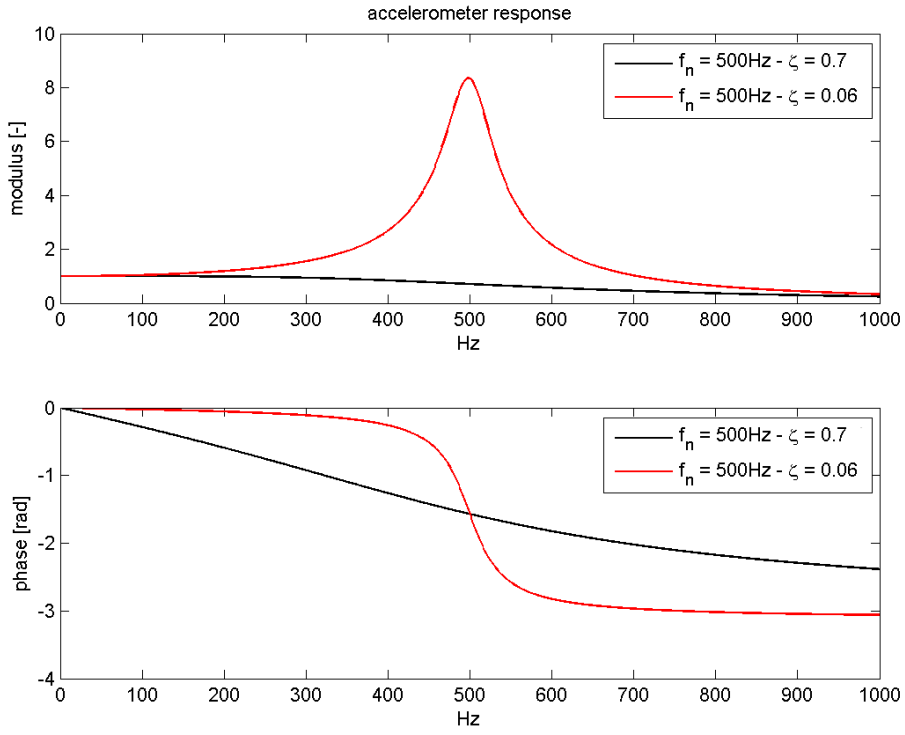

Figure A.5: model for the x to y transmissibility of two different accelerometers

Focusing on the region of 0-30Hz it is possible to notice how the 'lightly damped' accelerometer enhances the modulus of vibration (even if of just about +3‰ at 30 Hz), while the 'damped' accelerometers introduces a phase shift which increases linearly with frequency.

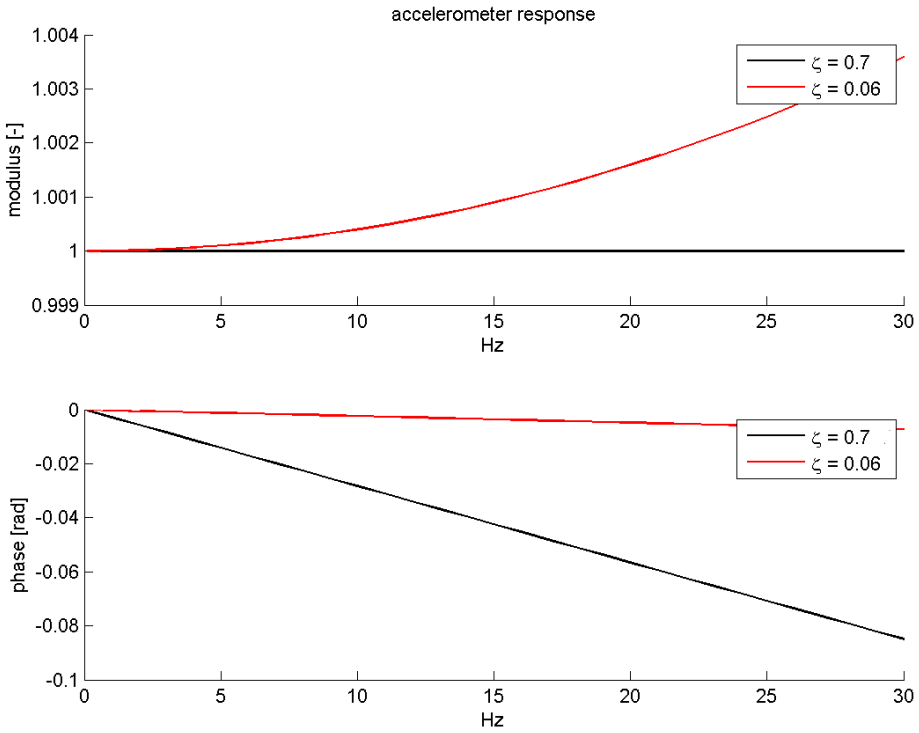

Figure A.6: model for the x to y transmissibility of two different accelerometers

It has to be noticed that the value of $\zeta = 0.7$ is chosen because having a linearly increasing phase lag means that all the signal components are shifted of the same amount of time, since

$$t = \varphi/\omega = k\omega/\omega = k$$

and the resulting will be lagging the true wave. If the time delay is not constant with frequency the wave will be distorted. Having a shift of $\varphi=0.08$ at 30Hz means that the time delay $t = 0.00042\ s$ and 1/t = 2350 1/s circa.

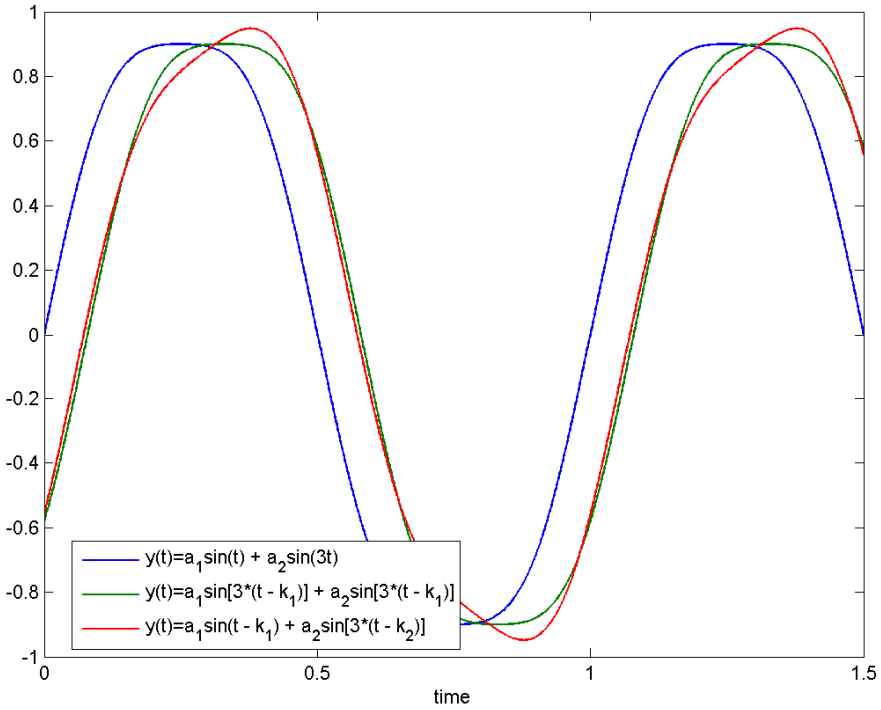

Figure A.7: distortion of a sinusoid due to a constant (green) and not constant (red) time delay

This time delay does not distort the signal, it just delays it. Anyway, problems arise when I'm simultaneously acquiring a signal coming from a device with different characteristics, such as a piezoelectric force cell.

Model Validation

As told before the model that I will use is the one degree-of-freedom. In order to validate it, I used the datasheet info of two available accelerometers, the force plate and a vibrator.

$$\frac{y}{x} = \frac{1-\Omega^2 - i2\zeta\Omega}{\left(1-\Omega^2\right)^2 + \left(2\zeta\Omega\right)^2} = \frac{\ddot{y}}{\ddot{x}} = H_{acc}$$

We want to show that the model could predict to phenomena due to transducer characteristics and predict the systematic error.

model	**resonance freq (Hz)**	**damping ratio (-)**
Entran J-type	400	0.7 (0.4 to 0.9)
Endevco 2265	1200	0.06

The values above are nominal and may vary in using conditions

Is it necessary to measure the apparent mass of the plate when performing any measurement, because the force read by the force cells contains the force generated by the mass per its acceleration.

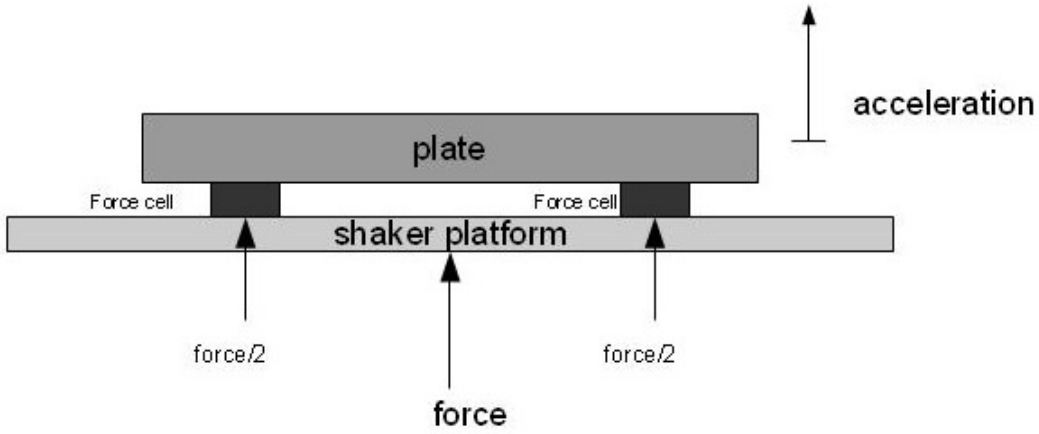

$$F^* = F + M_{plate} \times a_{plate}$$

If there's nothing on the plate

$$F = 0$$

Then

$$M_{plate} = \frac{F^*}{a_{plate}}$$

that is a real number because the inertial force has same direction of the acceleration.

Modelling the distortion in a_{plate}, the measured acceleration a^*_{plate} is the real acceleration multiplied per the response of the accelerometer.

$$a^*_{plate} = H_{acc} \cdot a_{plate}$$

so that

$$M^*_{plate} = \frac{F^*}{a^*_{plate}} = \frac{F^*}{H_{acc} \cdot a_{plate}}$$

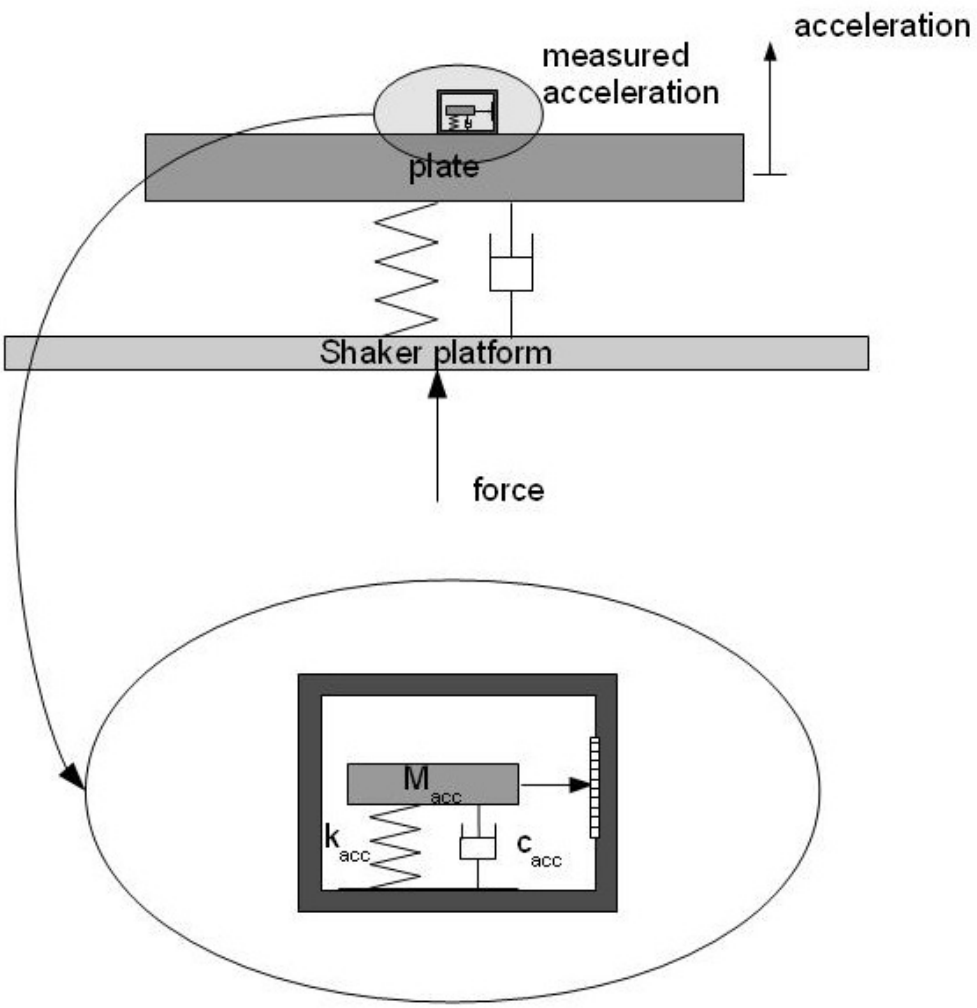

Figure A.8: model for the force plate apparent mass measurement

The experimental transfer function between acceleration and force is showed in Figure A.9. If we assume to know the static weight of the plate, we can see how the model can predict the phase error by using accelerometers datasheet parameters.

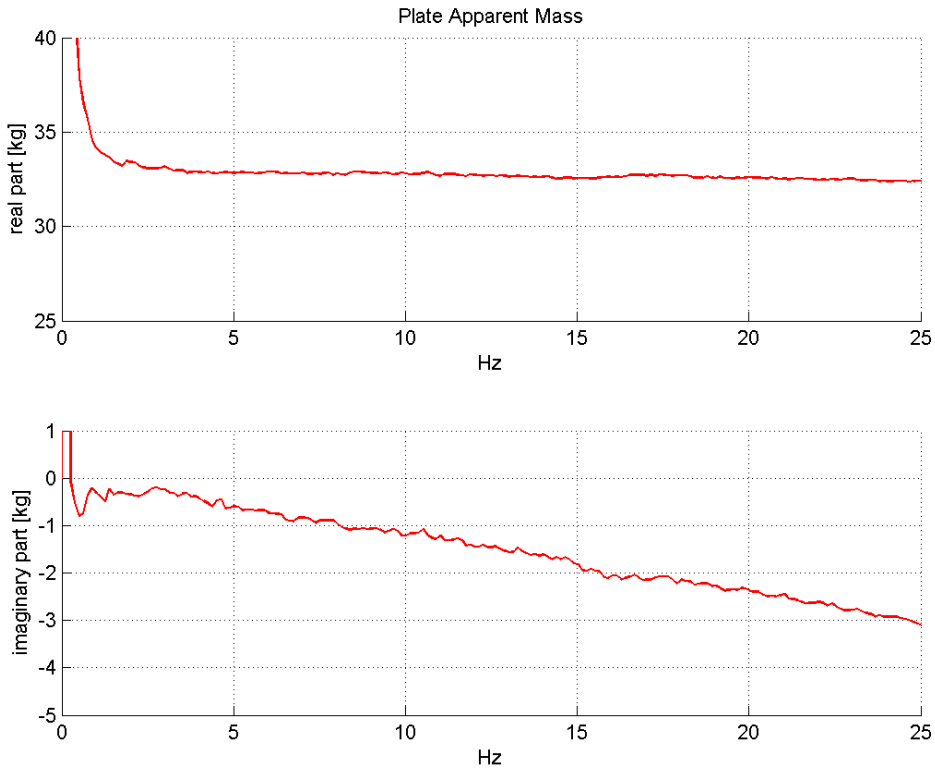

Figure A.9: experimental transfer function between force and acceleration of the unloaded plate

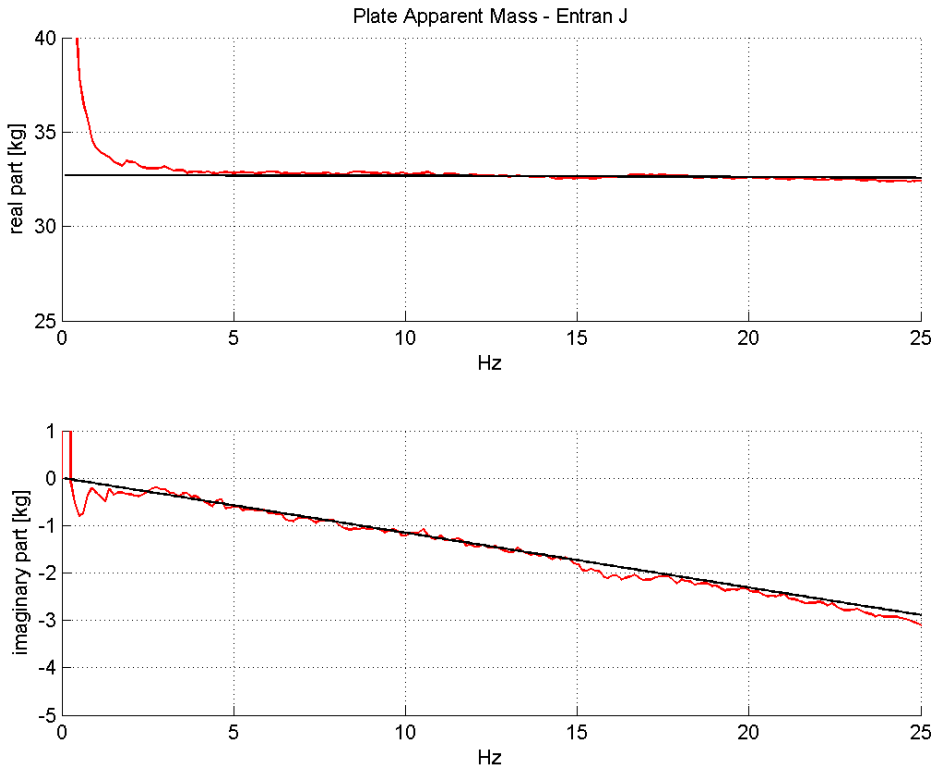

Figure A.10: modelling the Entran accelerometer – experimental data agreement, assuming the weight of the plate known

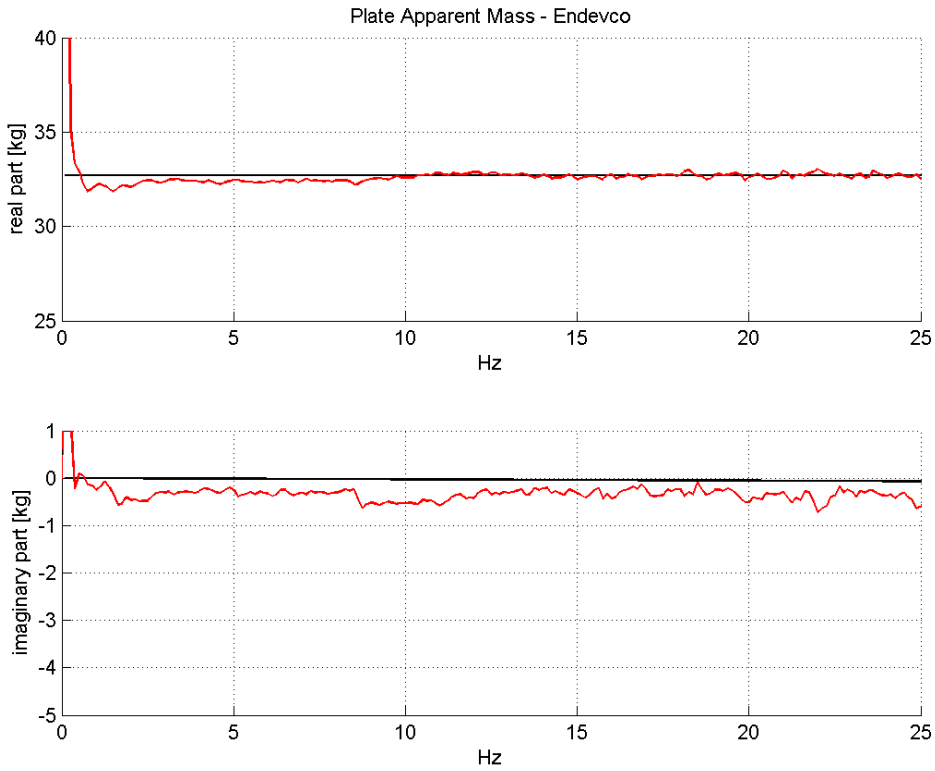

Figure A.11: modelling the Endevco accelerometer – experimental data agreement, assuming the weight of the plate known

In order to further test the model, measured and predicted transfer function between the tow accelerometers subjected to the same acceleration were compared. There is a good agreement between model and experimental data. There is a small difference, showing that the accelerometer seems to be more damped. This could be an effect of relatively low temperature during the test, because damping oil viscosity increases by decreasing temperature.

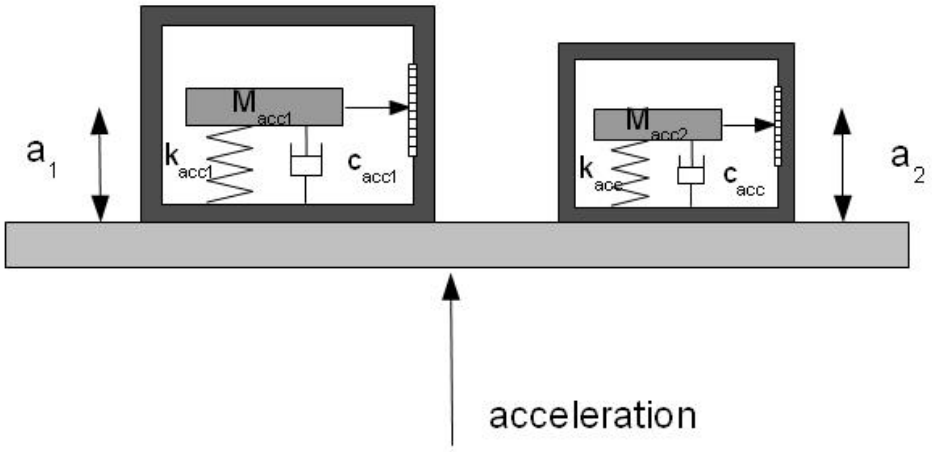

Figure A.12: model of two accelerometers on a shaker

$$\frac{a_1}{a_2} = \frac{a_1}{a}\frac{a}{a_2} = \frac{H_{acc1}}{H_{acc2}}$$

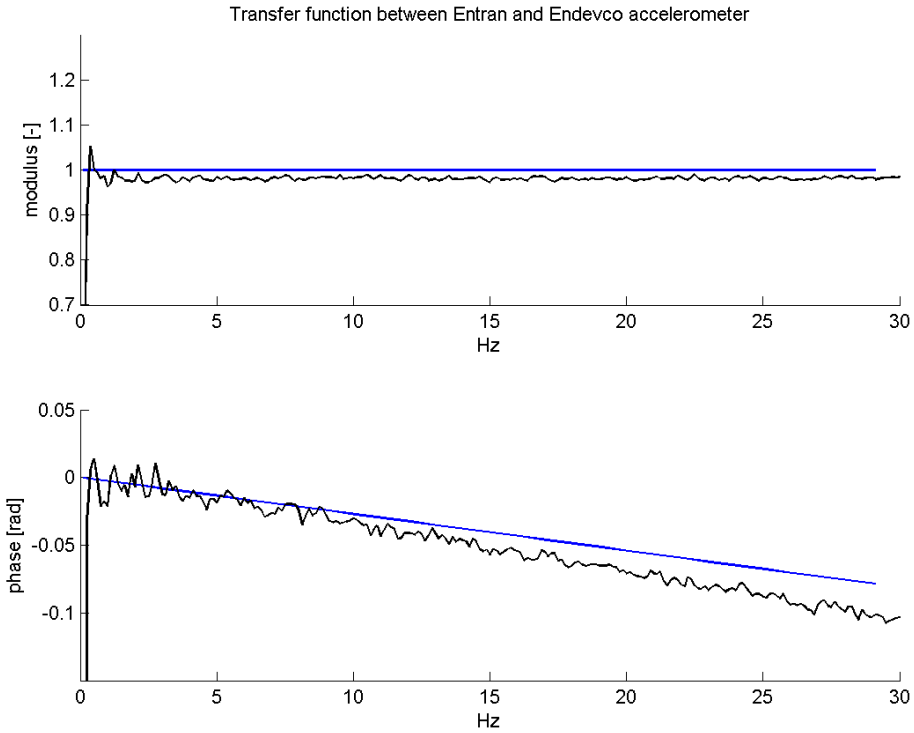

Figure A.13: transfer function between two accelerometers subjected to the same acceleration

Systematic error analysis

Once the model is validate, we can analyse the systematic error in the measurements

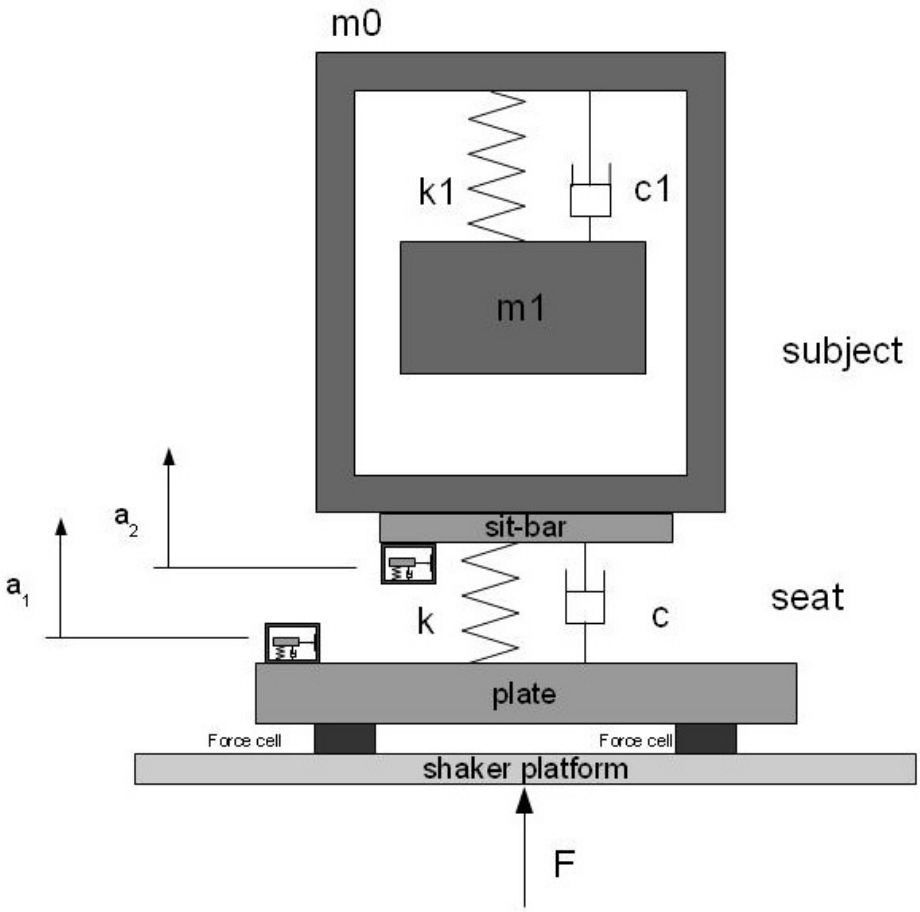

Figure A.14: experiment 1 setup

This setup allows measuring *S(ω)* and *AM(ω)* while they are coupled, so we can study differences in those functions due to "real" contact condition and spectra.

In order to model the errors it is necessary to define the parameters of the human-seat model.

Subject (Fairley and Griffin, 1989)	Foam seat (from experimental data)
m0 = 7.8	k = 60000
m1 = 43.5	k' = 200
k1 = 44130	c = 150
c1 = 1435	c' = 10000

$$S(\omega) = \frac{\bar{F}(\omega)}{d_{foam}} = \left(\frac{\bar{F}(\omega)}{a_{plate}(\omega) - a_{seat}(\omega)} \right) \omega^2$$

$$\bar{F}(t) = F(t) - M_{plate} \cdot a_{plate}(t)$$

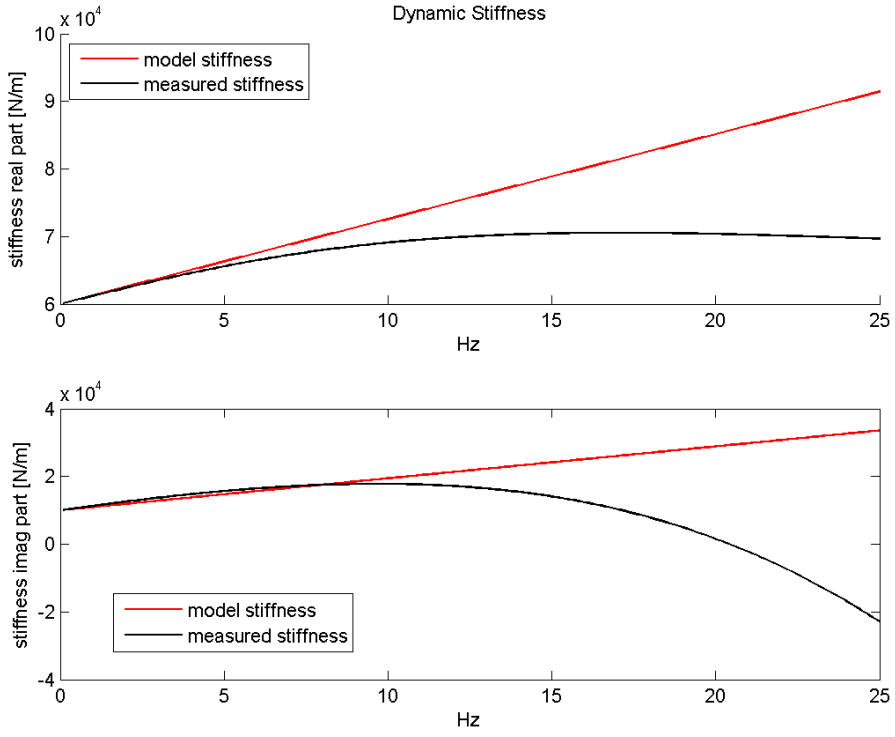

Figure A.15: error in the dynamic stiffness measurement with Entran accelerometer

The error is calculated as:

$$e\% = \frac{value - measured\_value}{value} \times 100$$

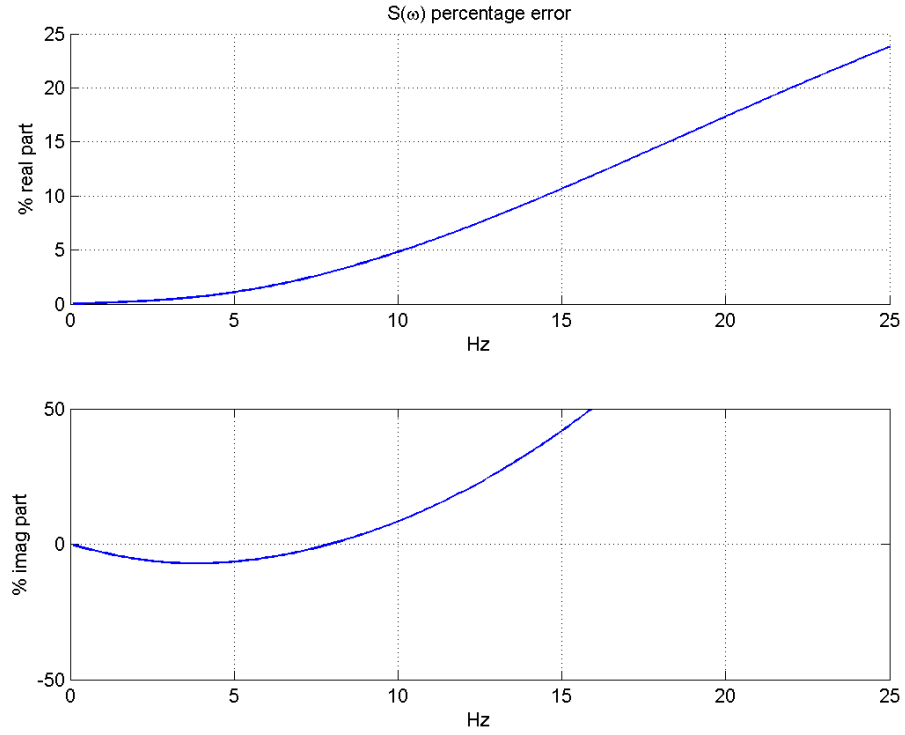

Figure A.16: percentage error in the dynamic stiffness measurement with Entran accelerometer

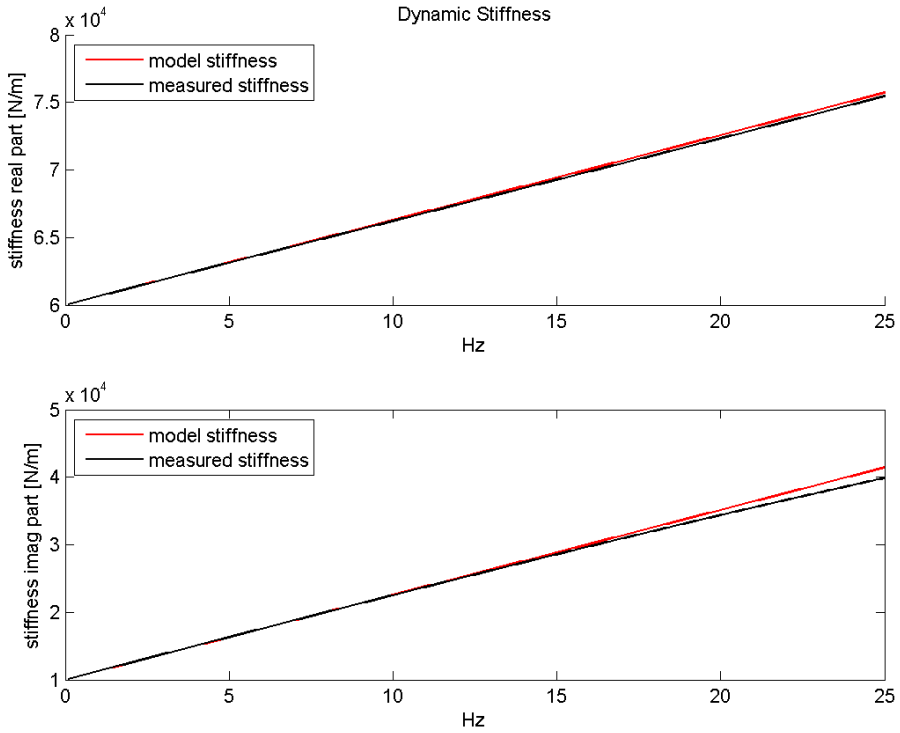

Figure A.17: error in the dynamic stiffness measurement with Endevco accelerometer

Systematic error in the measurement of dynamic stiffness are less than the 5% when using a Endevco 'lightly damped' accelerometer: those error is acceptable for the present study.

Conclusions

The models seemed to show a good agreement with experimental data, meaning that the electric part of the measurement instrumentation does not introduce significant distortions in the measurements. It is then possible to have a prediction of the systematic error.

It's possibly needed to have more accurate experimental validation of the model, for example by dummy tests and indenter tests.

Attention is needed when measuring seat Dynamic Stiffness on the indenter or when measuring it with a setup like the one in Experiment 1.

It is also possible to model the effect of errors in calibration.

It is possible to compensate, in three ways.

The first requires having a sampling rate at least equal to the time constant of the accelerometer. It is then possible to cancel the first samples in order to shift the time axis of the accelerometer backwards and eliminate the phase shift.

The second is to filter the signal in order shift it back in time.

It could also be possible, in the frequency domain, to add or subtract known values, obtained from experiments or from model.